PhD Program in Biomolecular Sciences

Department of Cellular, Computational and Integrative Biology – CIBIO

35th Cycle

Molecular mechanisms of Fam3c cardioprotective activity

Tutor:

Prof. Serena Zacchigna, M.D., Ph.D.

Advisor:

Prof. Mauro Giacca, M.D., Ph.D.

Ph.D. Thesis of

Antonio Mura

ICGEB, Trieste.

Academic Year 2022-2023

Declaration of Authorship

I, Antonio Mura, confirm that this is my own work and the use of all material from other sources has been properly and fully acknowledged.

Trieste, 10th January 2023

INDEX

ABSTRACT

Despite the urgent and broad need to develop new treatments for myocardial infarction (MI) and heart failure (HF), drug treatment to revert these pathologies has not evolved significantly over the last two decades. A key aspect underlying the epidemic burden of MI is the incapacity of the cardiac muscle to undergo regeneration in adult life. Damaged cardiac tissue typically results in irreversible loss of cardiomyocytes (CMs) with relative fibrosis and scarring. Although the massive effort so far made in trying and developing cardioprotective therapies, effective treatments have not been identified yet.

To systematically identify novel cardioactive biologicals, the Molecular Medicine Laboratory at ICGEB Trieste has generated a library of 1198 barcoded AAV vectors encoding for the mouse secretome and developed cardiac FunSel (cFunSel), a method for their in vivo unbiased selection ranking these factors for efficacy against MI. This strategy is based on the FUNctional SELection of molecules of interest without a priori knowledge on their function. After an iterative selection in mice subjected to MI, this method led to the identification of novel cardioactive proteins for which no information is currently available nor study has been performed relative to cardiac biology.

Among the selected hits identified by cFunSel, we focused our attention on Fam3c, a small, secreted protein ubiquitously expressed in all tissues with still unknown cardiac function. In vivo, cardiac Fam3c overexpression protected the heart after MI, preserving cardiomyocyte viability, sustaining ejection fraction, and preventing pathological remodelling. Fam3c overexpression in cardiomyocytes induced protective cardiac autophagy and decreased cardiomyocyte apoptosis in an in vitro model of cardiotoxicity. Moreover, Fam3c induced cardiomyocyte specific STAT3 activation in a Leukemia Inhibitory Factor receptor (LIFR)-complex dependent way. Although STAT3 participates in a well-known cardioprotective pathway, we demonstrate here that Fam3c induced autophagy is not mediated by STAT3 activation.

Fam3c, both expressed by cardiomyocytes and cardiac fibroblasts, was upregulated in an engineered heart tissue (EHT) model of cryoinjury and in the early phases after MI in mice. Fam3c upregulation upon cardiac injury is consequent to the upstream activation of TGF-β pathway and may reveal a new physiological mechanism to protect myocytes against acute ischemic damage, which can be exploited for therapeutic purposes.

1. INTRODUCTION

1.1 Cardiovascular disorders

1.1.1 Epidemiology

According to The World Health Organization (WHO), cardiovascular disorders (CVDs) are the first cause of death worldwide, taking an estimated 17.9 million lives each year.

As reported by the Global Burden of Disease Study 2019, 16% of the world total deaths are due to ischemic heart disease, followed by stroke and chronic obstructive pulmonary disease, second and third leading cause of death responsible for 11% and 6% of global deaths, respectively. Ischemic heart disease, also called coronary heart disease (CHD), is a pathological condition characterized by reduced blood flow supply to the cardiac tissue.

Since 2000, a massive increase has been reported in the number of deaths caused by CHD, rising by more than 2 million to 8.9 million deaths in 2019 (see Fig. 1). Furthermore, this burden of disease is expected to get worse in the next years. The WHO estimated that, by 2030, almost 23.6 million of people will die from CVDs.

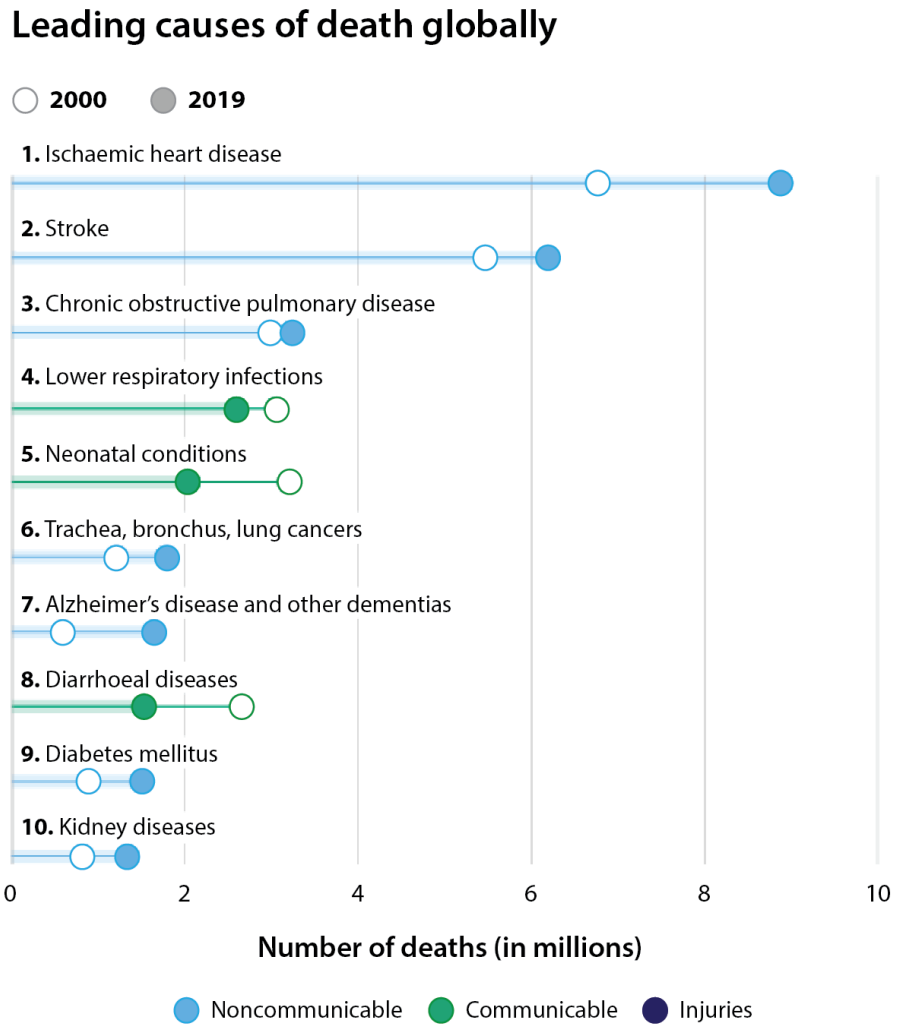

Figure 1: Leading causes of death globally. From WHO Global Health Estimates.

Among all different CVDs, myocardial infarction (MI) is the most clinically relevant condition. MI occurs when there is a decrease in the coronary blood flow, which results in deficient of nutrients and oxygen supply to the cardiac tissue. During MI, as a consequence of tissue damage, the heart can lose as many as 25% of the cells that are present in the left ventricle (Murry, Reinecke, & Pabon, 2006). This massive CMs loss is not accompanied by a sufficient renewal that would be required to compensate for this sudden cell death. By ^{14}C-carbon dating, the regenerative capacity of the normal adult heart was estimated to be less than 50% renewal in 70-year lifetime (Bergmann et al., 2009). The sudden loss of CMs during the adult life is a key aspect underlying the impact of MI and, more in general, heart failure (HF).

1.2 Molecular mechanisms of cardiomyocyte death

1.2.1 Overview of different types of cell death

The dynamic balance between cell death, proliferation, survival and differentiation is the key process that controls the development and tissue homeostasis of multicellular organisms. At a single cell level, all these events are essential and become even more important in pathological conditions. Both progressive and acute cell death are hallmarks of cardiac pathological conditions, including HF, MI and ischemia reperfusion injury. Recently, more than ten different types of cell death have been identified (Galluzzi et al., 2018). Among these, apoptosis, necrosis and autophagic cell death are considered the most common forms observed during the progression of heart disease (Whelan, Kaplinskiy, & Kitsis, 2010).

1.2.2 Apoptosis

Apoptosis is the most studied form of cell death. The word *apoptosis,* a Greek term that means “falling leaves in autumn”, was first used in 1972 to describe programmed cell death (Kerr, Wyllie, & Currie, 1972). Apoptosis can be induced by different cell stresses that stimulate pro-apoptotic signalling pathways resulting in the activation of the caspase proteases. Alteration in cell morphology, shrinkage of the cell, genomic DNA fragmentation, fragmentation into membrane-bound apoptotic bodies and rapid phagocytosis by neighbouring cells are considered its hallmark since many years (Kerr et al., 1972; Wyllie, 1980). Based on molecular mechanism of activation, apoptosis is divided into intrinsic and extrinsic apoptosis.

Intrinsic apoptosis is activated by both exogenous and endogenous stimuli, such as DNA damage, ischemia and oxidative stress. Mitochondria are the principal organelles involved in mediating this process. As well as other different cell types, CMs express various members of the B cell lymphoma-2 (Bcl-2) family proteins. Bcl-2 proteins induce mitochondrial translocation of the pro-apoptotic proteins Bax and Bak. This event causes mitochondrial membrane permeabilization, which leads to cytoplasmic release of cytochrome C. In the cytoplasm, cytochrome C forms a complex with apoptotic protease activating factor 1 (Apaf1) and the inactive form of

caspase-9, resulting in the initiation of caspase cascade reactions (Hutt, 2015). This complex, through adenosine triphosphate (ATP) hydrolysis, cleaves and activates caspase-9, which in turn cleaves and activates the downstream effector caspases-3 and -7, thereby executing programmed cell death. Among the Bcl-2 family members, anti-apoptotic and pro-apoptotic Bcl2 proteins have been shown to be transcriptionally regulated in heart disease (Condorelli et al., 1999).

On the other hand, extrinsic apoptosis is mainly regulated by death receptors: Fas cell surface death receptors (Fas), Tumor Necrosis Factor receptors (TNF) and TNF-related apoptosis-inducing ligand (TRAIL) receptors. Extrinsic apoptosis initiation is ruled by the binding of the ligand to its respective receptor with the help of adapter proteins. These receptors share a death domain of approximately 80 amino acids long that plays an essential role in transmitting the death signal to intracellular signalling pathways (Tartaglia, Ayres, Wong, & Goeddel, 1993). Death ligands, their receptors and different pro-apoptotic proteins form the death-inducing signalling complex (DISC), responsible for the induction of the caspase cascade. The DISC complex recruits and activates the initiator caspase-8 which in turn cleaves and activates the executioner caspase-3, leading the apoptotic signal (Barnhart, Alappat, & Peter, 2003). Moreover, the activation of caspase-8 can also trigger intrinsic apoptosis.

Fas, TNF receptor I and TRIAL are expressed in CMs, and their involvement in cardiovascular pathology has already been shown (Whelan et al., 2010). Several studies have reported decreased levels of TRAIL in patient with MI (Mori et al., 2010; Osmancik, Teringova, Tousek, Paulu, & Widimsky, 2013), suggesting that this is as a potential marker of prognosis for these patients.

Fig. 2 reports a schematic representation of both intrinsic and extrinsic apoptosis pathways.

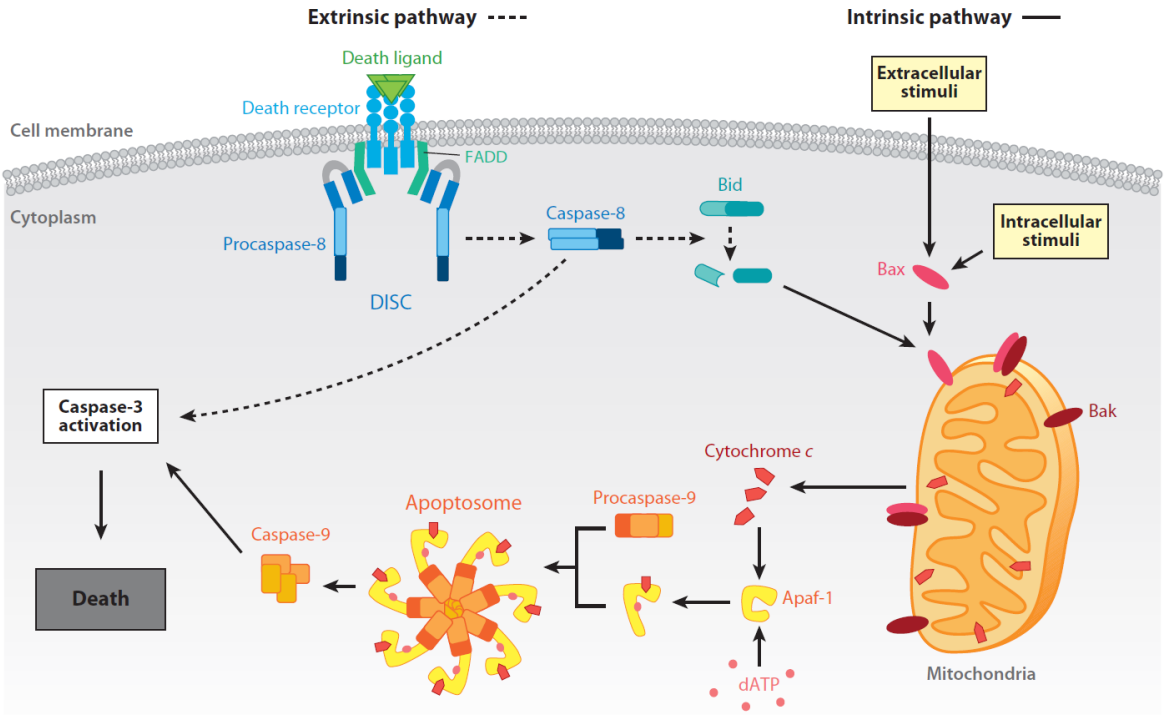

Figure 2: Overview of apoptosis. Apoptosis can be mediated by extrinsic and intrinsic pathway. The extrinsic pathway is activated by the binding of a death ligand to its receptor, which triggers the formation of the DISC complex. The DISC complex activates caspase-8, which results in activation of the downstream signalling cascade. The intrinsic pathway can be activated by both extracellular and intracellular stimuli that induce mitochondrial translocation of the pro-apoptotic proteins Bax and Bak. These events lead to mitochondrial membrane permeabilization and the release of cytochrome c into the cytoplasm. Cytosolic cytochrome c activates procaspase-9, which cleaves and stimulates caspase-9. At last, this triggers the downstream caspase-3, resulting in programmed cell death. From: (Whelan et al., 2010).

1.2.3 Necrosis

Unlike apoptosis, necrosis is another cell death process with different features. It results from the disruption of cellular membrane integrity, ATP depletion and consequent relative dysregulation of ion and water balance between intracellular and extracellular space. As a result of cellular membrane dysfunction, necrotic cells become swollen with concomitant swelling of mitochondria. These pathological events lead to membrane rupture and the release of cellular components, which induces an inflammatory response. In the past few decades, necrosis has been considered as a passive and non-regulated cell death process. Even though a great proportion of necrotic cell death is passive, regulated necrosis has also been shown

to exist and to be an important component of CVDs such as MI, HF and stroke. The execution of necrotic cell death could also be a finely regulated process by a set of signal transduction pathways and catabolic mechanisms (Golstein & Kroemer, 2007). These regulatory mechanisms are mainly classified into one of two pathways: mitochondrial mediated necrosis and death-receptor dependent necrosis, also called necroptosis.

During an ischemic condition such as MI, ATP depletion is followed by a shift from cardiac mitochondrial oxidative metabolism to anaerobic glycolysis with consequent increase of H^+ and Na^+. As illustrated in Fig. 3, cytoplasmic acidification results in the activation of proteases and a massive increase of water that generate lysosomal swelling, rupture of its membrane and activation of more proteases involved in the process.

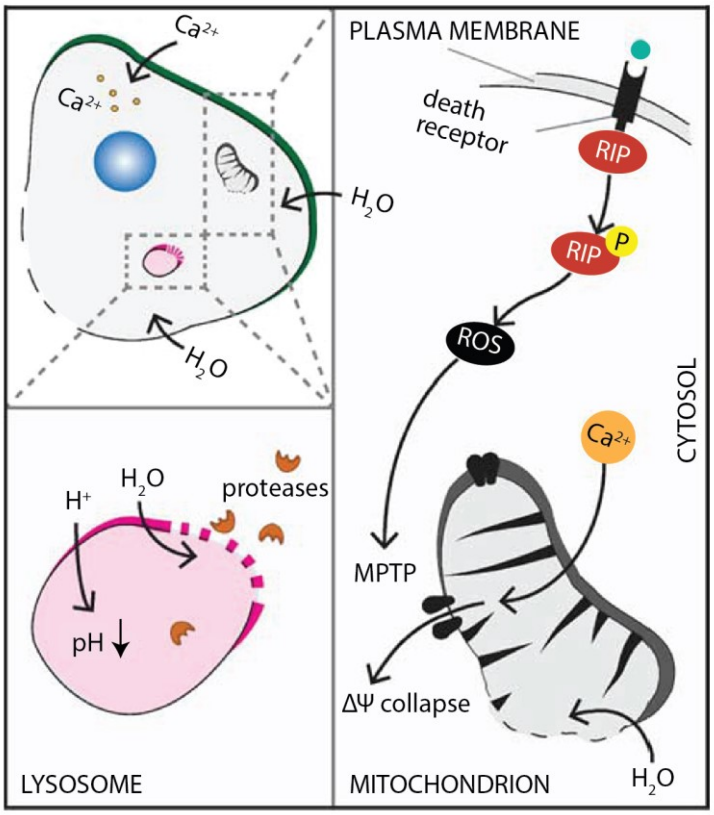

Figure 3: Necrosis pathway in cardiomyocytes. During stress condition, ATP depletion inhibits the action of cellular pumps with a consequent increase of intracellular levels of H^+ and Na^+. The sodium-calcium exchanger operates in reverse manner and provokes an increase of Ca^{2+} in the cytoplasm and in the mitochondrial matrix. High levels of mitochondrial Ca^{2+} together with elevated levels of ROS cause mitochondrial permeability transition pore (MPTP) opening and consequent necrosis. Adapted from: (Chiong et al., 2011).

In addition, inhibition of cellular pumps by ATP depletion can also result in a decrease in intracellular pH. In response to elevated Na^+, the sodium-calcium exchanger operating in reverse mode is less efficient in removing intracellular Ca^{2+} and provokes an increase of cytoplasmic Ca^{2+} that is transported into mitochondria. Increased level of Ca^{2+} in mitochondrial matrix compromises electron transport chain, elevates levels of reactive oxygen species (ROS) and causes long-lasting opening of mitochondrial permeability transition pore (MPTP) resulting in necrosis.

1.2.4 Autophagy

Although autophagy, together with necrosis and apoptosis, is an important mechanism that contributes to regulate cellular homeostasis, it is mainly described as a pro-survival mechanism. Autophagy is a highly conserved process among species and cell types, and it is primarily activated under stress conditions. Its main function is the recycling of dysfunctional organelles and damaged cellular components that are degraded by the lysosome.

Mainly three types of autophagic responses have been identified: chaperone-mediated autophagy (CMA), microautophagy and macroautophagy (Levine & Kroemer, 2008), as shown in Fig. 4.

CMA is a multi-step selective process through which cytosolic proteins carrying the KFERQ-like pentapeptide motif are delivered to lysosomes for degradation (Dice, 1990). Recognition of substrate proteins takes place in the cytosol through the binding of a constitutive chaperone, the heat shock-cognate protein of 70 kDa (HSC70), to the pentapeptide motif present in the amino acid sequences of all CMA substrates (Cuervo & Wong, 2014). Once bound to the chaperone, the substrate is targeted to the surface of the lysosomes, where it interacts with the cytosolic tail of the lysosomal-associated membrane protein 2A (LAMP-2A) (Cuervo & Dice, 1996). This binding promotes LAMP-2A multimerization into a higher-molecular-order complex at the membrane, where, after unfolding, the substrate is translocated into the lysosome and degraded by acidic hydrolases (Kirchner et al., 2019).

Microautophagy, first proposed by de Duve and Wattiaux more than 50 years ago, is a degradative process through which autophagic cargoes are directly taken up by

lysosomes and late endosomes through membrane invagination and degraded in the endolysosomal lumen (De Duve & Wattiaux, 1966; L. Wang, Klionsky, & Shen, 2022). Microautophagy can be both unselective and cargo-specific depending on the cellular context. While non selective microautophagy is involved in the degradation of randomly sequestered portions of cytosol (Mijaljica, Prescott, & Devenish, 2011), selective microautophagy is involved in the degradation of specific organelles: mitochondria (micromitophagy), nuclei (micronucleophagy), peroxisomes (micropexophagy) and endoplasmic reticulum (microreticulophagy) (L. Wang et al., 2022).

Macroautophagy (hereafter referred to as autophagy) is the most studied form of autophagy. Its molecular mechanism involves several conserved autophagy-related (Atg) proteins. At the initial step, the Unc-51-like kinase 1 (ULK1), focal adhesion kinase family interacting protein of 200 kD (FIP200), Atg13, and Atg101 are combined to form the Atg1 complex, which subsequently triggers the assembly of Beclin-1, Atg14, VSP15, and VSP34 comprising the Class III phosphatidylinositol 3-hydroxy kinase (PI3K) complex (D. Wu, Zhang, & Hu, 2019). Although autophagy is evolutionarily conserved across species (Schultz, Byman, Fex, & Wennstrom, 2017), Atg13 is not present in mammals and Atg1 associate with the Atg8 orthologues microtubule-associated protein light chain 3 (LC3). The PI3K complex is responsible for the membrane nucleation process generating an isolation membrane called phagophore. The phagophore then surrounds the material destined to be degraded creating the spherical double layer membrane termed autophagosome. Upon autophagy stimulation, the cytosolic form of LC3 (LC3-I) is conjugated with phosphatidylethanolamine to form LC3-phosphatidylethanolamine conjugate, which will be recruited to the autophagosomal membrane (LC3-II). Once the autophagosome is formed, it fuses with the lysosome leading to formation of the autolysosome, a single membrane structure. This event induces the release of the cargo into the acidic lysosomal environment. The degraded autophagic cargo is then transported back into the cytoplasm where it will be used by the cell in biosynthetic processes or to produce energy (Yorimitsu & Klionsky, 2005).

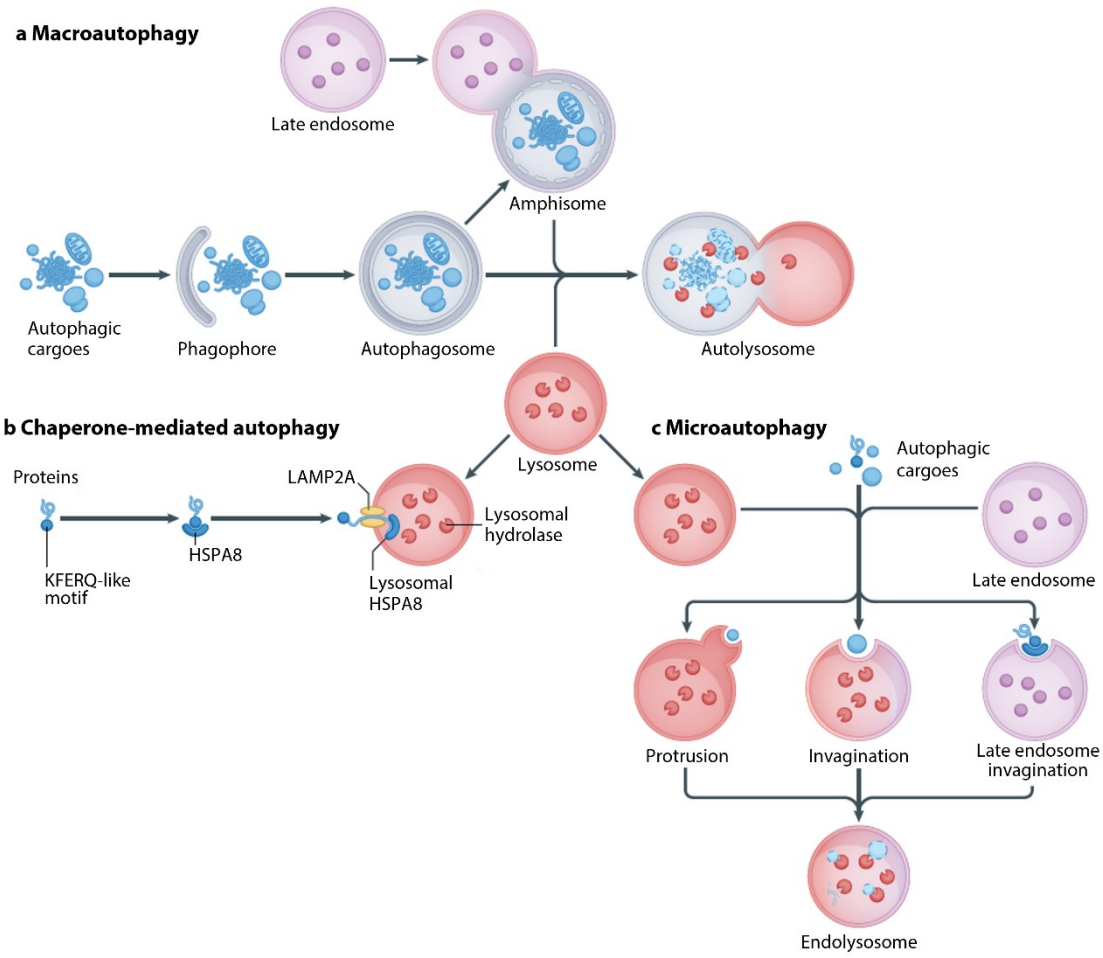

Figure 4: Overview of autophagy. During macroautophagy (**a**), molecules to be degraded are surrounded by a sequestering membrane termed "phagophore". The phagophore, after expansion, acquires a spherical shape to generate the autophagosome, a double membrane vesicle. The autophagosome fuses first with the late endosome and then with the lysosome to generate the autolysosome, the compartment where autophagic cargoes are degraded. During chaperone-mediated autophagy (**b**), cytosolic proteins carrying the KFERQ-like peptide motifs are recognised by chaperone proteins, delivered to the lysosome through lysosomal-associated membrane protein 2A (LAMP2A) and degraded within the acidic environment. During microautophagy (**c**), molecules to be degraded are directly sequestered by lysosomes and late endosomes. The autophagic cargoes are then degraded in the endolysosomal lumen. Adapted from: (L. Wang et al., 2022).

In post mitotic cells, such as CMs, the interplay between autophagy and cell death is a crucial process. Under ischemic condition, a decrease in autophagy leads to abnormal organelles and protein accumulation, thereby promoting apoptosis and necrosis. Since recycling of organelles is a strategy to survive in an environment poor of nutrients and oxygen such as the myocardium after MI, the role of autophagy supporting CM survival becomes essential. In a mouse model of MI, autophagy has

been shown to be induced in the acute phase while impaired in the later phase (X. Wu et al., 2014). In the same study, the significance of impaired autophagy was evaluated upon treatment with the autophagy enhancer rapamycin or autophagy inhibitor 3-methyladenine (3MA). Rapamycin improved postinfarction cardiac remodelling and dysfunction, while 3MA exacerbated it. Similar results were also observed in a rat model of MI in which rapamycin administration reduced the infarct size and ameliorated cardiac function (Aisa et al., 2017). Moreover, administration of bafilomycin A1, an autophagy inhibitor, significantly increased the infarct size in a mouse model of MI, while starved mice, in which nutrient deprivation stimulates autophagy, showed reduced infarct size (Kanamori et al., 2011). Interestingly, in adult mice the cardiac-specific deficiency of autophagy-related 5 (Atg5) led to left ventricular dilatation, contractile dysfunction and sarcomere disorganization (Nakai et al., 2007).

This evidence indicates that autophagy is an innate and essential process involved in the protection of myocytes against an ischemic insult. For these reasons, acute induction of autophagy has recently been considered a novel strategy for treating MI (Przyklenk et al., 2011).

1.3 Counteracting cardiomyocyte death

1.3.1 Pre- and post-ischemia conditioning

Despite the large efforts that have been made over the last years to treat MI, the restoration of blood flow to the ischemic zone is the only effective way to counteract ischemic damage. The restoration of blood and oxygen to injured cardiac tissue is essential to avoid massive cellular death, however, reperfusion causes itself CM death by inducing sudden oxidative stress (Ambrosio & Tritto, 1999), leading to the so-called ischemia reperfusion injury.

Reperfusion consists in the process of restoring blood flow to the ischemic region and can take place spontaneously or can be induced by invasive procedures

through different strategies. Among these, primary percutaneous coronary intervention (PCI), as recommended by the European and American guidelines, is the preferred reperfusion strategy in patients with myocardial infarction (Ibanez et al., 2018).

Protection of the myocardium against ischemia reperfusion injury can be obtained by conditioning protocols that consist in applying few periods of short coronary occlusion and reperfusion immediately preceding or following MI (ischemic pre- and post-conditioning, respectively).

Already in 1986, Murry and colleagues (Murry, Jennings, & Reimer, 1986) reported that pre-conditioning ischemia can reduce infarct size. This approach not only reduces CM death and endothelial dysfunction, but also contributes to the modulation of inflammatory response. The beneficial effect that follows ischemic pre-conditioning seems to be related to the release of various molecule which can trigger intracellular cardioprotective pathways (Hausenloy & Yellon, 2008). Although the cardioprotective effect induced by ischemic pre-conditioning is remarkable, it can only be clinically useful in patient with programmed cardiac-surgery interventions but unusable in patient with MI, since it must be performed prior to ischemia.

Myocardium is subjected to brief cycles of occlusion and reperfusion also in the case of post-conditioning. In this scenario, these actions are performed at the onset of reperfusion immediately after the blood flow restoration that follows the long period of ischemia. Similar to pre-conditioning, post-conditioning has also been shown to be protective against ischemia reperfusion injury. Post-conditioning has been reported to induce a reduction of infarct size, CM death and endothelial dysfunction (Penna et al., 2006; Z. Q. Zhao et al., 2003).

Without considering mechanical application, pre- and post-conditioning can be induced through a pharmacological approach with similar cardioprotective results in animal models. As far as pharmacological pre-conditioning is concerned, this can be achieved by using a range of different pharmacological agents, responsible to activate signalling cascades that can mimic ischemic pre-conditioning (Yellon & Downey, 2003). Concerning pharmacological post-conditioning, this can be induced

in the first minutes of blood flow restoration through the infusion of molecules already known to induce pre-conditioning (Penna, Mancardi, Raimondo, Geuna, & Pagliaro, 2008).

Both pre- and post-conditioning can be obtained by a remote approach. This procedure, so called remote ischemic pre- or post-conditioning, consists in the application of a transient and brief ischemic stimulus to a distant site from the heart, before and after reperfusion respectively. These procedures were also proven to protect the heart against ischemia and reperfusion injury (Bell & Yellon, 2012; Ludman, Yellon, & Hausenloy, 2010).

Unfortunately, these observations were not successfully translated into clinical application yet (Hausenloy et al., 2019). In addition, most of these studies were focused on treatments that increase the viable myocardial immediately after MI, essentially limiting CM death from sudden lack of oxygenation. However, the need to support the heart several hours later is tremendously important. In this phase, the extent of perfusion and collateral flow formation, as well as the efficiency in removal of dysfunctional organelles and activation of intracellular protective pathways, are essential to determine viability of the myocardium. These events, which are commonly activated several hours after an acute ischemic event, determine the fate of a large number of CMs in the so-called area-at-risk, for which the destiny is still uncertain. Indeed, this area can be as large as 88% of the original infarcted region (Lee, Ideker, & Reimer, 1981).

Since the adult heart has a limited capacity for regeneration and repair, it is essential to support and enhance CM survival after an ischemic insult to restore and maintain a proper cardiac contractile function.

1.3.2 Standard treatment regimens for myocardial infarction

Despite the urgent and broad need to develop new treatments for MI and HF, drug treatment for these conditions has not evolved significantly over the last two decades. Standard of care now includes angiotensin converting enzyme (ACE) inhibitors, angiotensin receptor blockers (ARBs), beta-blockers, mineralocorticoid receptor antagonists, ivabradin and, more recently, combined ARB-neprilysin

inhibitors (ARNIs-sacubitril/valsartan) and SGLT2 inhibitors (gliflozines); as reviewed by Heidenreich and colleagues (Heidenreich et al., 2022). Most of these drugs have been originally developed several decades ago, with the most recent one, the angiotensin II receptor blockers, dating back to the mid-1990s (Gottlieb et al., 1993). Equally surprising is the observation that not a single biological drug (protein, peptide, antibody, nucleic acid) exists for a condition that is as prevalent as HF (Packer, 2018). Although a remarkable progress in the clinical management of patients and the use of ventricular assist devices (Birks, 2013), the prognosis of HF remains poor. The mortality has been estimated at 6-7% at one year in patients with chronic HF to raise to up to 25% or more in hospitalized patients with acute HF (Crespo-Leiro et al., 2016).

1.4 Biotherapeutics

1.4.1 Overview of biotherapeutics: a new approach in modern medicine

Over the last decades, and even more in the current years, biotherapeutics have represented an essential component of modern medicine. Biotherapeutics or biologicals are therapeutic agents (DNA, RNA, peptide, protein) produced from a biological source or consisting in a biological molecule obtained synthetically. In the early ‘70s, a vast progress in the recombinant DNA techniques, including recombinant protein production, opened the door to a new strategy for the treatment of different pathologies. Using genetically engineered bacteria, yeast or mammalian cells, it has been possible to produce a large amounts of biological active human proteins. In 1982, the approval of recombinant human insulin has drastically improved the quality of life of diabetic patients. In the following years, recombinant proteins have revolutionized the treatment of a variety of disease in areas such as oncology, inflammatory and autoimmune diseases, hemophilia, cardiovascular disease, infectious diseases and rare genetic diseases (Zhong, Neumann, Corbo, & Loh, 2011). Currently, protein biotherapeutics occupy a large portion of the market

with more than 130 proteins, 140 peptide-based therapeutics and around 500 peptides in preclinical development (Haranath Chinthaginjala, 2021).

1.4.2 Biological therapies for cardioprotection

Cardioprotection includes all mechanisms that contribute to the preservation of the heart by reducing or even preventing myocardial damage (Kubler & Haass, 1996). It is based on the use of proteins, cells or genes to support cardiac function, reducing CM death and therefore limiting the detrimental cardiac remodelling occurring upon CM loss (Schwartz Longacre et al., 2011). Proteins, specially secreted proteins, are attracting more and more attention as target for therapeutic intervention since they can be properly dosed and easily administered through different delivery method such as subcutaneous, intravenous and intramuscular administration.

In the cardiac therapy field, not a single biological therapy exists today for any clinical application, ranging from cardioprotection, to therapy of HF and including cardiac regeneration. However, a few strategies have been attempted specifically for cardioprotection, based on recombinant factors. Among these the most extensive studies were with erythropoietin and relaxin.

Recombinant human erythropoietin (EPO) administration has shown a powerful cardioprotective effect in both permanent coronary ligation and ischemia/reperfusion model (Lipsic et al., 2006; Moon et al., 2003). However, results from clinical trials of patients with acute MI did not confirm the beneficial effect observed in animal studies (Belonje et al., 2008; Steppich et al., 2017).

Relaxin, a peptide hormone involved in the hemodynamic and renovascular adaptive changes occurring during pregnancy (Teichman et al., 2009), was thought to be a potential new treatment for HF. Pre-clinical studies with Serelaxin, the recombinant human form of relaxin-2, was shown to attenuate myocardial damage in mouse subjected to myocardial infarction (Valle Raleigh et al., 2017). In virtue of these promising pre-clinical studies, Serelaxin has undergone several clinical trials for chronic and acute failure (Ghosh et al., 2017). In the RELAXIN in Acute Heart Failure (RELAX-AHF), double-blinded, placebo-controlled trial, investigators found an improvement of dyspnoea relief with a 48-hour infusion of Serelaxin in the first 5

days, but the trial did not meet its secondary endpoint of cardiovascular death or hospital readmission for cardiac or renal failure (Teerlink et al., 2013). However, in patients treated with Serelaxin, a significant reduction in cardiovascular mortality at day 180 and a reduced worsening HF at 5 days was reported. To better evaluate the effect of this protein, another clinical trial was performed (RELAX-AHF-2). Surprisingly, RELAX-AHF-2 did not replicate the benefit of Serelaxin with respect to cardiovascular mortality that was seen in the previous RELAX-AHF-trial (Teerlink et al., 2013).

Various factors have probably contributed to these failures. First of all, most of pre-clinical experiments have been performed on young and healthy animals while ischemic heart disease affects patients above 50s, whose coronary artery can present both atherosclerosis and endothelial dysfunction, not present in animal models (Hausenloy et al., 2010; Heusch & Gersh, 2017). Furthermore, the presence of co-morbidities in patients affected by CVDs already under several medications, may have interfered with the cardioprotective treatments (Heusch & Gersh, 2017). Moreover, the time of medical intervention after symptoms onset dramatically impact on the cardioprotective effect. In fact, if reperfusion occurs in the first 30 minutes from symptom onset, its benefit could overcome the action of any additional therapy. On the other hand, if reperfusion happens after 4 hours or longer, only a limited portion of myocardium can be saved (Heusch & Gersh, 2017).

Finally, all the tested potential therapeutical agents have been first identified *in vitro*, and only after validation were evaluated *in vivo* in animal models. *In vitro* conditions cannot reproduce all the possible interactions of living organisms, thus the *in vitro* selected molecules may fail or result inefficient *in vivo* due to unexpected effects. All these limitations have contributed to the failure of novel therapies into clinical trials.

Consequently, there is an urgent need to identify new chemical/biological molecules that can protect CMs immediately after MI and throughout reperfusion. The achievement of this approach would be of immense therapeutic value.

1.5 *In vivo* functional selection of novel biotherapeutics

1.5.1 FunSel

Whit the aim to systematically search for factors able to counteract CM loss after cardiac damage, including MI, the Molecular Medicine Laboratory (MML) at the International Centre for Genetic Engineering and Biotechnology (ICGEB) has developed a novel procedure for the *in vivo* functional selection of beneficial factors that eventually could be used as therapeutics (Bortolotti et al., 2017; Ruozi et al., 2015; Ruozi et al., 2022). This technique, which was named FunSel (Functional Selection), is based on the use of adeno-associated virus (AAV) vectors, well known to be exquisite tools for highly efficient CM gene transfer (Chu et al., 2003; French, Mazur, Geske, & Bolli, 1994). In the past, the MML has generated an arrayed library of cDNAs individually cloned into the pGi-AAV backbone. The library corresponds to the mouse secretome and includes 1198 cytokines, growth factors, hormones, chemokines, interleukins, extracellular matrix proteins, secreted enzymes and other factors of unknown function encoded by the genome. The coding portion of each cDNA is under the control of a constitutive CMV IE promoter. After the coding sequence, each vector contains a unique 10-nt barcode, which univocally identifies each clone and that can be sequenced by Next Generation Sequencing (NGS). To allow recombinant vector production, Inverted Terminal Repeats sequences (ITRs) are present inside the pGi AAV-backbone. Fig. 5 shows the structure of the AAV constructs.

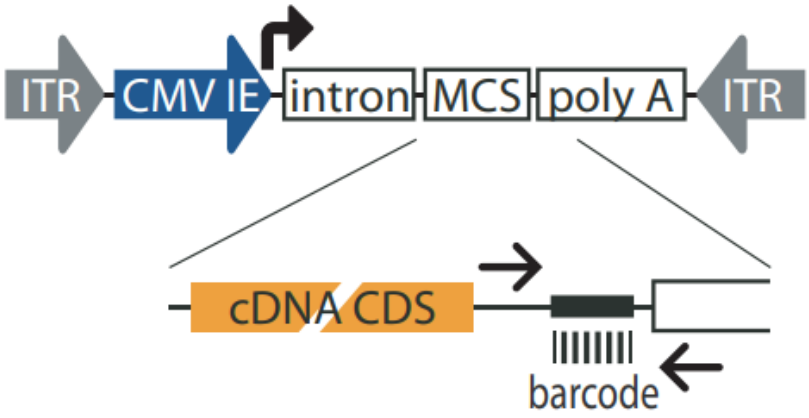

Figure 5: Schematic representation of the pGi vector plasmid used for the secretome library generation. The primers to amplify the 10-bp barcode region are indicated by black arrows. The pGi AAV backbone plasmid also contains two Inverted Terminal Repeats sequences (ITRs), essential for recombinant AAV vector production. CDS: coding sequence. CMV IE: cytomegalovirus immediate early promoter. From: (Ruozi et al., 2022).

Briefly, pools of 50 AAV9 vectors expressing different factors are injected into the heart of adult mice at a multiplicity of infection (MOI) by which theoretically each vector enters a different CM. To apply a selective stimulus, MI is induced by left descendent coronary artery ligation. Upon MI, most of CMs die due to the ischaemic damage, but myocytes expressing protective factors selectively survive.

After three weeks, vector DNA is recovered from the survived myocardium and the frequency of each factor is determined by barcode amplification through Next Generation Sequencing using the Illumina platform. Vectors expressing factors contributing to CM protection or regeneration are thus selected and become enriched over the others, while vectors encoding detrimental factors are lost. An outline of FunSel technique is showed in Fig. 6.

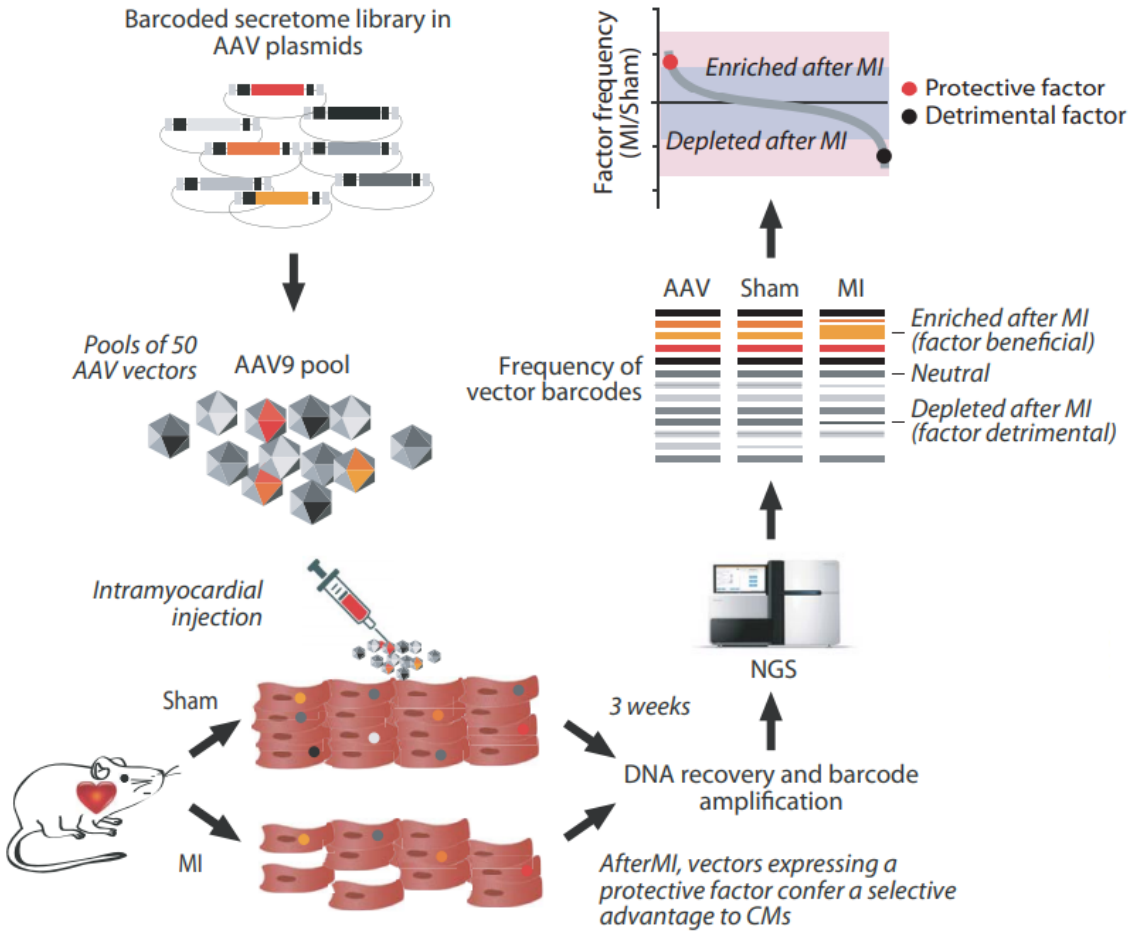

Figure 6: Schematic illustration of FunSel. A pool of plasmids coding for different factors is used to generate a Pool of AAV9 vectors, which are then administered to the heart; each vector transduces different cardiomyocytes. Selection is then applied by inducing MI. After three weeks, barcoded vector DNA is PCR-amplified and sequenced by next generation sequencing (NGS). Factors exerting cardioprotective activity are relatively enriched. From: (Ruozi et al., 2022).

The *in vivo* screening of the entire FunSel library for selection after MI was recently completed. The top performers included proteins already reported to exert cardioprotective action, such as Midkine (Mdk) (Sumida et al., 2010) and Relaxin-1 (Rln-1) (Martin, Romero, & Salama, 2019) and proteins for which no information is currently available nor study has been performed relative to cardiac biology. These last are two members of Family with sequence similarity 3 (Fam3), Fam3b and Fam3c (Cao et al., 2005; Pilipenko, Reece, Choo, & Greinwald, 2004), Chordin-like 1 (Chrdl-1) (Nakayama et al., 2001), the NHL repeat-containing protein 3 (Nhlrc3) (H. Chen et al., 2017) and the HtrA (Htra1) protein (Pallen & Wren, 1997).

1.6 The FAM3 gene family

In 2002, searching for new cytokines, Zhu and colleagues identified a novel cytokine-like gene family that was termed Family with Sequence Similarity 3 (FAM3). This comprises four genes: Fam3a, Fam3b, Fam3c and Fam3d (Y. Zhu et al., 2002). Each of these genes encodes a protein of 224-235 amino acids in length that has no homology with any known cytokine. As shown in table 1, the homology at amino acid level between the different FAM3 proteins is 31.6-53.3%. The function and mechanisms of action of this new class of family protein is still not completely understood (Wilson, Robert-Cooperman, & Burkhardt, 2011; X. Zhang et al., 2018). Crystal structure of Fam3b showed that the FAM3 family proteins exhibit a unique β-β-α fold (Johansson et al., 2013), different from the originally predicted four-helix bundles typical of cytokines.

Homology of the novel cytokine family members at the amino acid level				
	FAM3A	FAM3B	FAM3C	FAM3D
FAM3A	---	31.6	47.4	53.3
FAM3B		---	32.5	28.0
FAM3C			---	50.2
FAM3D				---

Table 1: Homology of the FAM3 protein family. Adapted from: (Y. Zhu et al., 2002).

Fam3a, Fam3b and Fam3c are considered as novel regulators of hepatic glucose and lipid metabolism. Fam3a was shown to represses hepatic gluconeogenesis and lipogenesis. Its overexpression in diabetic mice leads to improved glucose intolerance, hyperglycemia and insulin resistance together with attenuated hepatic glucose production and steatosis (C. Wang et al., 2014). Moreover, Fam3a protects

mouse liver after ischemia reperfusion injury by activating the Akt survival pathway and repressing inflammation and oxidative stress (Z. Chen, J. Wang, et al., 2017).

The Fam3b protein, also named PANcreatic-DER-ived factor (PANDER) due to its high expression in pancreatic islets (Cao et al., 2003), was found to be elevated in the serum of diabetic patients and it negatively correlated to pancreatic β cell function (Shehata, Kamal, El-Hefnawy, & El-Mesallamy, 2017). Fam3b seems to act differently according to cell types. In human colon cancer cells (HCT8, HCT116), lung carcinoma cell (A549), microglia (N9) and muscle cell (C2C12), the knockdown of Fam3b induced cell death through a p53-dependent pathway (Mou et al., 2013), while its overexpression results in apoptosis in pancreatic α and β cells (Cao et al., 2003; Yang et al., 2005). In a type II diabetes mouse model, physical exercise leads to a reduction in Fam3b liver expression with an increase in Fam3a protein (J. Li et al., 2011; C. Wang et al., 2014), suggesting a crosstalk among FAM3 gene family members in diabetic patients. Recently, the Fibroblast Growth Factor Receptors (FGFRs) 1 to 4 were putatively identified as receptors for Fam3b (F. Zhang et al., 2021). In the same study, Fam3b was shown to promote posterior axis development in *Xenopus* embryos through the FGFR/ERK signalling pathway. The binding of Fam3b to FGFR was also confirmed in mammalian cells (F. Zhang et al., 2021).

Fam3d is a gut-secreted protein, which is highly expressed in the mouse gastrointestinal tract and was found to be regulated by nutritional status (de Wit et al., 2012). The literature data about this protein is limited compared to the other members of the family. In 2016, Fam3d was identified as a new endogenous chemotaxis agonist for the formyl peptide receptors (Peng et al., 2016) and a possible role in inflammation was proposed. Recently, deficiency in Fam3d was shown to be associated with impaired integrity of the colonic mucosa, increased epithelial hyper-proliferation, reduced anti-microbial peptide production and increase sensitivity to chemically induced colitis associated with high incidence of cancer (Liang et al., 2020). These last observations underline the essential role of Fam3d in colon homeostasis.

1.6.1 Fam3c

Human Fam3c gene is located on chromosome 7q31.31 and contains 12 exons. Its protein product is a secreted protein that is processed at its N-terminus resulting in a full-length 25 kDa molecule that can be reduced to 18 kDa (Csiszar et al., 2014; Waerner et al., 2006). Four conserved cysteines stabilize the protein folding generating covalent bonds between cysteine 58 and 86 and 64 and 221. Unlike the other three FAM3 factors, Fam3c has an additional fifth cysteine (cysteine 58) which is responsible for covalent self-association (Kral et al., 2017). Thanks to this additional amino acid residue, Fam3c can exist as both monomer and covalent dimer. The dimer form was demonstrated to be the active form responsible for endothelial-mesenchymal transition (EMT) and cancer progression (Jansson et al., 2017). The homology between human and rodent Fam3c is very high. As shown in Fig. 7**,** blasting mouse Fam3c against the correspondent rat and human protein sequence reveals 97% and 94% identity, respectively.

Fam3c has been shown to participate in different biological processes. These include retinal laminar formation, Alzheimer's disease, bone density regulation, hepatic glucose and lipid metabolism (H. Chen et al., 2017; Hasegawa, Liu, Tooyama, Murayama, & Nishimura, 2014; Katahira, Nakagiri, Terada, & Furukawa, 2010). In 2006, Fam3c was identified as a key player in TGF-β-induced epithelial-EMT, tumor formation and progression in late stage of carcinoma (Waerner et al., 2006). Since Fam3c shows similarity to the interleukins and it is involved in EMT, it is also called interleukin-like EMT inducer (ILEI).

Figure 7: Amino acid sequence of human, mouse and rat Fam3c.

ILEI was observed to be ubiquitously expressed in all tissues (Pilipenko et al., 2004) and mainly in the most secretory epithelia of several organs: salivary and mammary gland, human pancreas and duodenum (Y. Zhu et al., 2002). In normal tissues, the secreted protein is localized within granule structures in proximity to the nucleus. However, in pathological conditions, such as colorectal cancer (Z. H. Gao et al., 2014) or hepatocellular carcinoma (Lahsnig et al., 2009) an enhanced Fam3c diffuse cytoplasmic staining has been reported. This peculiar localization, together with increased amounts of Fam3c secretion in several malignant tumors, have made Fam3c a good prognostic marker in patients with esophageal squamous cell carcinoma (Y. H. Zhu et al., 2015) and a potential therapeutic target for other cancer types.

Fam3c also participates in the regulation of biological functions in normal tissues. Chen and colleagues demonstrated that, in the liver, Fam3c activates heat shock factor 1 (HSF1) which induces CALM1 transcription and calmodulin (CaM) protein level to activate the phosphatidyl inositol 3-kinase (PI3K)–Akt pathway. The activation of the CaM-Akt pathway represses gluconeogenic and lipogenic gene expression in an insulin and Ca^{2+}-independent manner, contributing to regulate hepatic glucose and lipid metabolism. In the same study, the authors reported that, in obese diabetic mice, Fam3c expression was reduced in the liver. Its hepatic restoration improved insulin resistance, hyperglycemia and fatty liver, leading to a beneficial approach to regulate glucose/lipid metabolism under sever insulin resistance. Furthermore, both *in vitro* and *in vivo*, Fam3c represses the mTOR-SREBP1-FAS lipogenic pathway in hepatocytes, contributing to its beneficial effect on fatty liver (Z. Chen, L. Ding, et al., 2017).

In 2009 a large-scale genome-wide association study performed in a Korean population revealed a correlation between Fam3c and bone mineral density (Cho et al., 2009). Some years later, this correlation was confirmed in a different population by two independent genome-wide association studies (Martinez-Gil et al., 2018; L. S. Zhang et al., 2012). A study published in 2015 to evaluate the role of Fam3c in bone biology generated a Fam3c knock-out (KO) mouse. This mouse showed normal appearance, behavior and fertility but changes in bone morphology and mineral density were observed. In the same KO model, bone marrow cells showed

an increased osteogenic differentiation with a reduced number of trabeculae and decreased breaking strength in the lateral direction of tibiae. Moreover, inactivation of the gene led to increased cortical mineral density, indicating a role of Fam3c in osteoblast differentiation and bone homeostasis (Maatta et al., 2016). One year later, the same group found a correlation between Fam3c and TGF-β1. The latter is a cytokine stored in the human bone matrix that regulates osteoblast differentiation. In a pre-osteoblast murine cell line (MC3T3-E1), TGF-β1 affects osteoblast differentiation by inhibiting the ability of bone morphogenetic protein-2 (BMP-2) to induce MC3T3-E1 mineralization (Spinella-Jaegle et al., 2001). During osteoblast differentiation, intracellular Fam3c and TGF- β1 regulate each other. TGF-β1 induces the expression of Fam3c while Fam3c negatively acts on TGF-β1: the TGF-β1 mRNA levels were markedly decreased in cells overexpressing Fam3c and significantly increased in cells in which Fam3c was silenced upon siRNA treatment (Bendre, Buki, & Maatta, 2017).

As reported by Kraya and colleagues, high levels of Fam3c were detected in serum of high-autophagy melanoma patients. Similar results were observed in vitro from supernatant of high autophagy melanoma cell lines, suggesting Fam3c as a candidate autophagy biomarker in melanoma (Kraya et al., 2015).

In 2014, a correlation between Fam3c and Alzheimer's disease (AD) was also reported. In AD patients, the levels of Fam3c were found to be decreased (Hasegawa et al., 2014). In the same work, the transgenic overexpression of Fam3c in AD model mice markedly decreased the accumulation of amyloid- β peptide (Aβ), a hallmark of AD, and improved memory deficit. Moreover, Fam3c expression levels in mouse brain was reported to change during developmental stages: protein levels peak in the post-natal period and then decline with age (L. Liu, Watanabe, Akatsu, & Nishimura, 2016). The decline of Fam3c expression may cause accumulation of Aβ and eventual development of AD (L. Liu et al., 2016) suggesting Fam3c as plausible target for AD therapy.

Until 2019, nothing was known about the Fam3c receptor. In this contest, a recent study performed in breast cancer stem cells showed that Fam3c acts on the leukemia inhibitory factor (LIF) receptor (LIFR) (Woosley et al., 2019). The binding

of Fam3c to LIFR induces signal transducer and activator of transcription 3 (STAT3) activation through its phosphorylation at Tyrosine 705 (Tyr705), driving both EMT and breast cancer stem cells (BCSC) formation.

1.7 Canonical STAT3 pathway

The signal transducer and activator of transcription (STAT) protein family was initially identified as a family of transcription factors that modulate the expression of a variety of genes involved in the regulation of cell proliferation, differentiation, apoptosis, metastasis, angiogenesis and immune response (Johnston & Grandis, 2011). The STAT family includes seven mammalian STATs: STAT1-4, STAT5a, STAT5b and STAT6, which are activated in response to specific extracellular stimuli through tyrosine phosphorylation-mediated activation, mainly mediated by Janus kinases (JAKs) (Awasthi, Liongue, & Ward, 2021).

The STAT3 gene encodes for an 89 kDa protein of 770 amino acids, composed of six functional domains. The N-terminal domain is involved in higher order complex formation and is followed by a coiled-coiled domain that allows protein-protein interaction. Adjacent to this, there is the DNA binding domain through which STAT3 binds the promoter of specific genes, followed by a linker region and by the Src homology-2 (SH2) domain, which is responsible for STAT3 dimerization. In addition, located at C-terminal domain, there is the transcription activation domain (TAD), where phosphorylation occurs (Zouein et al., 2015). The canonical STAT3 pathway is activated by a large number of extracellular stimuli, including the entire family of Interleukin (IL)-6-type cytokines, comprised of IL-6, IL-11, IL-22, IL-27, IL-31, cardiotrophin 1 (CT-1) ciliary neurotrophic factor (CNTF), cardiotrophin-like cytokine factor 1 (CLCF1), oncostatin M (OSM), leukemia inhibitory factor (LIF) (Garbers et al., 2012; Jones & Jenkins, 2018) and by growth factors including epidermal growth factor (EGF), fibroblast growth factor (FGF) and insulin-like growth factor (IGF) (Lo et al., 2005; Mitsuyama et al., 2007). In non-stimulated cells, STAT3, as other STATs protein, is kept inactive in the cytoplasm. However, upon binding of ligands

to their respective receptors, JAKs are activated and phosphorylate STAT3 at Tyr705, inducing STAT3 dimerization and translocation into the nucleus where it functions as a transcriptional activator. An illustration of the STAT3 signalling pathway is shown in Fig.8.

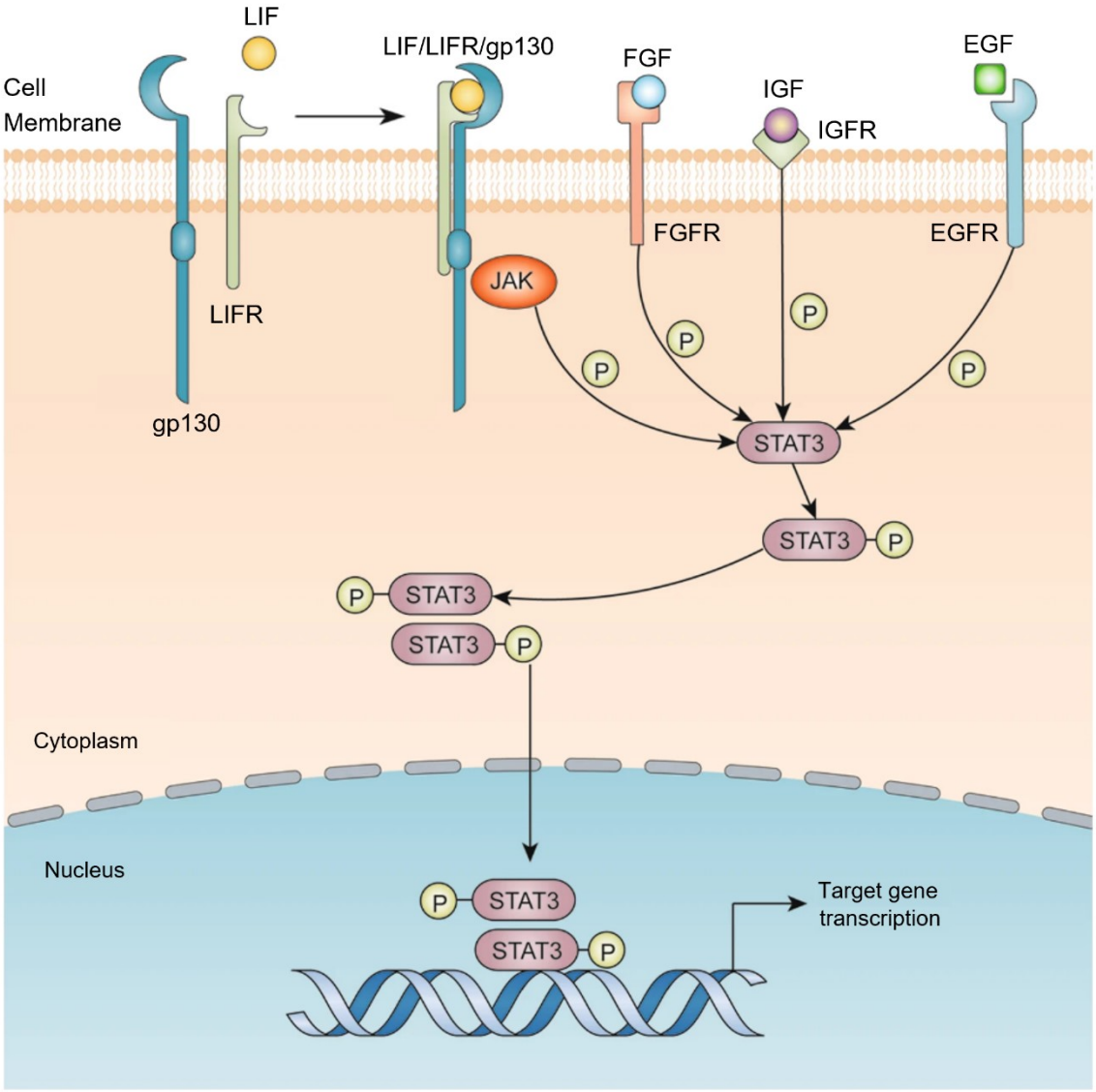

Figure 8: Canonical STAT3 pathway. Activation of the canonical STAT3 pathway is exemplified through the illustration of the LIF receptor. LIF exerts its biological function through two proteins: LIF receptor (LIFR) and gp130. The binding of LIF to LIFR induces its heterodimerization with gp130, resulting in the formation of the LIF/LIFR/gp130 functional complex. This in turn activates the JAK protein, which phosphorylates and activate STAT3. Growth factors such as FGF, IGF and EGF can also phosphorylate STAT3 by binding their respective receptors. Once phosphorylated, STAT3 homodimerizes and translocates into the nucleus where it binds the promoter regions of target genes inducing their transcription. Adapted from: (Ma, Qin, & Li, 2020).

In addition to Tyr705, STAT3 can be phosphorylated at Ser727. The involvement of serine phosphorylation may boost STAT3 activity but is not able to induce DNA binding (Wen & Darnell, 1997; Wen, Zhong, & Darnell, 1995).

While normal cells display transient physiological STAT3 activation, tightly regulated by stimulatory and inhibitory molecules, many cancer cells depend on the constitutive activation of STAT3 for survival and cell transformation (Hu et al., 2015). Although the involvement of STAT3 in cancer is well documented and aberrant regulation of STAT3 is reported in nearly 70% of cancers (Levy & Inghirami, 2006; Turkson & Jove, 2000), STAT3 is a signalling molecule and transcription factor that plays important protective roles in the heart. It participates in mechanisms that contribute to protection against myocardial infarction, fibrosis, hypertrophy, hypertension, myocarditis and diabetic cardiomyopathy, as reviewed by Harhous and colleagues (Harhous, Booz, Ovize, Bidaux, & Kurdi, 2019). During cardiac ischemia, STAT3 is phosphorylated at Tyr705; a further increase in phosphorylation was reported during reperfusion (Fuglesteg et al., 2008; O'Sullivan, Breen, Gallagher, Buggy, & Hurley, 2016). Since STAT3 knockout significantly increase infarct size following ischemia reperfusion (Hilfiker-Kleiner et al., 2004) and multiple evidence already showed a cardioprotective role of STAT3 (Harhous et al., 2019), a possible cardioprotective mechanism exerted by Fam3c may related to STAT3 pathway activation.

2. AIM OF THE THESIS

The work presented in this thesis was aimed to understand the molecular mechanism behind the cardioprotective activity exerted by Fam3c after myocardial infarction in mice. Providing an accurate overview of the Fam3c mechanism of action is of compelling interest in anticipation of the potential translational perspectives of this factor against myocardial infarction. For this purpose, the following specific objectives were pursued:

- Evaluation of apoptosis in primary cardiomyocytes upon Fam3c treatment; the ability of Fam3c to modulate apoptosis was investigated in a doxorubicin model of cardiac damage.
- Involvement of Fam3c in the autophagic pathway (both in immortalized cell line and primary cells).
- Identification of the Fam3c receptor in cardiomyocytes.
- Involvement of the STAT3 pathway in Fam3c biology.
- Investigation on the reciprocal crosstalk between Fam3c and TGF-β signalling.
- Evaluation of Fam3c gene expression upon cardiac damage, both *in vitro* (cryoinjured EHT) and *in vivo* (after myocardial infarction in mice).

3. MATERIALS AND METHODS

3.1 CELL CULTURE METHODS AND ANALYSIS

3.1.1 NIH-3T3 and HEK-293T cell lines

NIH-3T3 murine fibroblasts and human kidney HEK-293T cells were obtained from ATCC (CRL-1658 and CRL-3216 respectively) and grown in Dulbecco's modified Eagle medium (DMEM) + [GlutaMAX-I] + [Pyruvate] 1 g/L D-Glucose (Life Technologies), supplemented with 10% Fetal bovine serum (FBS, Life Technologies), 100 U/ml penicillin and 100 µg/ml streptomycin (Sigma), at 37°C in a humidified 5% CO2 incubator.

3.1.2 Plasmid DNA transfection of HEK-293T cells

HEK-293T cells were transfected using FuGENE® HD as transfection reagent (Promega). The cDNA coding region of mouse Fam3c and GFP was individually cloned, upon PCR amplification with gene specific primers, into the Xho I and Not I sites of the pGi plasmid, a modified version of the pZac2.1, under the control of the CMV IE promoter, see Fig. 5. The optimized ratio of pDNA:lipids was 1:3. Briefly, the recommended amount of plasmid DNA was diluted in Opti-MEM medium (Life Technologies). The proper amount of FuGENE® was added to the mix, which was then vortexed and incubated 15 minutes at room temperature. After the formation of DNA/lipid complexes, the mix was added to cells.

3.1.3 Isolation of murine neonatal cardiomyocytes and cardiac fibroblasts

Primary cardiomyocytes were isolated from heart of neonatal mouse and rats using the Neonatal Heart Dissociation Kit (Miltenyi Biotec) according to the manufacturer's instructions. The purpose of this procedure is to dissociate the neonatal hearts into single-cell suspensions by combining enzymatic degradation with mechanical

dissociation, to disrupt the extracellular matrix, which maintains the structural integrity of the tissue.

Briefly, hearts from 0 to 1-day old CD1 mice or Wistar rats were retrieved and transferred into a 10 cm dish containing PBS; ventricles were separated from both the atria and the great vessels, cut into pieces of ~2 mm diameter and collected in a fresh tube. The digestion mix, obtained by combining the enzyme mix 1 (Enzyme P + Buffer X, previously heated at 37° C for 5 minutes) and the enzyme mix 2 (Buffer Y + Enzyme A + Enzyme D), was transferred together with the harvested tissue into the MACS C Tube where the fragments dissociation was performed. The C Tube was attached onto the sleeve of the gentleMACS™ Dissociator for the mechanical dissociation steps; afterwards the digestion was run at 37°C for 1h.

After the run termination, 7.5 ml of Dulbecco's modified Eagle medium 4.5 g/l glucose (DMEM, Life Technologies), containing 5% FBS, 20 mg/ml vitamin B12 (Sigma), 100 U/ml penicillin and 100 µg/ml streptomycin (Sigma), were added to the Tube. Then, the digested tissue was filtered through a 40 µm, cell strainer (BD Falcon) to remove any remaining large particles from the single-cell suspension. After that, the cell strainer was washed with 3 ml of DMEM and the filtrate was centrifuged at 600 x g for 5 minutes to pellet the cells, which were then resuspended in a Red Blood Cell Lysis Solution to remove erythrocytes and incubated for 2 minutes at room temperature. Then cells were washed twice by centrifugation (PBS solution + Enzyme A) and resuspended in complete medium. The collected cells were pre-plated on 100-mm plastic dishes at 37 °C in 5% CO_2 and humidified atmosphere for 2 hours, to allow the attachment of cardiac fibroblasts. After this pre-plating step, the cardiomyocyte-containing supernatant was collected, and cells were counted. CMs cells were plated at the appropriate density in Primaria 96- well plates (BD Falcon) or Primaria 6-well plates (BD Falcon), according to the experiment. Mouse cardiac fibroblasts adhered on the plate have been cultured for 48 hours in DMEM, 1 g/L D-Glucose (Life Technologies), supplemented with 5% FBS and used to verified endogenous levels of Fam3c.

3.1.4 Doxorubicin and Chloroquine

Doxorubicin hydrochloride (Sigma) was added to the cardiomyocyte culture medium at different final concentration (from 0.5 up to 5.0 μM for 24 hours). Chloroquine diphosphate salt (Sigma) was added at the final concentration of 10 μM for 4 hours.

3.1.5 HEK-293T conditioned media

HEK-293T cells were transfected with GFP or Fam3c coding plasmids. 24 hours post transfection, cells were starved in 0 % FBS until next day. 48 hours post transfection supernatant was recovered, centrifuged 2 minutes at RT and used to treat for 30 minutes neonatal mouse cardiomyocytes previously starved for 6 hours in 0% FBS. For the conditioned media experiment, neonatal mouse cardiomyocytes were carefully washed in PBS and supernatant recovered from control and transfected HEK-293T cells was added on the cells.

3.1.6 Isolation of adult mouse cardiac fibroblasts

Primary murine cardiac fibroblasts were isolated from heart of adult CD1 mice by tissue digestion and mechanical shearing. For this, tissue was minced and then digested for 1 h at 37 °C with a magnetic stirrer using the following enzyme mix: Enzyme A + Enzyme P + Enzyme D, from Neonatal Heart Dissociation Kit (Miltenyi Biotec). Dissociated tissue was passed through a 70 μm cell strainer and centrifuged at 450 × *g*. The resulting cell pellet was resuspended in Dulbecco's modified Eagle medium (DMEM) + [GlutaMAX-I] + [Pyruvate] 1 g/L D-Glucose (Life Technologies), supplemented with 10% Fetal bovine serum (FBS, Life Technologies), 100 U/ml penicillin and 100 μg/ml streptomycin (Sigma), at 37°C in a humidified 5% CO2 incubator, and fibroblasts were allowed to attach on plastic tissue culture plates for 2 hours. Medium was changed, and cells were left to recover overnight in a humidified incubator at 37 °C in 5% CO_2 before being immediately used for experiments. Human recombinant TGF-β1 (Proteintech, HZ-1011) was added at a dose of 25 ng/ml for 48 hours in absence of serum to stimulate fibroblast to myofibroblast transition.

3.1.7 Rat engineered heart tissue

Rat fibrin-based engineered heart tissue (EHT) has been produced by Molecular Cardiology group at ICGEB, Trieste, Italy. To generate fibrin-based EHTs a reconstitution mixture was prepared on ice as follow. Final concentration of cells: 4.1^10^6 cells/mL, 5 mg/mL bovine fibrinogen (Sigma F8630), DMEM 2X (20% DMEM 10x, 20% heat inactivated horse serum [Thermo Fisher 26050-088], 1% penicillin/streptomycin [Thermo Fisher 15140-122]). Casting molds were prepared by adding 1.5 mL 2% agarose in PBS (Invitrogen 15510-027) per well in 24-well culture dishes and placing Teflon spacers inside. After agarose jellification, the spacers were removed (LxWxD 12 x 3 x 4 mm) and silicone post racks were placed onto the dishes with pairs of posts reaching into each casting mold. For each EHT 100 µL reconstitution mix was mixed briefly with 3 µL thrombin (100 U/mL, Sigma Aldrich T7513) and pipetted into the agarose slot. For fibrinogen polymerization, the constructs were placed in a humidified cell culture incubator at 37°C, 7% CO_2 for 2 hours. To allow the removal of the constructs from agarose casting molds, cell culture medium (300 µL) was then added in each well. Racks were transferred to new 24-well cell culture dishes. EHTs were maintained in 37°C, 7% CO_2 humidified cell culture incubator. EHT medium consisted of DMEM (Biochrom F0415), 10% horse serum (Thermo Fisher 26050-088), 1% penicillin/streptomycin (Thermo Fisher 15140-122), insulin (10 µg/mL, Sigma-Aldrich I9278), and aprotinin (33 µg/mL, Sigma Aldrich A1153) and was changed every two days. EHTs were monitored daily and are considered mature approximately 10 days after the development of coherent beating.

3.1.8 Crioinjury model of rat EHT

The Molecular Cardiology group at ICGEB, Trieste, Italy, built a custom-made system to deliver cryoinjury to the middle section of EHTs. Briefly, a 50 ml tube was connected through a copper pipe to a 23G or a 26G needle that was bent to facilitate the contact with the EHTs in a discrete fashion. The tube was filled with liquid nitrogen and the lid was used to direct the flow through the needle, thus creating a cryo-probe. The EHT was placed in contact with the needle, while the liquid nitrogen was flowing, for 1 or 4 seconds and a clear area of freezing could be observed. The

removal of the plunger would determine a stop of the flow through the needle and a rise in temperature that allows to safely detach the EHT. After the procedure, EHTs were placed in complete medium to recover.

3.1.9 AAV vectors

All AAV vectors were produced by the AVU unit at the ICGEB, Trieste, Italy (http://www.icgeb.org/avu-core-facility.html) as described previously (G. P. Gao et al., 2002). Briefly, infectious AAV6 and AAV9 vector particles were generated in HEK-293 cells by co-transfecting each vector plasmid together with the packaging plasmids expressing AAV and adenovirus helper functions, pDP6 (PlasmidFactory). Viral stocks were obtained by $CsCl_2$ gradient centrifugation; rAAV titers, determined by measuring the copy number of viral genomes in pooled, dialyzed gradient fractions were in the range of $1x10^{12}$ to $1x10^{13}$ genome copies per milliliter.
Cardiomyocytes were transduced with AAV6-control (empty vector), AAV6-GFP and AAV6-Fam3c the day after plating using a multiplicity of infection (MOI) of $5x\ 10^4$ viral genomes particles per cell. The day after transduction the medium was changed. The correspondent AAV9 were generated in parallel and used for *in vivo* transduction of cardiac tissue as previously established in the laboratory (3.0×10^{11} and 3.9×10^{12} viral genomes particles per animal).

3.1.10 Immunofluorescence

Primary neonatal mouse and rat cardiomyocytes were fixed with 4% PFA for 10 min, permeabilized with 0.5% Triton X-100 in PBS for 10 min, followed by 1 hr blocking in 2% BSA (Roche). Cells were then stained overnight at 4°C with mouse monoclonal antibody against sarcomeric α-actinin (EA-53, Abcam), rabbit monoclonal antibody against GFP (Ab6556, Abcam), rabbit monoclonal antibody against p-STAT3 (#9131, Cell Signalling) diluted in blocking solution. Cells were washed with PBS-Tween and incubated for 2 hours with the proper secondary anti mouse or anti rabbit antibodies (Invitrogen) conjugated to Alexa Fluor-488 or -594 (Invitrogen). Nuclei were counterstained with Hoechst 33342 (Life Technologies).

3.2 MOLECULAR BIOLOGY PROTOCOLS

3.2.1 Recombinant protein production

Recombinant mouse Fam3c protein (rFam3c) was produced taking of advantage of the Flp-In CHO cell line. Briefly, an expression vector containing His tagged-Fam3c gene sequence (pcDNA 5/FRT) has been integrated into the genome of CHO Flp-In cells via Flp recombinase-mediated DNA recombination at the FRT site (O'Gorman, Fox, & Wahl, 1991). Integration of the expression construct induces Fam3c transcription and confers hygromycin antibiotic resistance to positively select transfected cells. The supernatant of Flip-In Fam3c cells was then collected and the His-tagged Fam3c protein was purified with Ni-NTA agarose beads or Nichel loaded column for larger scale production. Imidazole 0,5 M was used for protein elution. The purified protein was desalted and concentrated using Amikon columns (15 kDa cut-off). Once produced and purified, Coomassie Blue staining and silver staining gels (SDS-PAGE) were exploited to monitor protein purity and concentration.

3.2.2 siRNAs transfection

All siRNAs (siGENOME SMARTpools) were purchased from Dharmacon (GE Healthcare), see table 2. Transfection of human or mouse siRNAs was performed using a standard reverse transfection protocol, with a final siRNA concentration of 50 nM. For experiments performed in 96-well plates, 15 µl of 500 nM siRNAs were transferred to 96 well plates. Transfection reagent, Lipofectamine RNAiMAX Transfection Reagent (0.2 µl per 96-well, Life Technologies) diluted in 35 µl of OPTI-MEM (Life Technologies) was then added to the siRNAs arrayed on 96-well plates and incubated at RT for 30 min. Mouse CMs, suspended in 100 µl antibiotic-free culture medium, were then seeded onto the 96-well plates at 25.000 cells per well and incubated at 37°C, 5% CO2. Transfections performed in 6-well plate format were done using the same procedure but transferring 7 ul from the 20 µM siRNAs stock to each well. 5.7 µl of Lipofectamine RNAiMAX were diluted in 600 µl of OPTI-MEM and then added to siRNAs. 30 min. after, 600.000 neonatal mouse

cardiomyocytes or 600.000 HEK-293T cells per well, resuspended in 2.5 ml of culture medium, were seeded on the transfection reagents in the plate.

Probes	Probe ID
Mouse Lifr	L-040750-00-0010, ON-TARGETplus (16880)
Mouse gp130	L-040007-01-0010, ON-TARGETplus (16195)
Human Lifr	L-008017-01-0005, ON-TARGETplus (3977)

Table 2: List of Dharmacon siRNAs.

3.2.3 RNA extraction

Primary cardiomyocytes seeded onto 6-well were washed twice in PBS and then cells were lysed in 1 ml of TRIzol Reagent (Life Technologies) and incubated for 3 min at RT. Heart sections of CD1 mice were lysate with 1 ml TRIzol and dissociated using MagNA Lyser green beads (Roche) at 6500 rpm for 60 seconds. After this, the heart homogenate was put in 1.5 ml tubes and incubated for 3 minutes at RT. From here the procedure of RNA extraction from primary cells or heart tissue is the same, although specified. 0.2 ml of chloroform per ml of TRIzol was added to cells lysate (or heart homogenate). The tubes were shaken vigorously for 15 s and incubated for 10 min at RT. Samples were then centrifuged at 12,000 x g for 10 min at 4°C. After the centrifugation, the upper aqueous phase, was transferred to a new tube and 0.5 ml isopropanol was added. The tubes were shaken vigorously for 15 s and incubated for 10 min at RT. Samples were then centrifuged at 12,000 x g for 10 min at 4°C. After the centrifugation, the upper aqueous phase was removed and 1 ml of 75% Ethanol was added. Samples were then centrifuged at 12,000 x g for 5 min at 4°C. After the centrifugation, the upper aqueous phase was removed and tubes were then left opened under chemical hood to allow the complete evaporation of the EtOH. Finally, 40 µl or 70 µl of RNase-free water were added to resuspend the RNA obtained from primary neonatal cardiomyocytes or from heart tissue, respectively.

3.2.4 Reverse Transcription PCR

Total RNA concentration was measured using Nanodrop 1000 (Thermo Scientific). 1 µg of total RNA was used for cDNA synthesis. The RNA was diluted into 11 µl of RNAse-free water and treated with 2 µl of RNAse-free DNAse I (Roche), 1.5 µl of Buffer 10x (Roche) and 0.5 µl of PRI (Roche) for 15 min, at RT. DNAse I was then inactivated by rising the temperature to 75°C for 5 min. After DNAse digestion, RNA was incubated with 2 µl of 10 mM dNTPs (Promega), 2 µl of random primers (Invitrogen, 1:20 dilution) and 5 µl of RNAse-free water for 5 min at 65°C. Reverse transcription was performed by using 8 µl of 5x First-Strand Buffer (Invitrogen), 4 µl of DTT 0,1 M (Invitrogen) and 2 µl of PRI (Protector Rnase Inhibitor). The samples were incubated for 2 min at 37°C and then 2 µl of Maloney murine leukemia virus reverse transcriptase (M-MLV RT, Invitrogen) was added. The reverse transcription reaction was performed as follows: 10 min at 25°C (RT activation), 50 min at 37°C (RT reaction), 15 min at 72°C (RT inactivation).

3.2.5 Real-Time PCR

Quantification of gene expression was performed by quantitative real-time PCR using the TaqMan assay (Applied Biosystems). GAPDH or HPRT was used as housekeeping gene for normalization. cDNA (1 µl) was treated with 10 µl of TaqMan mix (Qiagen – not correct), 8 µl of RNAse-free water, 1 µl of the TaqMan probes and analysed by using a standard TaqMan protocol using a CFX96TM Real-Time System (Bio-Rad) (95°C for 10 min, followed by 40 cycles of 95°C for 15 sec and 60°C for 1 min), according to the manufacturer's recommendations. A list of the used probes is summarized in the table 3.

Target	Probe ID
Mouse Fam3c	Mm00506842_m1
Mouse Hprt	Mm01545399_m1
Mouse Gapdh	Mm99999915_g1
Mouse TGF-β	Mm01178820_m1
Rat Fam3c	Rn01500658_m1
Rat Hprt	Rn01527840_m1

Table 3: List TaqMan probes.

3.2.6 Western blotting

Protein expression was evaluated by western-blot: cells were washed in ice-cold PBS and proteins were harvested in RIPA buffer (20 mM Tris-HCl, pH 7.4; 150 mM NaCl; 1 mM EDTA; 1 mM EGTA; 0.5% NaDOC; 0.5% NP-40 and 0.1% SDS) containing Protease Inhibitor Cocktail Tablets (Roche), Phosphatase Inhibitor Cocktail (Thermo Fisher Scientific) and 1 mM PMSF. Cell lysates were then sonicated with Bioruptor (Diaagenode) for 30 minutes using 3 pulses of 10 minutes each. After this step, samples were centrifuged at 13.000 rpm for 10 minutes at 4°C, the supernatants were collected and protein concentration was determined by the Bradford method (Bio-Rad Laboratories). Protein extract (30-50 µg) was resolved on 10-12% SDS-PAGE and transferred to nitrocellulose membranes (GE Healthcare). Immunoblots were blocked in 5% BSA in TBS-Tween (50 mM Tris-HCl, pH 7.4; 200 mM NaCl; and 0.1% Tween 20), overnight at 4°C and incubated for 2 hours at room temperature with the primary antibodies for LC3B (1:2000; L7543 Sigma-Aldrich), Fam3c (1:1000; Ab72182 abcam), pSTAT3 (1:1000; 9131 Cell Signalling), STAT3 (1:1000; 9132 Cell Signalling), Lifr (1:300; sc-515337 Santa Cruz) and gp130 (1:1000; 3732 Cell Signalling) and then for 1 hr at room

temperature with the HPR-conjugated goat anti-rabbit secondary antibody (1:5000; 31460 Thermo Fisher Scientific) or goat anti-mouse secondary antibody (1:3000; 62-6520 Thermo Fisher Scientific). To evaluate autophagy in vitro, LC3-II protein levels were analysed 48 hours after HEK-293T cells transfection or 72 hours after cardiomyocytes AAV6 vector transduction (MOI: $5x10^4$ vg per cell). Cells were analysed under basal condition or upon 4 hours of treatment with the lysosomotropic alkalinizing agent chloroquine (10 μM Sigma-Aldrich), to inhibit autophagosome-lysosome fusion and analyze endogenous autophagic flux. To evaluate the ability of Fam3c to modulate the STAT3 pathway, primary mouse CMs were starved for 6 hours in 0 % FBS and treated for 30 min with home-made produced rFam3c (500 ng/ml). To evaluate the ability of TGF-β to modulate Fam3c protein expression, NIH-3T3 cells and adult mouse cardiac fibroblasts were treated with rTGF-β (25 ng/ml, 48 hours, Proteintech, HZ-1011).

In all the experiments, as a gel loading control, the membranes were incubated for 1 hours with conjugated mouse monoclonal anti-β-Actin (1:20000; A3854 Sigma-Aldrich). Proteins were detected by enhanced chemiluminescence (GE Healthcare). Band intensity was analysed using the ImageJ software.

3.2.7 TUNEL and caspase 3/7 assays for apoptosis detection

TUNEL assay was performed on primary neonatal mouse cardiomyocytes treated with doxorubicin (1.0 μM, 24 hours). Cells were fixed with 4% paraformaldehyde (PFA) and permeabilized with 0.5% Triton X-100 for 10 min. After 1 h in blocking solution (2% BSA) at room temperature, primary neonatal mouse cardiomyocytes were stained with the primary antibody against sarcomeric a-actinin (1:200, EA-53 Abcam) for 2 hours. Alexa Fluor-488 donkey anti-mouse (1:500, A-21202 Thermo Fisher Scientific) was used as a secondary antibody. Apoptotic cells were visualized by in situ cell death detection kit, TMR red (Roche Diagnostics), according to the manufacturer's instructions. Nuclei were stained with Hoechst 33342 (1:5000 in PBS, Life Technologies).

Apoptosis for mouse and rat neonatal cardiomyocytes treated with doxorubicin (1.0 and 1.5 μM, respectively) was evaluated 24 h after treatment using the Caspase-Glo 3/7 Assay System (Promega) according to the protocol provided by the supplier.

3.3 ANIMAL MODEL

3.3.1 Myocardial infarction

Myocardial infarction was produced in adult CD1 mice (8–12 weeks old), by permanent left anterior descending (LAD) coronary artery ligation. Briefly, mice were anesthetized with an intraperitoneal injection of ketamine and xylazine, endotracheally intubated and placed on a rodent ventilator. Body temperature was maintained at 37°C on a heating pad. Beating heart was accessed via a left thoracotomy. After removing the pericardium, a descending branch of the LAD coronary artery was visualized with a stereomicroscope (Leica) and occluded with a nylon suture. Ligation was confirmed by the whitening of a region of the left ventricle, immediately post-ligation. To evaluate heart function and morphology, transthoracic two-dimensional echocardiography was performed in mice anaesthetized with isoflurane keeping the heart rate over 450 bpm, using a Vevo 2100 Ultrasound (Visual Sonics) equipped with a MS550D 22–50 MHz linear array solid-state transducer. B-mode multi- planar tracings in parasternal short and long axis views (modified Simpson's method) were used to measure left ventricular anterior and posterior wall thickness, septum thickness and left ventricular internal diameter at end-systole and end-diastole, which were used to calculate left ventricular fractional shortening and ejection fraction. For all infarcted animals, echocardiography was performed after 15, 30 and 60 days and the hearts were collected at 60 days after infarction (n=8 per group).

3.4 STATISTICAL ANALYSIS

Data are presented as mean ± standard error of the mean (SEM). Statistical analysis was performed by using a commercially available software package (GraphPad Prism). Student's T-test was used to compare two groups while one-way ANOVA with Tukey post-hoc test has been used to compare means of two or more samples to determine whether there is statistical evidence that the associated population

means are significantly different. Analysis of morphological and functional measurements at different time points among groups was performed using two-way ANOVA for repeated measurements, followed by pairwise post hoc analysis.

For all the statistical analyses, significance was accepted at $p<0.05$.

4. RESULTS

4.1 Fam3c preserves heart function upon myocardial infarction

The FunSel in vivo screening led to the identification of novel cardioprotective factors without a priori knowledge on their function. The cardioprotective activity of the selected hits, including Fam3c, was further evaluated in a mouse model of myocardial infarction (MI). In brief, mice underwent permanent coronary artery ligation and then received an intramyocardial injection of AAV serotype 9 vector (AAV) expressing Fam3c or a control empty vector (AAV9-control) into the infarct border zone (Fig. 9A). Echocardiographic follow up of infarcted animals for 2 months clearly demonstrated that Fam3c overexpression was effective in maintaining cardiac function and preventing post-MI pathological remodelling compared to control animals (Ruozi et al., 2022). Indeed, as shown in Fig. 9B and 9C, Fam3c significantly preserved left ventricular (LV) ejection fraction and reduced LV-end diastolic volume post infarction. Moreover, histological analysis performed on heart section after animal sacrifice showed a significant reduction of the LV infarct size and preservation of LV mass in the AAV9-Fam3c treated mice (Fig. 9D and 9E). The Masson trichrome stain performed 60 days after MI highlighted a strong reduction of the fibrotic scar in the infarct zone.

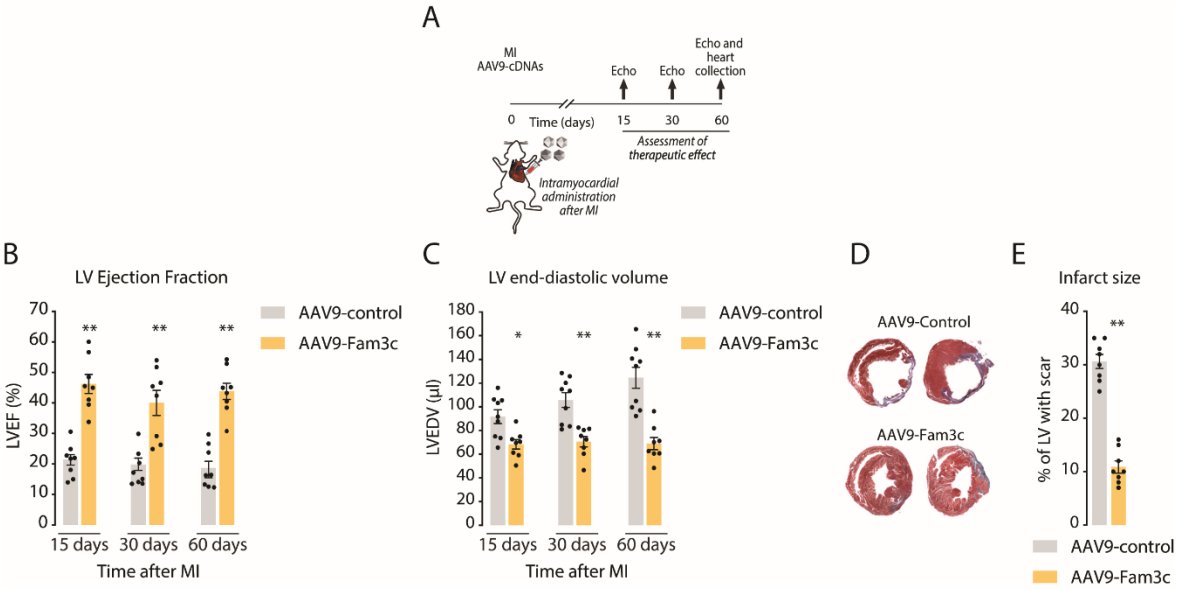

Figure 9: Cardioprotective effect of Fam3c after myocardial infarction. (**A**) Experimental protocol. Mice were intramyocardially injected with AAV9-control or AAV9-Fam3c (1.0×10^{11} vg per animal). (**B** and **C**) Echocardiographic analysis of infarcted mice at 15, 30, and 60 days after MI and vector administration. Data are means ± SEM (N = 8 per group); *p < 0.05 and **p < 0.01 versus AAV9-Control; two-way ANOVA with Bonferroni post hoc correction. LVEF, left ventricular ejection fraction; LVEDV, left ventricular end-diastolic volume. (**D**) Representative images of Masson's trichrome stains of heart transverse sections 60 days after MI and vector injection. Fibrotic areas are stained blue. (**E**) Quantification of left ventricle (LV) infarct size. Data are means ± SEM (N = 8 per group); **p < 0.01 versus AAV9-Control; one-way ANOVA. Adapted from (Ruozi et al., 2022).

4.2 In vitro model of cardiotoxicity induced by doxorubicin

Although Fam3c dramatically protects cardiac tissue after MI, the molecular mechanisms behind its cardioprotective activity are still unknown. To understand the Fam3c mechanism of action in cardiomyocytes, we developed an in vitro model of cardiotoxicity. We took advantage of the well-known cardiotoxic agent doxorubicin to mimic cardiac damage in mouse primary cardiomyocytes. Doxorubicin is a widely used effective chemotherapeutic agent. However, its use is limited due to its adverse effect on cardiac cells in the short and the long term (Slordal & Spigset, 2006; Youssef & Links, 2005).

Primary neonatal mouse CMs were treated for 24 hours with increasing doses of doxorubicin (from 0.5 up to 5 µM). CM morphological shape and viability were

monitored over time. As shown in Fig. 10A, doxorubicin treatment induced a massive shrinkage of the sarcomeric cardiac structure in a dose dependent manner. A significant decrease in the number of CMs was reported when cells were treated with the highest doses tested, from 3 up to 5 µM (Fig. 10A and 10B).

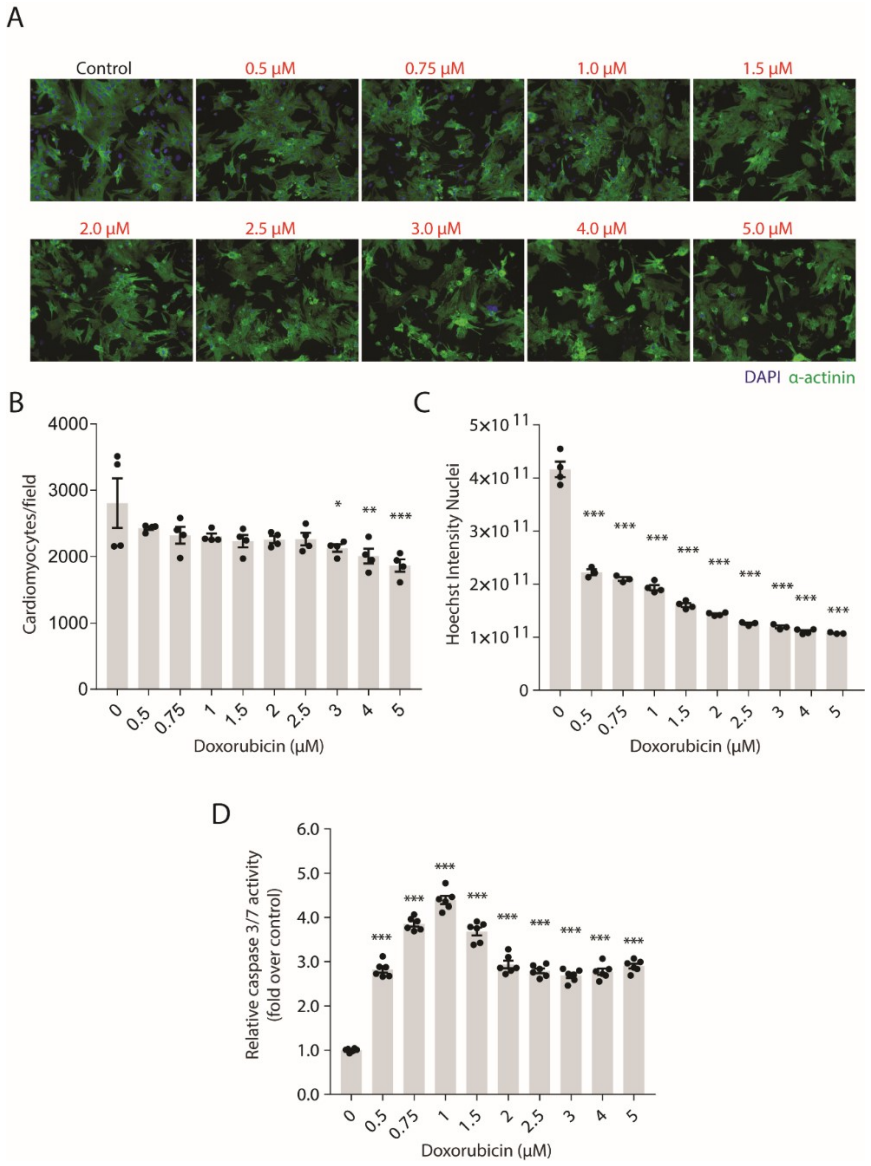

Figure 10: Cardiotoxic effect of doxorubicin. (**A**) Representative images of neonatal mouse CMs treated for 24 hours with increasing doses of doxorubicin as indicated (α-actinin-DAPI). (**B** and **C**) The graphs report the number of CMs per well and the intensity of DAPI nuclear staining, respectively. Data are mean ± SEM (15 field per well, n=4 technical replicates); *p<0.05, **p<0.01, ***p<0.001; one-way ANOVA. (**D**) Activation of caspase 3/7 in neonatal mouse CMs treated for 24 hours with increasing doses of doxorubicin as indicated. Data are mean ± SEM (n=6 technical replicates); ***p<0.001; one-way ANOVA.

Noteworthy, doxorubicin treatment induced a massive decrease in nuclear DAPI staining (Fig. 10A and 10C), possible due to its ability to intercalate into DNA inducing DNA damage (S. Zhang et al., 2012).

Since doxorubicin is known to cause cardiotoxicity mainly through the upregulation of death receptor-mediated apoptosis (L. Zhao & Zhang, 2017), cleaved caspase 3/7 activity was evaluated in the drug-treated CMs. Starting from the lowest concentration, doxorubicin treatment induced a significant increase of caspase 3/7, with the highest activation at 1 μM, (Fig. 10D). Thus, this condition was selected for the subsequent investigations in vitro using Fam3c.

4.3 Evaluation of the most effective AAV serotype for the transduction of primary neonatal cardiomyocytes

All the previous in vivo experiments were performed with AAV vector serotype 9 (Ruozi et al., 2022). For our ex vivo experiments, we assessed the relative efficiency of AAV9 and AAV6 in transducing isolated neonatal CMs. As shown by the immunofluorescence images in Figs. 11A and 11B, AAV6-GFP outperformed AAV9-GFP in transducing cultured mouse CMs. Transduction efficiency was dose dependent (relative quantification in Fig. 11C) and the most effective Multiplicity of Infection (MOI) was $5.0*10^4$ viral genomes (vg) per cell, without cellular toxicity. Similar results were also obtained when transducing rat CMs, as shown in Figs. 11D and 10E and by the relative quantification in Fig. 11F.

For this reason, all the in vitro experiments that required gene overexpression in CMs were performed transducing cells with AAV serotype 6 vectors (MOI $5.0*10^4$ vg per cell).

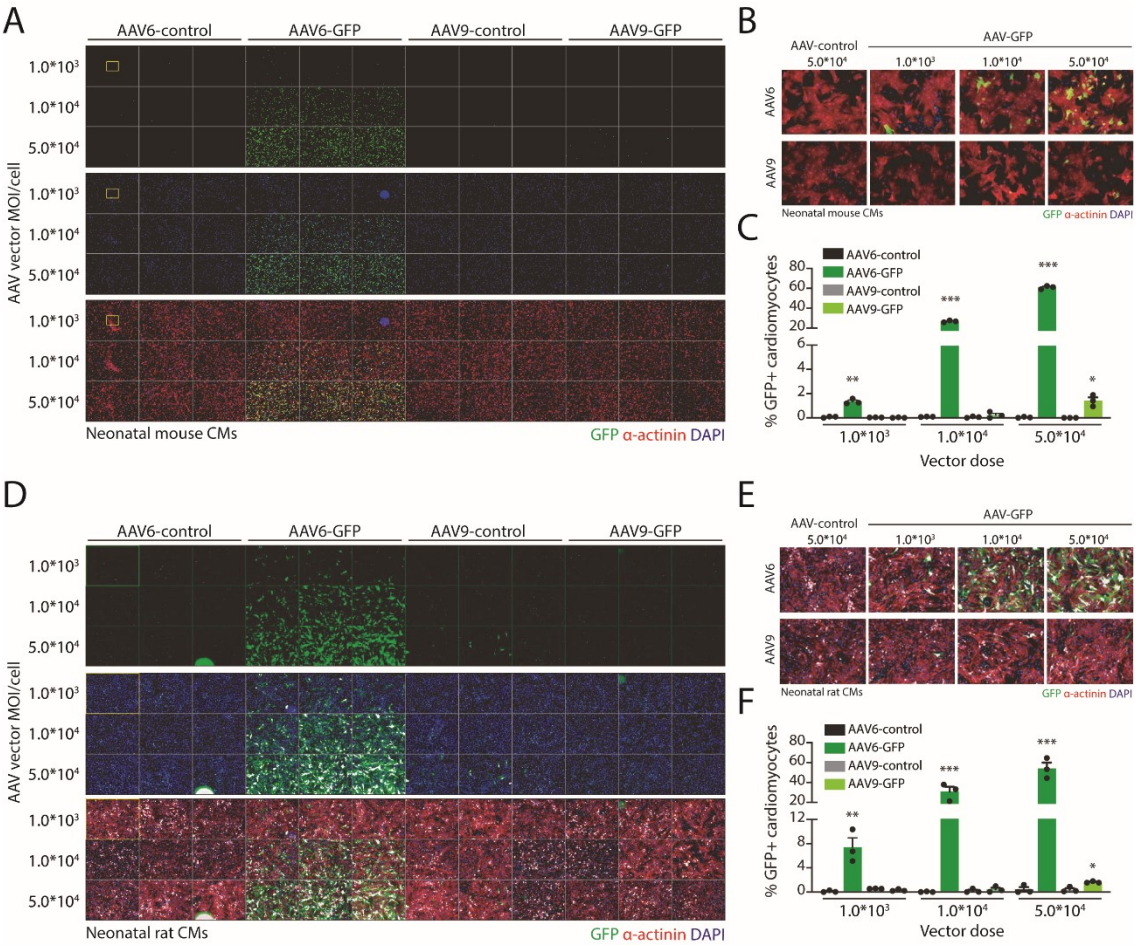

Figure 11: Evaluation of AAV serotype efficacy in mouse and rat cardiomyocytes. (**A**) Representative images of neonatal mouse CMs transduced with increasing MOIs ($1.0*10^3$, $1.0*10^4$, $5.0*10^4$ vg/cell) of AAV6 or AAV9 vectors as indicated. (**B**) Higher magnification of transduced mouse CMs with the indicated vectors and MOIs, (GFP-α-actinin-DAPI). (**C**) Quantification of transduced mouse CMs. The graph reports the number of GFP-positive (green), α-actinin-positive (red) cells 72 hr after transduction. (**D-E-F**) Representative images and relative quantification of AAV transduced rat CMs, as in A-C, (GFP-α-actinin-DAPI). Data are mean ± SEM (15 field per well, n=3 technical replicates); *p<0.05, **p<0.01, ***p<0.001; one-way ANOVA.

4.4 Fam3c is an anti-apoptotic agent

The cardioprotective effect of Fam3c was tested in the optimized doxorubicin-induced model of cardiac damage. Neonatal mouse CMs were transduced with AAV6-control or AAV6-Fam3c and then treated for 24 hours with 1 μM doxorubicin.

Effective Fam3c overexpression was confirmed 72 hours after AAV treatment at both mRNA and protein levels (Fig. 12A and Fig. 12B).

As shown in Fig. 12C and in line with Fig. 10D, 1 μM doxorubicin-exposed CMs showed a significant increase in caspase 3/7 activation, highlighting apoptotic events. Caspase activation was significantly reduced when CMs were pre-treated with AAV6-Fam3c, both in mouse and rat cells (Fig. 12C and 12D respectively).

Doxorubicin treatment significantly increased cardiac apoptosis also when we measured as the number of TUNEL-positive cells (Bernard et al., 2011; Gupta et al., 2018). AAV6-control CMs treated with doxorubicin showed a significant increase of TUNEL positive cells in comparison with untreated cells, while Fam3c overexpression rescued this pathological effect (Fig. 12E, and 12F). Together, these results suggest that CM-specific Fam3c expression preserves cardiac function and structure by preventing apoptosis in CMs. Prevention of apoptosis was most likely the reason why FunSel had originally selected these factors in vivo.

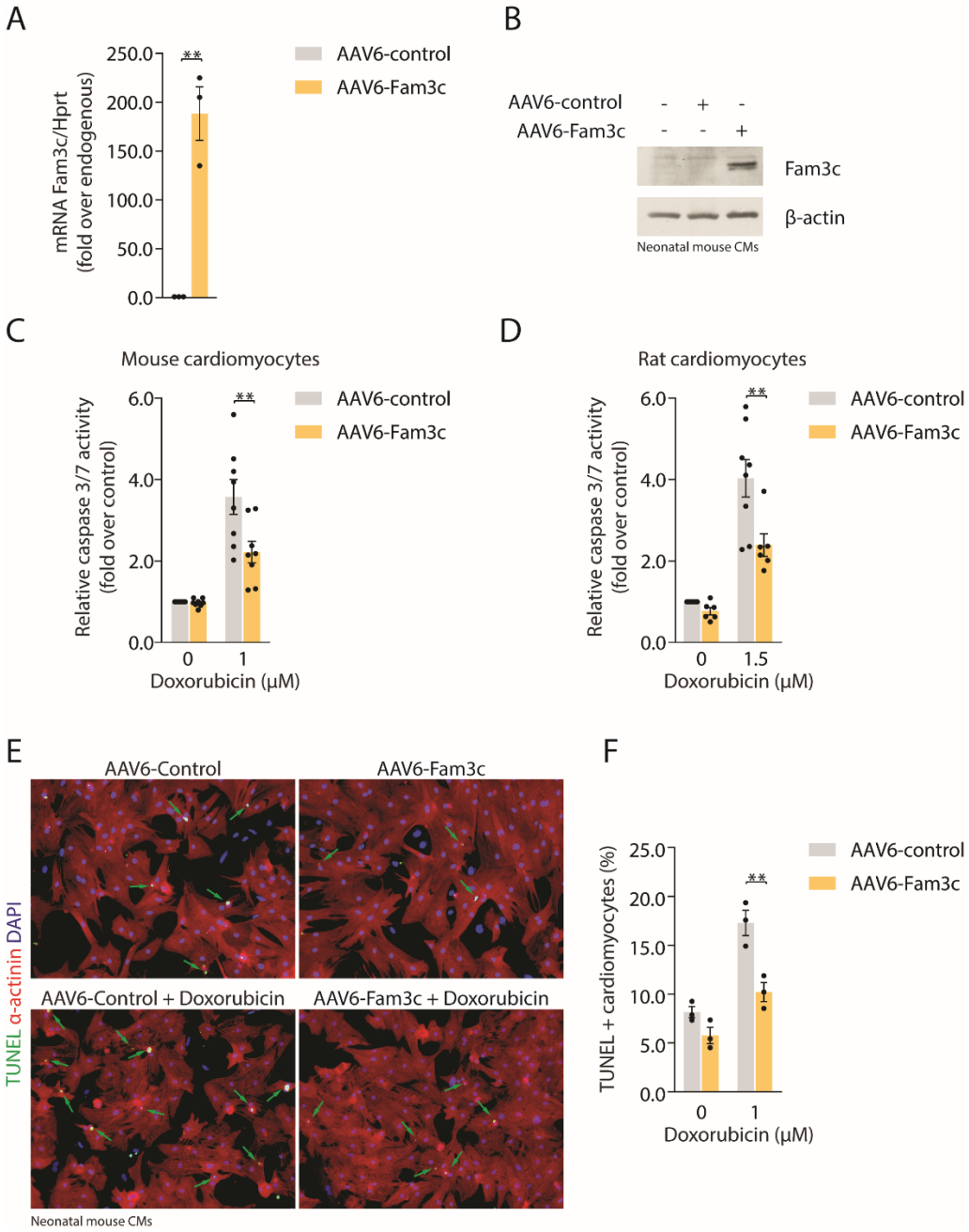

Figure 12: Fam3c exerts anti-apoptotic effect on cardiomyocytes. (**A**) Levels of Fam3c transgene expression 72 after AAV6 transduction of neonatal mouse CMs. Quantification of transgene expression was obtained by qPCR. Data are mean ± SEM (n=3 biological experiments); **p<0.01; t-test. (**B**) Representative western blot showing expression of Fam3c 72 hours after AAV6 transduction of neonatal mouse CMs (representative image of 3 different biological replicates). (**C** and **D**) Evaluation of caspase 3/7 activation in neonatal mouse and rat CMs transduced with AAV6-control or AAV6-Fam3c in the presence of doxorubicin (1-1.5 μM, 24 hours). Data are mean ± SEM (n=8 biological experiments of 6 technical replicates each); **p<0.01; one-way ANOVA. (**E**) TUNEL staining of neonatal mouse CMs transduced with AAV6-control or AAV6-Fam3c in the presence of doxorubicin (1 μM, 24 hours), TUNEL-α-actinin-DAPI. Green arrows indicate apoptotic cells. (**F**) The graph reports the number of TUNEL (green), α-actinin-positive (red) CMs (% of total). Data are mean ± SEM (15 field per well, n=3 biological replicates of 3 technical replicates each); *p<0.05, **p<0.01; one-way ANOVA.

4.5 Fam3c promotes cardioprotective autophagy

As already discussed in paragraph 1.2.4, the recycle of dysfunctional and damaged organelles by autophagy becomes essential in an environment poor of nutrients and oxygen such as the myocardium after MI or after doxorubicin-induced stress. For this reason, we investigated the role of Fam3c in the stimulation of cardioprotective autophagy.

As a first approach, we evaluated whether Fam3c induces autophagy in the well-studied mammalian Human Embryonic Kidney 293 cell line (HEK-293T) by monitoring LC3 protein levels. When HEK-293T cells were transfected with a Fam3c or GFP coding plasmid, we found that Fam3c promoted evident increase of the translipidated form of LC3 (LC3-II), a well-established marker of autophagosome formation (Fig. 13A and 13B).

An increase of LC3-II can be observed in the presence of either increased autophagy or impaired autophagic flux. To avoid data misinterpretation, it has been previously demonstrated that the administration of an autophagic inhibitor, such as chloroquine or bafilomycin, is fundamental to distinguish between these two possibilities (D. L. Li et al., 2016). When HEK-293T cells were treated with chloroquine (10 μM, 4 hours) after transfection, we still observed a significant increase of LC3-II in Fam3c transfected cells, in comparison with GFP-treated cells (Fig. 13A and 13B). This result clearly indicates that the LC3-II accumulation mediated by Fam3c is a real induction of autophagy rather than an impairment of autophagic flux.

Moving to neonatal mouse CMs, we demonstrated that AAV6-mediated Fam3c overexpression increases LC3-II levels in both the absence and presence of chloroquine (Fig. 13C and 13D), thus confirming the ability of Fam3c to also increase autophagic flux in primary CMs.

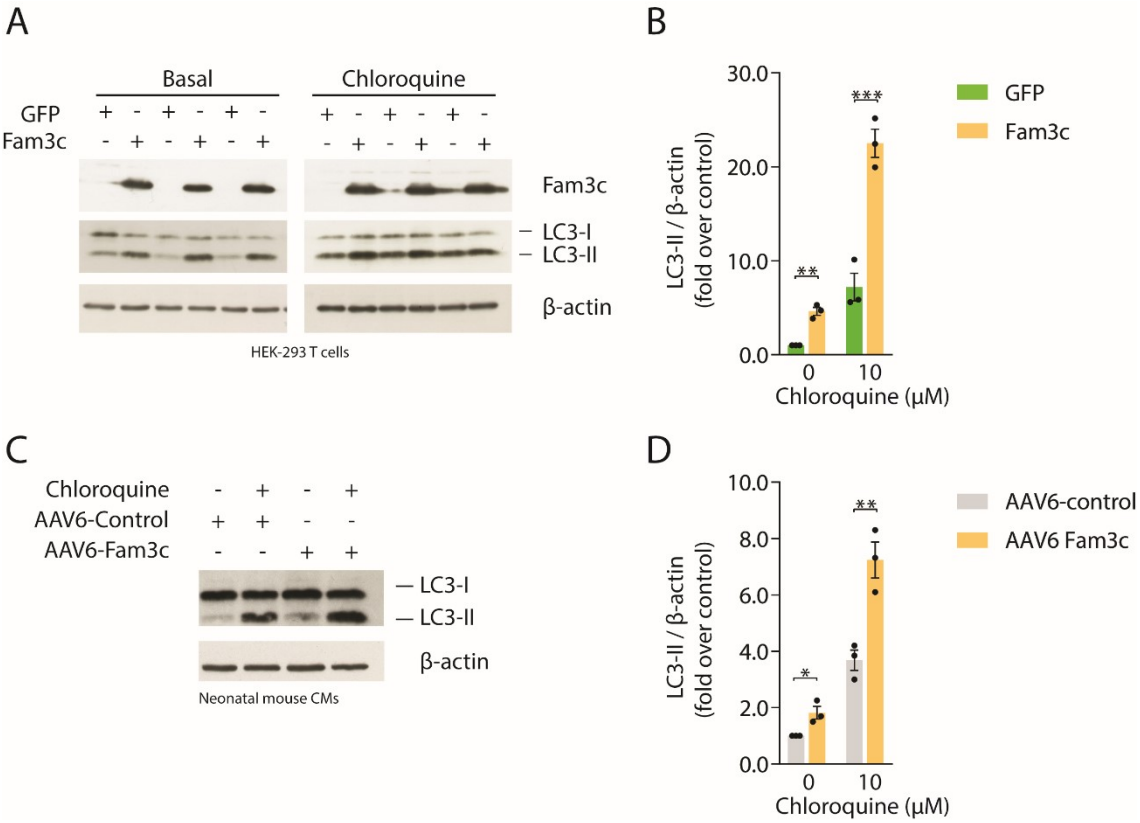

Figure 13: Fam3c induces autophagy in HEK-293T cells and primary cardiomyocytes. (**A** and **B**) Representative western blot and relative densitometric quantification showing LC3 lipidation (conversion from LC3-I to LC3-II) in HEK-293T cells. Cells were treated for 48 hours with GFP or Fam3c coding plasmid in the presence or absence of the lysosomotropic alkalizing agent chloroquine (10 μM, 4 hours). Data are mean ± SEM (n=3 biological replicates); **p<0.01, ***p<0.001; one-way ANOVA. (**C** and **D**) Representative western blot and relative densitometric quantification of LC3 lipidation in neonatal mouse CMs. Cells were treated for 72 hours with indicated vectors in the presence or absence of chloroquine (10 μM, 4 hours). Data are mean ± SEM (n=3 biological replicates); **p<0.01, ***p<0.001; one-way ANOVA.

4.6 Fam3c cardioprotective action is partially mediated by the STAT3 pathway

Until 2019, no information was available on the Fam3c receptor(s). Recently, it has been shown that Fam3c can interact with LIFR to activate the STAT3 pathway in breast cancer stem cells (Woosley et al., 2019). Since STAT3 it is a well-known cardioprotective factor (Fuglesteg et al., 2008) (O'Sullivan et al., 2016), we

investigated whether the ability of Fam3c to activate STAT3 and its downstream cascade was also maintained also CMs.

We transfected HEK-293T cells with a GFP or a Fam3c coding plasmid (Fig. 14A) and, 48 hours post transfections we collected both cell lysate and supernatants to verify Fam3c protein expression and secretion (Fig. 14B). Conditioned media from untransfected, GFP or Fam3c transfected HEK-293T cells was then used to treat mouse CMs (30 minutes) to evaluate the level of activated STAT3. As shown in Fig. 14C and 14D, mouse CMs treated with Fam3c-conditioned media showed a significant STAT3 activation, shown as phosphorylation at Tyrosine 705 residue (Darnell, Kerr, & Stark, 1994).

Since the use of conditioned media does not allow a proper dose-response study, we decided to move to the use of a Fam3c recombinant protein. In house-made murine recombinant Fam3c protein (rFam3c) was produced by taking advantage of the Flp-in CHO cell line. The full-length cDNA of Fam3c was tagged with a Histidine (His) tag at the C terminus of the protein (after removal of the stop codon) and cloned into the pcDNA 5/FRT plasmid. A stable Fam3c cell line was generated in Flp-In CHO cells exploiting a co-transfection with a Flippase. The His-tagged protein was detected by direct Western Blot analysis in both lysate and medium. Concentrated supernatant was used for affinity protein purification using a Nickel based column; rFam3c purity was confirmed by Coomassie blue and silver staining gels (Fig. 14E). As shown in Fig. 14F, we tested the effect of rFam3c in mouse CMs and, in line with what observed with Fam3c-conditioned media treatment, we observed activation of STAT3.

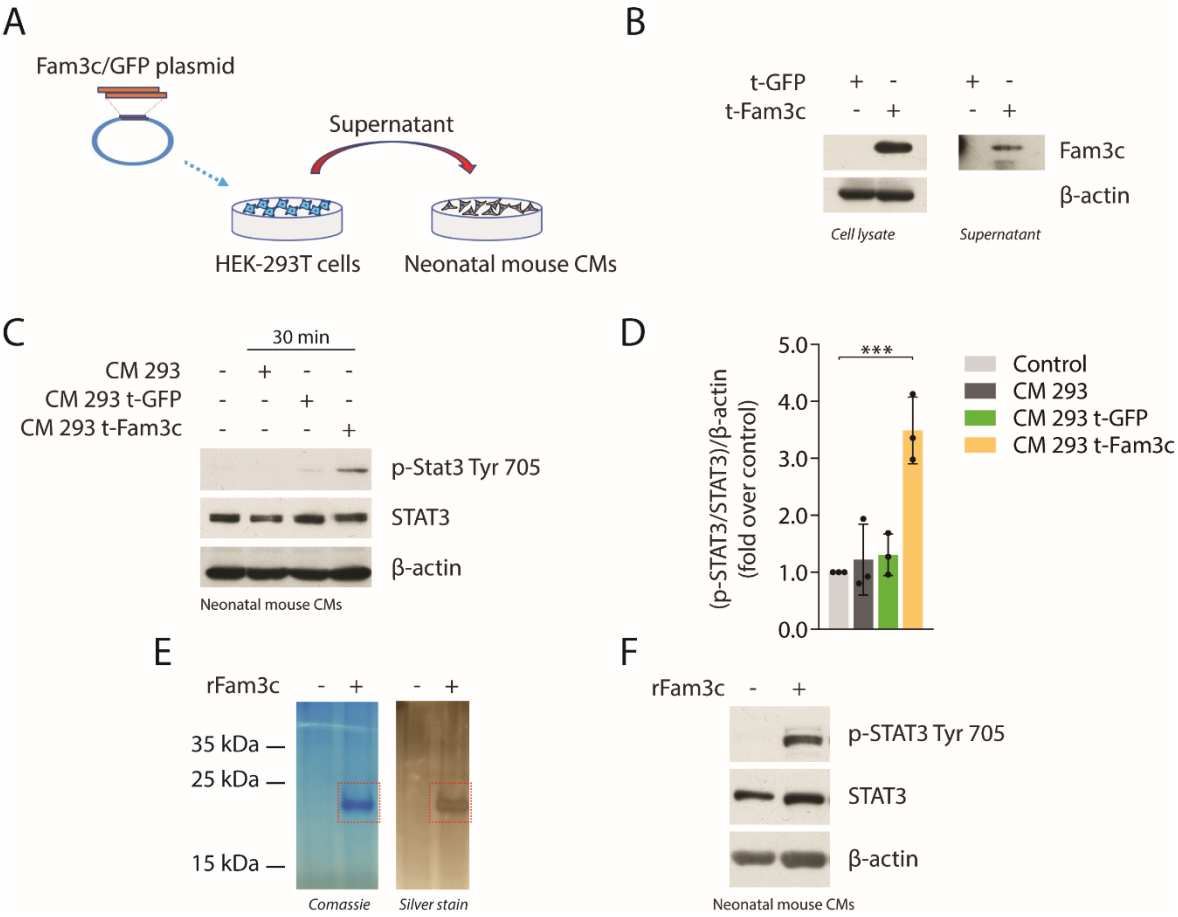

Figure 14: Fam3c activates STAT3 pathway. (**A**) Schematic representation of neonatal mouse cardiomyocytes treated with conditioned media (CM) from HEK-293T cells. Briefly, 48 hours post transfection, CM from HEK-293T cells was collected and used to treat mouse CMs previously starved for 6 hours in the absence of FBS. (**B**) Representative western blot showing Fam3c protein expression in whole cell lysate and supernatant (representative image of 3 different biological replicates). (**C** and **D**): Representative western blot and relative densitometric quantification of neonatal mouse CMs treated for 30 minutes with CM of untreated, GFP or Fam3c transfected HEK-293T cells. Data are mean ± SEM (n=3 biological replicates); ***p<0.001; one-way ANOVA. (**E**) Coomassie and silver staining gel of home-made produced recombinant Fam3c protein (rFam3c). (**F**) Representative western blot of neonatal mouse CMs treated for 30 minutes with rFam3c (representative image of 3 different biological replicates).

4.7 Fam3c selectively activates STAT3 in cardiomyocytes through the Leukemia Inhibitory Factor receptor complex

To date, the only work that correlates Fam3c to cardiac biology is the one from our laboratory (Ruozi et al., 2022). Since the previous study on the Fam3c-STAT3 axis were performed by Woosley et al. in breast cancer stem cells (Woosley et al., 2019), we investigated whether Fam3c could also activate the STAT3 pathway through the Leukemia Inhibitory Factor-receptor complex in CMs. Since the main Lifr ligand is a cytokine that exerts its action through the heterodimerization of gp130 and Lifr (Giese et al., 2005), neonatal mouse CMs were treated with rFam3c in the presence or absence of both siRNAs against Lifr and gp130. Effective Lifr and gp130 knockdown was verified by western blot analysis (Fig. 15A and 15B, respectively). As shown in Fig. 15C, rFam3c treatment induced a strong STAT3 activation that was abolished knocking down Lifr (Fig. 15C and 15D). A similar result was obtained in CMs treated with rFam3c in the presence of the siRNA against gp130 (Fig. 15E and 15F). These results confirmed that Fam3c also activates STAT3 through the Leukemia Inhibitory Factor-receptor complex in CMs.

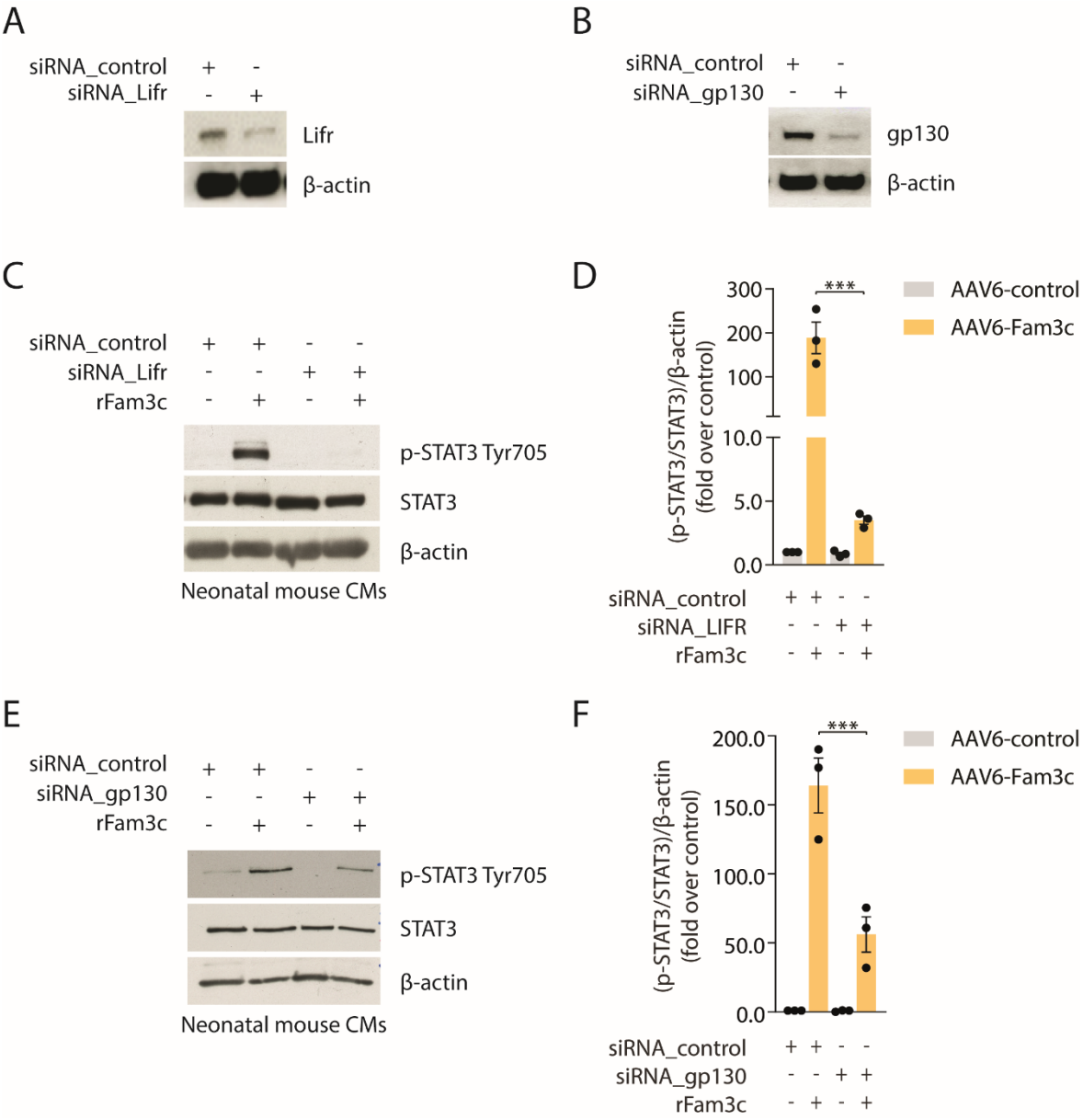

Figure 15: Fam3c activates STAT3 through Leukemia Inhibitory Factor Receptor complex. (**A** and **B**) Representative western blot showing reduced Lifr and gp130 protein expression respectively, 72 hours after siRNA knockdown in neonatal mouse CMs. (**C** and **D**) Representative western blot and relative densitometric quantification of neonatal mouse CMs treated with recombinant Fam3c (rFam3c) after Lifr knockdown. (**E** and **F**) Representative western blot and relative densitometric quantification of neonatal mouse CMs treated with rFam3c after gp130 knockdown. Data are mean ± SEM (n=3 biological replicates); ***p<0.001; one-way ANOVA.

Primary neonatal mouse CMs isolation is a technically challenging process. After heart muscle dissociation, CMs are the main cell population purified (approximately 85-90%, data not shown), however cardiac fibroblasts could also be present, thus challenging the interpretation of western blot analysis using a total cell lysate.

To better understand whether STAT3 activation driven by Fam3c is cardiomyocyte- fibroblast- or both cell type-specific, we moved to an immunofluorescence approach in which it is easier to discriminate each cell type through specific cell markers. As shown in Fig. 16A, CMs were easily identified using sarcomeric α-actinin as a cardiac marker. In line with the western blot analysis, immunofluorescence images confirmed the rFam3c ability to activate STAT3 in a Lifr-gp130 dependent manner (Fig. 16A). Moreover, we also proved that all STAT3 phosphorylation events triggered by rFam3c are within CMs (Fig. 16A and relative quantification in Fig. 16B and 16C) and not in non-CM cells.

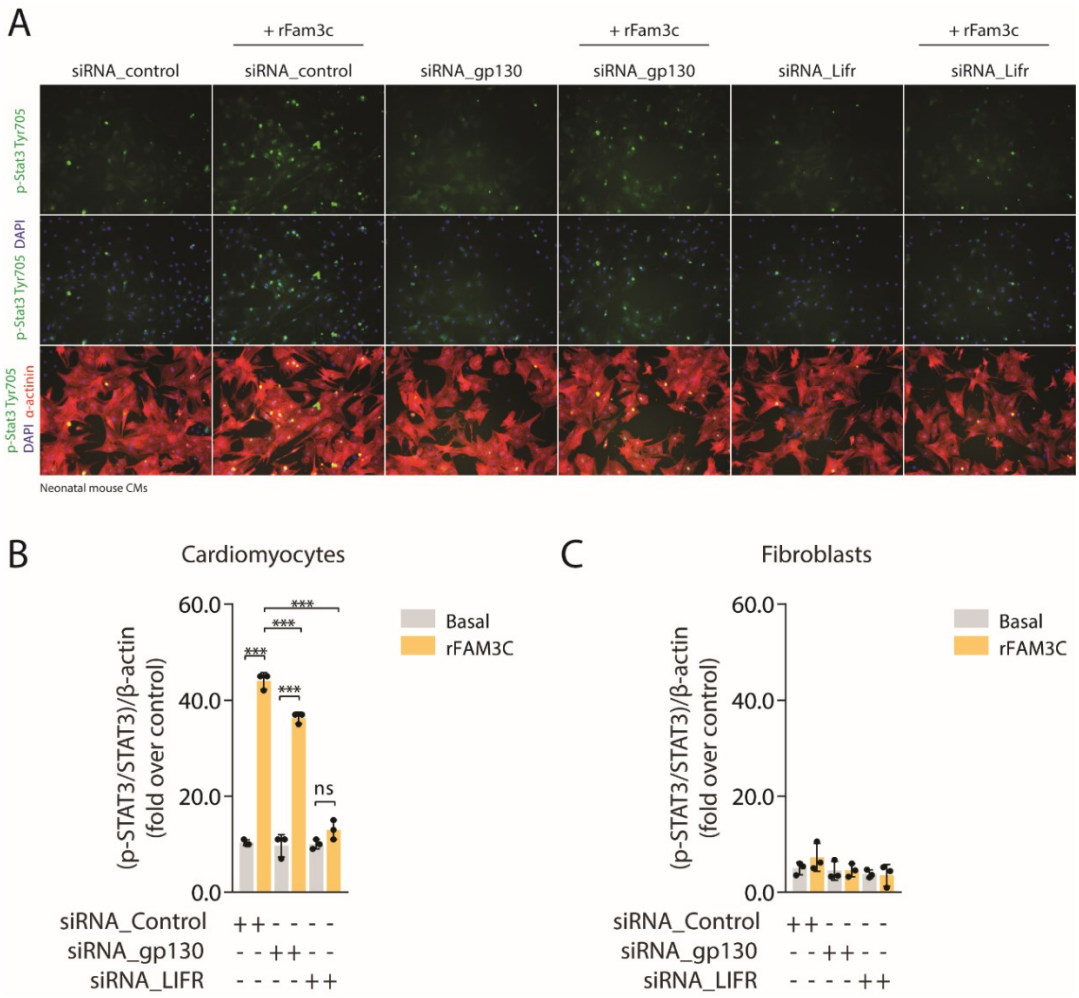

Figure 16: Fam3c activates STAT3 selectively in cardiomyocytes through Leukemia Inhibitory Factor receptor complex. (**A**) Representative immunofluorescence images of neonatal mouse CMs treated with rFam3c for 30 minutes in the presence of control siRNA, siRNA targeting gp130 or Lifr, p-STAT3-α-actinin-DAPI. (**B** and **C**) Quantification of p-STAT3-positive (nuclear green), α-actinin-positive (red) cardiomyocytes and p-STAT3-positive (nuclear green), α-actinin-negative cardiac fibroblasts, respectively. Data are mean ± SEM (15 field per well, n=3 technical replicates); ***p<0.001; one-way ANOVA.

4.8 Fam3c induced autophagy is not mediated by LIFR

Our previous experiments showed that Fam3c induces autophagy in both primary neonatal CMs and HEK-293T cells, suggesting a possible conserved mechanism of action in different cell types. We initially speculated on the possibility that Fam3c-mediated autophagy could be induced, at least partially, through the activation of the STAT3 pathway. To verify this possibility, HEK-293T cells were transfected with GFP or Fam3c coding plasmid in the presence or absence of the siRNA targeting Lifr. As shown in Fig. 17A, Fam3c induced autophagy through a massive conversion of LC3-II both in the presence or absence of the anti- Lifr siRNA (Fig. 17A and 17B). These data clearly indicate that Fam3c-induced autophagy is not mediated by STAT3 activation.

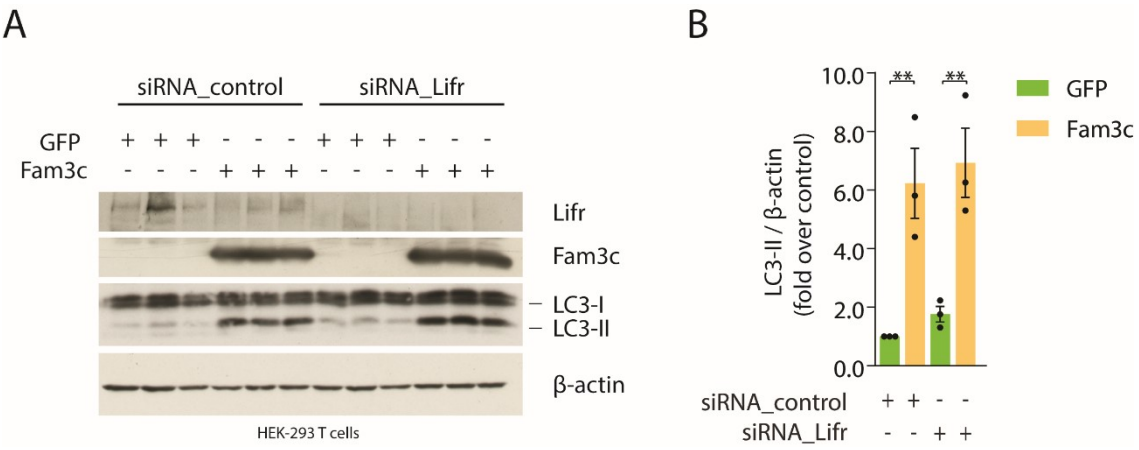

Figure 17: Fam3c induces autophagy in a LIFR independent way. (**A** and **B**) Representative western blot and relative densitometric quantification showing LC3 lipidation of HEK-293T cells transfected for 48 hours with GFP or Fam3c coding plasmid in the presence or absence of siRNA against Lifr. Data are mean ± SEM (n=3 biological replicates); ***p<0.001; one-way ANOVA.

4.9 Fam3c expression in cardiac fibroblasts and its modulation by Transforming Growth Factor β (TGF- β)

All the previous experiments were focused on CMs as the main cell population of interest. However, due to the growing evidence on the essential contribution of

fibroblasts on scar remodelling and cardiac function, we also decided to investigate the effect of Fam3c on cardiac FBs. First, we evaluated the basal expression level of Fam3c in FBs in comparison to CMs. As shown by real time-PCR in Figs. 18A and 18B, Fam3c is more expressed in cardiac FBs than in CMs, when normalizing over either endogenous glyceraldehyde phosphate dehydrogenase (Gapdh) or hypoxanthine guanine phosphoribosyl-transferase (Hprt).

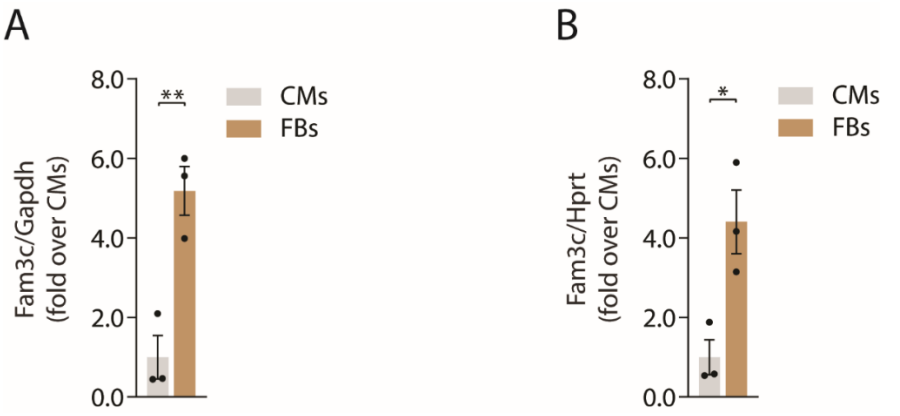

Figure 18: Fam3c is more expressed in cardiac fibroblasts than cardiomyocytes. (**A** and **B**) Endogenous Fam3c mRNA levels in neonatal mouse cardiomyocytes (CMs) and neonatal cardiac fibroblasts (FBs) normalized over endogenous glyceraldehyde phosphate dehydrogenase (Gapdh) or hypoxanthine guanine phosphoribosyl-transferase (Hprt), respectively. Data are mean ± SEM (n=3 biological replicates); *p<0.05, **p<0.01, t-test.

Cardiac FBs play an important role after MI, especially upon TGF-β signalling upregulation. The activation of TGF-β is protective against ischemic myocardial damage during the early phase after MI, however, its beneficial effects are lost if its expression is sustained, thereby leading to cardiac pathological remodelling and scarring (Ikeuchi et al., 2004).

A correlation between Fam3c and TGF-β has already been reported in other cellular models. A few studies have demonstrated that TGF-β treatment increases Fam3c expression in different cell types, mainly in tumor tissues (Chaudhury et al., 2010; Noguchi et al., 2017; X. Zhao et al., 2018). To date, however, there is no evidence on conserved mechanisms in cardiac cells.

Speculating about a possible correlation between Fam3c and TGF-β in cardiac cells, we decided to co-culture CMs and FBs and treat these cells with a concentration of

recombinant TGF-β known to promote cardiomyocyte hypertrophy and cardiac fibroblast activation (Lijnen, Petrov, Rumilla, & Fagard, 2003; Schultz Jel et al., 2002). For this purpose, rat neonatal CMs and FBs were co-cultured at a ratio 1:3; CMs were stained with the specific cardiac marker Troponin. As shown in Fig. 19A and in the relative quantification (Figs. 19B and 19C), TGF-β stimulation for 48 hours induced both CM hypertrophy and activation of FBs, the latter seen as an increase of smooth muscle alpha-actinin (α-SMA) (N. G. Frangogiannis, Michael, & Entman, 2000).

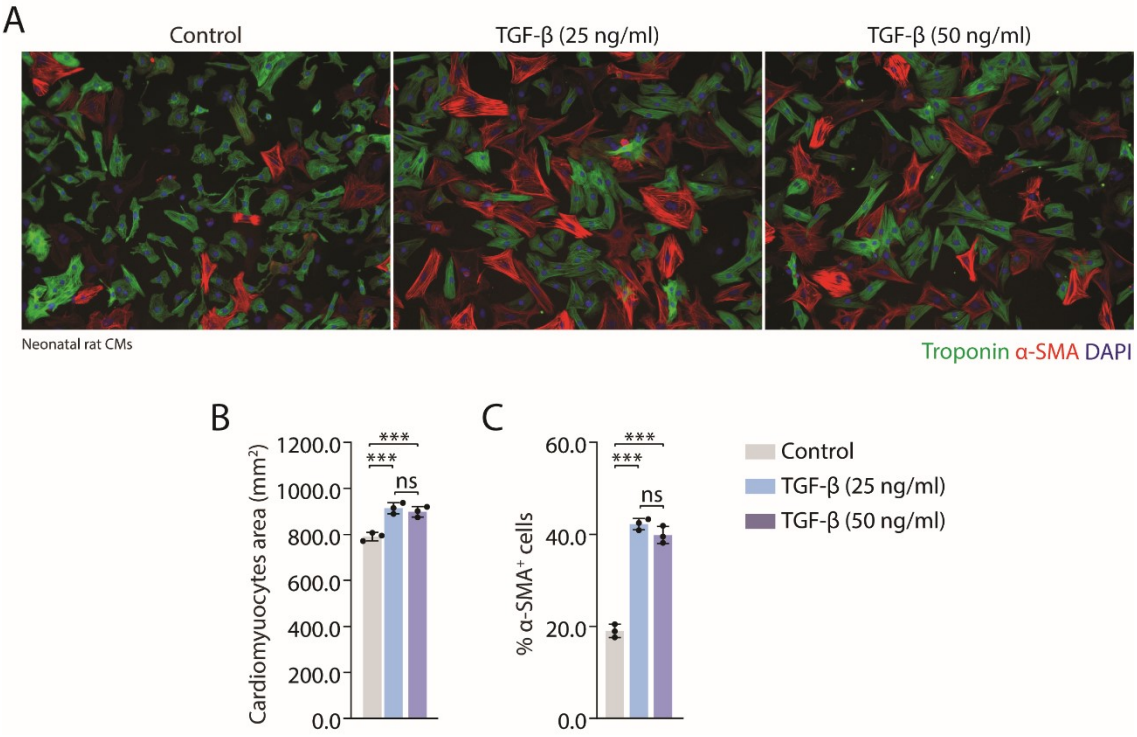

Figure 19: TGF-β induces cardiac hypertrophy and fibroblast activation. (**A**) Representative immunofluorescence images of neonatal rat CMs and FBs starved in 0.1% FBS and treated with TGF-β (25-50 ng/ml, 48 hours), Troponin-α-SMA-DAPI. (**B** and **C**) Quantification of CM area (Troponin -positive cells) and α-SMA positive cells, respectively. Data are mean ± SEM (9 fields per well, n=3 technical replicates); ***p<0.001; one-way ANOVA.

Since fibroblasts are the major targets of TGF-β signalling in the heart (N. Frangogiannis, 2020), we investigated whether TGF-β directly modulated the Fam3c expression level in NIH-3T3 fibroblasts and in primary adult mouse cardiac fibroblasts. No significant difference was found between 25 ng/ml and 50 ng/ml TGF-β treatment in the induction of either cardiac hypertrophy or fibroblast activation

(Fig. 19A). Therefore, we selected the lowest concentration for the subsequent experiments.

When NIH-3T3 fibroblasts were treated with TGF-β for 48 hours, an increase of intracellular and secreted Fam3c protein was observed (Fig. 20A and Fig. 20B, respectively). A similar effect on Fam3c was also observed in adult mouse cardiac FBs when treated with TGF-β (Fig. 20C).

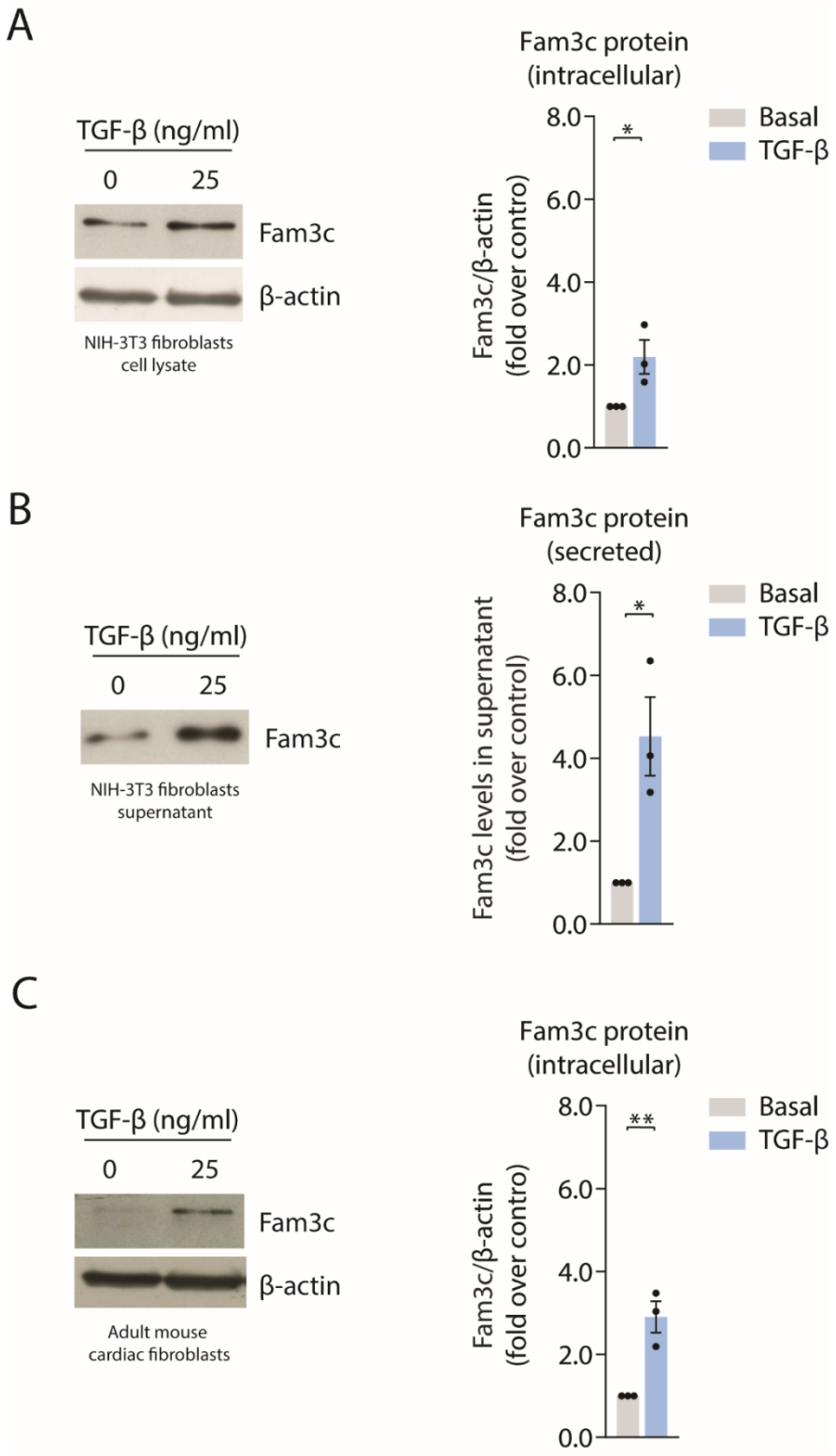

Figure 20: Transforming Growth Factor β (TGF-β) increases Fam3c protein levels. (**A** and **B**) Representative western blots and relative densitometric quantification showing increased level of intracellular and secreted Fam3c protein in NIH-3T3 fibroblasts treated with TGF-β (25 ng/ml, 48 hours). (**C**): Representative western blot and relative densitometric quantification showing increased level of intracellular Fam3c in adult mouse CMs treated with TGF-β (25 ng/ml, 48 hours). Data are mean ± SEM (n= 3 biological replicates); *p<0.05, **p<0.01, t-test.

Since the sustained TGF-β signalling activation after MI is deleterious for the heart by promoting FB proliferation and enhancing the fibrotic response, we investigated whether Fam3c could regulate activation of the TGF-β signalling pathway. Neonatal mouse CMs were treated with AAV6-Fam3c or a control vector; Fam3c transgene expression was verified by qPCR. We observed that Fam3c overexpression did not promote TGF-β transcription in vitro. We further proved this observation also in vivo in adult CD1 mice that were intramyocardially injected with AAV9-Fam3c at two different MOIs (Figs. 21C and Fig. 21D).

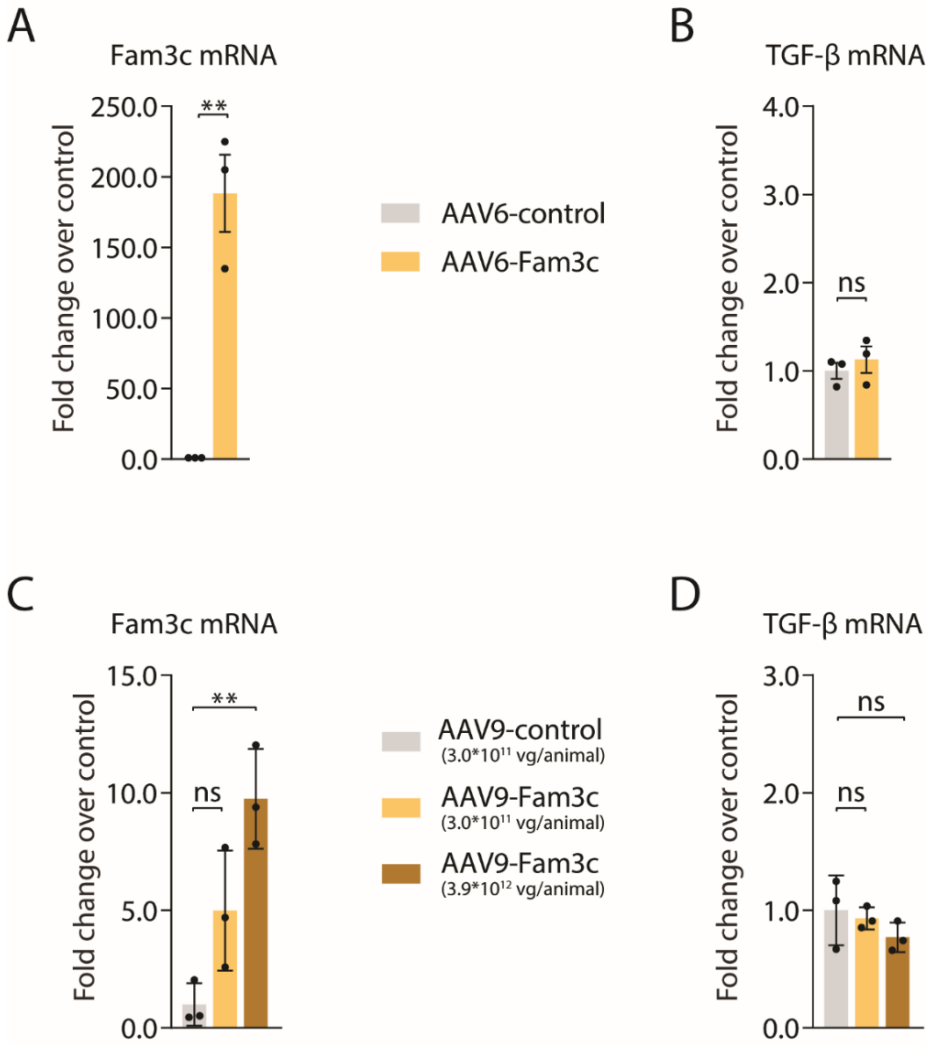

Figure 21: Fam3c does not affect TGF-β expression. (**A**) Fam3c transgene expression 72 hours post AAV6-Fam3c administration in neonatal mouse CMs. (**B**) Endogenous level of TGF-β expression 72 hours post AAV6-Fam3c in neonatal mouse CMs. Data are mean ± SEM (n=3 biological replicates); **p<0.01, t-test. (**C**) Levels of Fam3c transgene expression upon AAV9-Fam3c intracardiac delivery in CD1 mice at different MOIs, as indicated. (**D**) Endogenous levels of TGF-β expression upon AAV9-Fam3c intracardiac delivery in CD1 mice at different MOIs, as indicated. Data are mean ± SEM (n=3 biological replicates); **p<0.01, one-way ANOVA.

4.10 Fam3c is upregulated upon cardiac injury

As TGF-β levels change early after MI (Sanders et al., 2016), we wondered whether Fam3c levels could also change after cardiac injury. For this purpose, we took advantage of the possibility of engineering cardiac tissue in the laboratory. Cardiac tissue engineering aims to reproduce as accurately as possible the function and biology of cardiac muscle, during development or maturity, health or disease (Montero et al., 2020). In collaboration with the Molecular Cardiology Unit at ICGEB, using rat CMs and following a fibrin casting method originally developed by the Thomas Eschenhagen laboratory in Hamburg (Hansen et al., 2010) we generated engineered heart tissue (EHT) to mimic the beating heart in 3D. In addition to basal conditions, we also induced a damage in the 3D tissue by cryoinjury, a well-established in vivo model that partially mimics MI (Gonzalez-Rosa & Mercader, 2012). In this model, cryoinjury generates an extended injury border zone that exhibits classic markers of remodelling found in surviving cardiac tissue at the edge of a MI (Strungs et al., 2013). Mature EHT were generated and, 10 days after the development of synchronous beating, were injured with liquid nitrogen (Fig. 22A). 24 hours after injury, the force of contraction (which was calculating by analysing the displacement of silicon post on which EHTs are anchored) was significantly impaired. This reduction become substantial after 7 days, when a decrease of 50% was observed with no recovery of contractile activity (data not shown). We then performed a time course analysis by collecting EHTs at different time points after cryoinjury to analyse the expression levels of Fam3c. We found a significant increase of Fam3c expression 3 days post injury (Fig. 22B) in comparison to uninjured EHT.

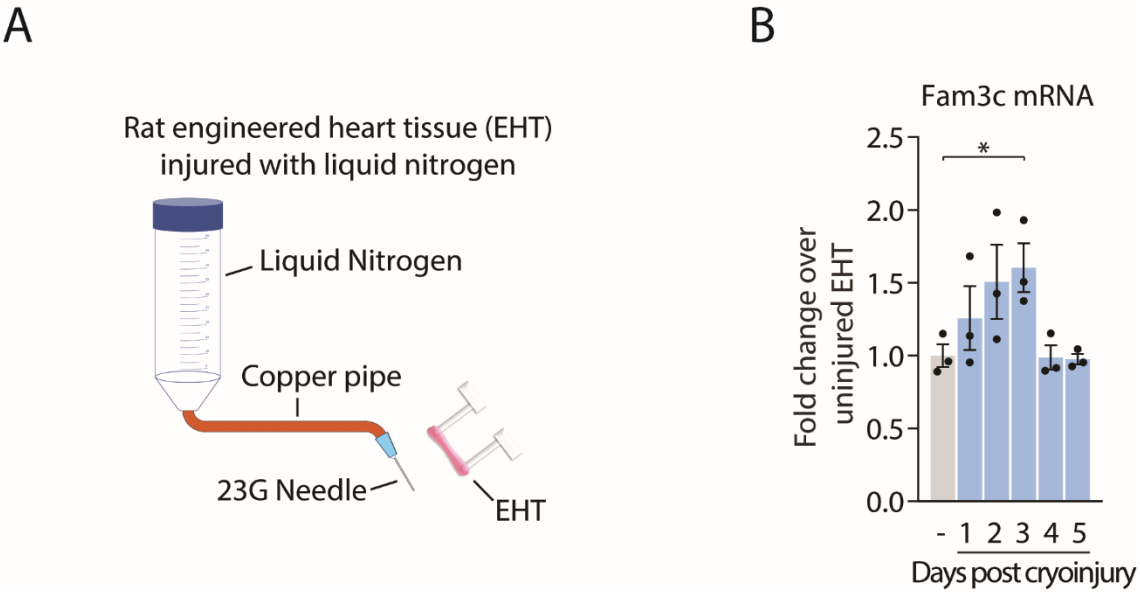

Figure 22: Fam3c levels increase in cryoinjured Engineered Heart Tissue (EHT). (**A**) Schematic representation of rat EHT injured with liquid nitrogen. (**B**) Endogenous Fam3c mRNA levels at different time points after cryoinjury. Data are mean ± SEM (n=3 biological replicates); *p<0.01, one-way ANOVA.

Starting from this in vitro evidence of Fam3c activation after injury, we moved to an in vivo mouse model of MI induced by the permanent ligation of left descendent coronary artery, as in the previous FunSel experiments that led to the identification of Fam3c as a cardioprotective agent. After MI, we performed a time course study by sacrificing the animals for a gene expression analysis at different time points. Total RNA was extracted from the collected left ventricle free walls (Fig. 23A) and TGF-β and Fam3c expression was analysed.

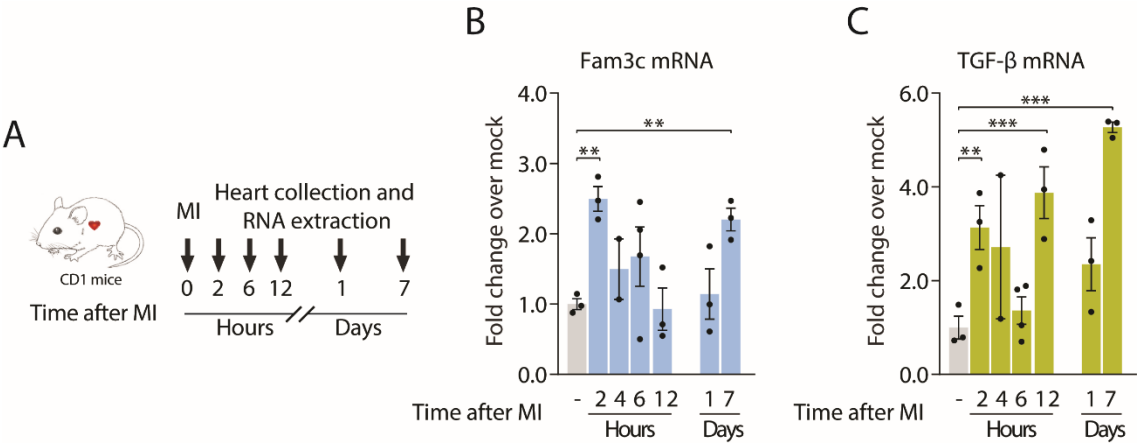

Figure 23: Fam3c is upregulated after myocardial infarction. (**A**) Experimental protocol: myocardial infarction (MI) was induced in CD1 mice by permanent ligation of the left descendent coronary artery. Mice were sacrificed at different times (from hours to days) after MI and RNA was extracted from the collected left ventricular tissue. (**B** and **C**) Fam3c and TGF-β mRNA levels were monitored after MI. Data are mean ± SEM (n=3 per time point, three samples per animal); **p<0.01, ***p<0.001; one-way ANOVA.

As shown in Fig. 23B, Fam3c mRNA levels were significantly upregulated post MI. Monitoring TGF-β levels, we found a significant increase of its transcript with a peak at day 7 post MI (Fig. 23C), in line with previous studies (Sanders et al., 2016). Noteworthy, a superimposable trend was observed for Fam3c, consistent with the conclusion that its expression is regulated by the upstream activation of the TGF-β pathway. The endogenous Fam3c upregulation after injury could reveals a new, endogenous cardioprotective mechanism to counteract cardiac damage.

5. DISCUSSION

Despite the extensive effort made in developing therapies against cardiac dysfunction, treatment of myocardial infarction or other forms of cardiac damage has not significantly evolved over the last several decades. While the available medical, surgical and support device therapies have profoundly modified the natural history of cardiovascular conditions, an increasing number of patients who survive the acute event of MI inevitably progress towards heart failure (Heusch & Gersh, 2017). Prognosis of advanced heart failure remains grim, with 50% of patients dying withing 5 years from diagnosis (Roger et al., 2012).

A main problem behind the massive impact of cardiac disease on human health is the inability of the adult mammal cardiac tissue to regenerate after injury. Unlike lower vertebrates that have the ability to regenerate the heart when this is damaged (Poss, Wilson, & Keating, 2002; Witman, Murtuza, Davis, Arner, & Morrison, 2011), mammals show a cardiac regenerative ability limited to the fetal stage, with a very rapid decline within the first week after birth (Porrello et al., 2011). The human CMs turnover has been estimated to be ~0.04% in the first year after birth and ~0.01% per year in the adult life, according to studies based on radiocarbon dating (Alkass et al., 2015; Bergmann et al., 2009; Bergmann et al., 2015). The evidence of limited CM renewal in adulthood mammal heart and its negative impact after MI has encouraged the scientific community to try and counteract cardiac cell loss with a pro-regenerative approach. Several groups have attempted to push adult CM re-entry into the cell cycle, for example by using microRNAs (miRNAs) (F. Gao et al., 2019), small interfering RNA (siRNAs) targeting cell-cycle regulatory proteins (Chen et al., 2018) or components of the signal transduction pathways that are known to regulate cardiomyocyte proliferation [(the Hippo, Notch and Wnt/beta-catenin pathways - reviewed in ref. (Cannata, Ali, Sinagra, & Giacca, 2020; Giacca, 2020). For example, as far as microRNAs are concerned, a strong pro-proliferative effect was achieved in a mouse model of MI by viral gene delivery of miRNAs (has-miR199a-3p, has-miR-590-3p, miR-106b-25) (Eulalio et al., 2012; Raso et al., 2021) or trough lipid emulsion delivery of synthetic miR302-367 (Tian et al., 2015). Recent

evidence has shown that the intramyocardial administration of the pro-proliferative miR199a-3p in infarcted pig results in effective tissue renewal with improved heart function (Gabisonia et al., 2019). Although these data put the basis of new attractive regenerative approaches, cardiac regeneration by the stimulation of the endogenous capacity of cardiomyocyte to proliferate is still in infancy and needs to overcome significant translational challenges.

An alternative to remuscularise the damaged myocardium is through cell therapy. Putative stem cell therapy of various derivation has been tested for over a decade for their presumed regenerative potential. However, to date no evidence exists that any stem cell for the heart exists and can be used for regenerative purposes (Chien et al., 2019; Eschenhagen et al., 2017). Cardiomyocytes can be generated from embryonic stem cells or induced pluripotent stem cells and can be either injected into the heart as cell suspensions (Chong et al., 2014; Y. W. Liu et al., 2018), or after formation of engineered myocardial tissue (Tiburcy et al., 2017; Weinberger et al., 2016; Zimmermann et al., 2006). However, administration of cells is highly arrhythmogenic and implantation of 3D tissue patches is highly invasive and requires open chest surgical intervention.

A more effective and intuitively more applicable approach would be to prevent the loss of myocardial tissue immediately after damage rather than regenerating the myocardium after damage has occurred. Considering that the loss of CMs during MI can involve as many as 25% of the total 2-4 billion cells in the left ventricle (Murry et al., 2006), preventing death becomes of paramount importance in light of the difficulty of regenerating such a large number of cells. As already discussed in the Introduction, some biotherapeutics such as VEGF, EPO and Serelaxin have already showed significant efficacy counteracting cardiac dysfunction after MI in preclinical animal models. However, they have largely failed when moved to human trials, possible due to the discrepancy between animal models and co-morbidities in patients affected by CVDs.

Recently, our group has performed a fully unbiased, systematic, in vivo screening in the ischemic heart named FunSel to search for cardioprotective factors. Cardiac FunSel has identified three previously undescribed proteins (Chrdl1, Fam3b and

Fam3c) that showed powerful cardioprotective activity after MI (Ruozi et al., 2022). These factors exerted their beneficial action upon AAV overexpression in the left ventricle, but also when released from the liver as circulating proteins. Noteworthy, induction of cardiac autophagy and protection from apoptosis are common mechanisms of action for Chrdl1, Fam3b and Fam3c, reinforcing the notion that autophagy exerts a protective role after MI (Sciarretta, Maejima, Zablocki, & Sadoshima, 2018). Understanding the molecular mechanisms behind the cardioprotective properties of these proteins is of great scientific interest, and becomes crucial to improve the quality of the biotherapeutics derived from these factors and to minimize the risk of any side effects when moving towards clinical application.

While Chrdl-1 mainly protects the heart by blocking the negative effects of BMP4 on CMs, inhibiting cardiac fibrosis and preventing pathological remodelling (Ruozi et al., 2022), the molecular mechanisms that drive the beneficial effect of Fam3b and Fam3c remain still poorly understood. These are two members of the Fam3 family for which there is no information in relation to cardiac biology. Fam3b, also known as PANcreatic DERived factor (PANDER) is mainly expressed in the pancreas, where it is involved in the regulation of glucose homeostasis and β cell function (Cao et al., 2003; Robert-Cooperman et al., 2010). Fam3c, also called Interleukin-Like Epithelial-to-mesenchymal transition Inducer (ILEI), is ubiquitously expressed in human tissue and is involved in several biological processes including hepatic and lipid metabolism, osteogenic differentiation, retinal laminar formation and brain amyloid- β (Aβ) peptide production, as reviewed by Zhu and colleagues (Y. Zhu et al., 2021). The secreted form of Fam3c protein was also found to be elevated in conditioned media of cells activating the autophagic machinery (Kraya et al., 2015) and in the secretome of doxorubicin resistant cells (Yao, Zhang, Chen, Hu, & Xu, 2011), suggesting a possible role of Fam3c as a player in resistance to chemotherapy.

By studying the role of Fam3c in damaged CMs in vitro, we observed a remarkable anti-apoptotic effect upon doxorubicin treatment, suggesting a protective role for this protein not only after ischemia, as shown by Ruozi et al (Ruozi et al., 2022), but also after anthracycline induced damage. Indeed, despite the great efficacy of

doxorubicin for the treatment of several cancer types, the usage of this drug is limited by its important cardiotoxicity. Different elements are shared between the pathogenesis of ischemic damage and anthracycline cardiotoxicity, including DNA damage, mitochondrial stress (Ichikawa et al., 2014; Suliman et al., 2007) and accumulation of reactive oxygen species (Doroshow & Davies, 1986). Interestingly, an impairment of autophagic flux was also previously reported in CMs upon doxorubicin administration (D. L. Li et al., 2016). In this context, we found that Fam3c induces CM autophagy, an essential mechanism to recycle dysfunctional organelles damaged by oxidative stress or cardiotoxic agents.

Previous investigations on the Fam3c mechanism of action has revealed a role of the Lifr-STAT3 axis in other cells than CMs (Woosley et al., 2019). STAT3 is a transcription factor activated by phosphorylation, which promotes translocation of the factor from the cytoplasm to the nucleus. In the heart, STAT3 activation contributes to protect against MI, fibrosis, hypertrophy, hypertension, myocarditis and diabetic cardiomyopathy (Harhous et al., 2019). Among the cardioprotective mechanisms commonly attributed to STAT3, its subcellular localization pattern affects apoptosis and autophagy. STAT3 is predominately localised in the cytoplasm in resting cells, but its role as a DNA-binding transcription factor depends on its ability to translocate into the nucleus. Concerning apoptosis, nuclear STAT3 upregulates anti-apoptotic proteins, suppresses transcription of pro-apoptotic genes and regulates expression of growth factors (Harhous et al., 2019). Moreover, nuclear STAT3 can fine-tune autophagy through transcriptional regulation of several autophagy-related genes, while its cytoplasmic form inhibits the autophagic process (You et al., 2015).

Our experiments revealed that, also in CMs, STAT3 is activated by Fam3c through Lifr receptor complex. This conclusion is supported by our observation that the downregulation of both gp130 and Lifr virtually abolish STAT3 phosphorylation and nuclear translocation. However, despite our data also clearly show that Fam3c-induced autophagy is not mediated by STAT3 activation, thus suggesting that this effect might be mediated by additional mechanisms and by an unknown receptor. In this context, a recent human binary protein interactome study reported the interaction between Fam3c and Free fatty acid receptor 2 (FFAR2) (Luck et al.,

2020), a G-coupled protein receptor mainly expressed in the gastrointestinal tract with a moderate expression in the heart (A. Wang, Gu, Heid, Akers, & Jiang, 2009). FFAR2 regulates a vast variety of biological processes such as energy metabolism, inflammation, intestinal cellular homeostasis and glucose metabolism (Lymperopoulos, Suster, & Borges, 2022). Since Fenchol, a natural FFAR2 agonist, increased lysosomal activity and reduced senescence in neuronal cells (Razazan et al., 2021), a regulation of autophagic pathway by FFAR2 might not be excluded. Further studies will be required to first evaluate whether Fam3c might interact with FFAR2 in CMs and if this interaction might eventually correlate with the ability of the factor to induce cardiac autophagy.

Our experiments based on the administration of an AAV9 vector expressing Fam3c immediately after MI have revealed that this factor reduces the extent of the infarct scar and protects the heart against negative ventricular remodelling, as concluded from echocardiographic monitoring of the treated animals over time and histological analysis of the hearts at 1 and 2 months after MI. Since a role for endogenous Fam3c in the heart has never been reported earlier, we were surprised to observe that MI itself induces expression of this factor in the heart, thus with a presumable protective effect. To the best of our knowledge, this is the first study to demonstrate that Fam3c transcription becomes upregulated following cardiac injury.

In the early time points after MI, it is well established that TGF-β signalling protects the heart by repressing the expression of pro-inflammatory cytokines and mediating resolution of the inflammatory infiltrate. In the last few years, a few studies performed in different cell lines have reported that TGF-β signalling modulates Fam3c expression (Chaudhury et al., 2010; Noguchi et al., 2017; X. Zhao et al., 2018). However, to date there is no prove that this mechanism is conserved in cardiac cells. Considering the similar trend observed between Fam3c and TGF-β after MI, we hypothesised that the increase of Fam3c could be driven by TGF-β. Our data showing increased Fam3c expression in cardiac fibroblasts following recombinant TGF-β treatment further reinforced this hypothesis. Our current model, which is shown in Fig. 24, envisages that the increased TGF-β release in the infarcted myocardium triggers the production of Fam3c by cardiac fibroblasts, activating the pro-survival STAT3 pathway through the Lifr complex and promoting

cardiac autophagy through a still unidentified receptor. The ultimate outcome of these combined effects is to limit CM death.

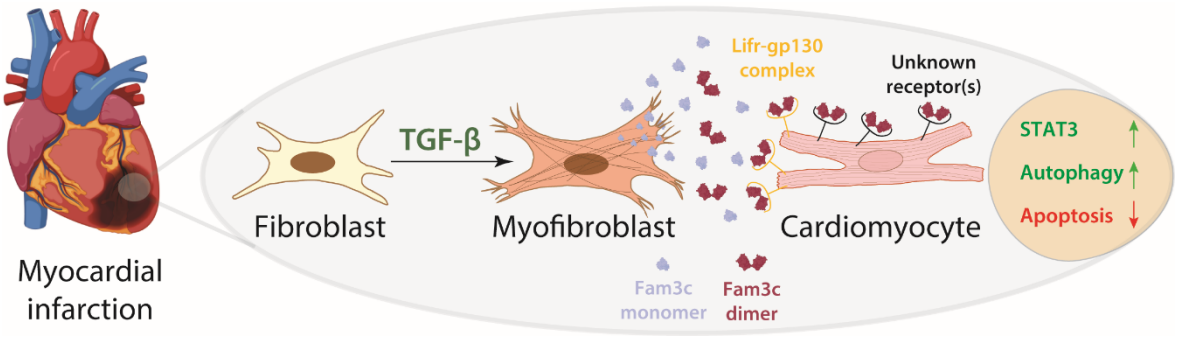

Figure 24: Schematic representation of the mechanisms for Fam3c upregulation after myocardial infarction. TGF-β upregulation after myocardial infarction drives the conversion of cardiac fibroblasts into myofibroblasts. TGF-β signalling increases the production of Fam3c which, as secreted factor, binds the Lifr-gp130 complex and other unknown receptor(s), activating pro-survival STAT3 pathway, cardiac autophagy and limiting cardiac apoptosis. *Parts of this figure were created with BioRender.com.*

We are well aware that further experimental evidence is needed to fully support this model. First, the amount of Fam3c protein (in addition to its mRNA) after cardiac injury still needs to be evaluated.

Second, total RNA extraction from cardiac tissue does not allow the identification of the cell type responsible for increased Fam3c expression. Cardiac fibroblasts are by far the most likely cell source for Fam3c, but this needs to be formally proven. This is particularly relevant after MI, when neutrophils, mononuclear cells, dendritic cells and lymphocytes sequential infiltrate the injured myocardium (J. Liu, Wang, & Li, 2016). In this respect, however, it is worth noting that we also observed an increase of Fam3c levels even when analysing cryoinjured EHT, a cardiac tissue model that lacks the immune and inflammatory infiltrate. This further supports the speculation that the increase of Fam3c after injury is most likely related to the resident cardiac cell population. In this context, the use of single-cell RNA sequencing will definitely shed light on the source of Fam3c.

Third, we have no information on the relevance for cardiac repair of Fam3c expression in the injured heart. We are currently awaiting the generation of a new conditional knock out mouse in which we will be able to inactivate the Fam3c gene in cardiomyocytes in both normal conditions and after MI. The use of this mouse will generate definitive information on the role of Fam3c in the normal process of myocardial repair after MI and in other conditions of cardiac damage, including anthracycline toxicity.

In conclusion, our data disclose both a novel, endogenous mechanism of response to cardiac damage and a potential cardioprotective protein that could progress towards clinical translation. The observation that Fam3c maintains its cardioprotective activity even when expressed from the liver as a circulating protein (Ruozi et al., 2022), supports the development of a recombinant factor that could be administered to patients immediately after MI, with the intent to limit the massive CM death due first to ischemia, and later to reperfusion.

6. PUBLISHED PAPERS

Ruozi, G., Bortolotti, F., **Mura, A**., Tomczyk, M., Falcione, A., Martinelli, V., Vodret, S., Braga, L., Dal Ferro, M., Cannata, A., Zentilin, L., Sinagra, G., Zacchigna, S., Giacca, M. 2022. *Cardioprotective factors against myocardial infarction selected in vivo from an AAV secretome library*. **Sci Transl Med** 14, eabo0699.

Part of my PhD work has been dedicated to an in vivo study aiming to identify novel cardioprotective molecules. In this context, our group has generated a library of 1198 barcoded AAV vectors encoding for the mouse secretome and developed cardiac FunSel (cFunSel), a method for their in vivo unbiased selection ranking them for efficacy against myocardial infarction (MI). Among the selected proteins, Chordin like 1 (Chrdl1), family with sequence similarity 3 member b and c (Fam3b and Fam3c) were the most effective factors sustaining cardiac function, preserving cardiomyocyte viability and preventing pathological remodelling after MI. Production of secreted and circulating Chrdl1, Fam3c and Fam3b from the liver was also able to protect the heart after MI, thus supporting the use of the three cardioprotectors as recombinant proteins.

My contribution to this work:

- I contributed to factor characterization.
- I contributed to evaluate the ability of the selected factors to modulate autophagy.
- I verified effective transgene expression (both at mRNA and protein level) in the heart and in primary cardiomyocytes after AAV9 and AAV6 transduction, respectively.
- I optimized and evaluated the effective production of overexpressed protein in the liver and in the serum after liver-specific AAV vector injection.
- I took part in the revision process.

7. REFERENCES

Aisa, Z., Liao, G. C., Shen, X. L., Chen, J., Li, L., & Jiang, S. B. (2017). Effect of autophagy on myocardial infarction and its mechanism. *Eur Rev Med Pharmacol Sci, 21*(16), 3705-3713.

Alkass, K., Panula, J., Westman, M., Wu, T. D., Guerquin-Kern, J. L., & Bergmann, O. (2015). No Evidence for Cardiomyocyte Number Expansion in Preadolescent Mice. *Cell, 163*(4), 1026-1036. doi: 10.1016/j.cell.2015.10.035

Ambrosio, G., & Tritto, I. (1999). Reperfusion injury: experimental evidence and clinical implications. *Am Heart J, 138*(2 Pt 2), S69-75. doi: 10.1016/s0002-8703(99)70323-6

Awasthi, N., Liongue, C., & Ward, A. C. (2021). STAT proteins: a kaleidoscope of canonical and non-canonical functions in immunity and cancer. *J Hematol Oncol, 14*(1), 198. doi: 10.1186/s13045-021-01214-y

Barnhart, B. C., Alappat, E. C., & Peter, M. E. (2003). The CD95 type I/type II model. *Semin Immunol, 15*(3), 185-193. doi: 10.1016/s1044-5323(03)00031-9

Bell, R. M., & Yellon, D. M. (2012). Conditioning the whole heart--not just the cardiomyocyte. *J Mol Cell Cardiol, 53*(1), 24-32. doi: 10.1016/j.yjmcc.2012.04.001

Belonje, A. M., Voors, A. A., van Gilst, W. H., Anker, S. D., Slart, R. H., Tio, R. A., . . . investigators, H. I. (2008). Effects of erythropoietin after an acute myocardial infarction: rationale and study design of a prospective, randomized, clinical trial (HEBE III). *Am Heart J, 155*(5), 817-822. doi: 10.1016/j.ahj.2007.12.036

Bendre, A., Buki, K. G., & Maatta, J. A. (2017). Fam3c modulates osteogenic differentiation by down-regulating Runx2. *Differentiation, 93*, 50-57. doi: 10.1016/j.diff.2016.11.005

Bergmann, O., Bhardwaj, R. D., Bernard, S., Zdunek, S., Barnabe-Heider, F., Walsh, S., . . . Frisen, J. (2009). Evidence for cardiomyocyte renewal in humans. *Science, 324*(5923), 98-102. doi: 324/5923/98 [pii]

10.1126/science.1164680

Bergmann, O., Zdunek, S., Felker, A., Salehpour, M., Alkass, K., Bernard, S., . . . Frisen, J. (2015). Dynamics of Cell Generation and Turnover in the Human Heart. *Cell, 161*(7), 1566-1575. doi: 10.1016/j.cell.2015.05.026

Bernard, Y., Ribeiro, N., Thuaud, F., Turkeri, G., Dirr, R., Boulberdaa, M., . . . Desaubry, L. (2011). Flavaglines alleviate doxorubicin cardiotoxicity:

implication of Hsp27. *PLoS One, 6*(10), e25302. doi: 10.1371/journal.pone.0025302

Birks, E. J. (2013). Molecular changes after left ventricular assist device support for heart failure. *Circ Res, 113*(6), 777-791. doi: 10.1161/CIRCRESAHA.113.301413

Bortolotti, F., Ruozi, G., Falcione, A., Doimo, S., Dal Ferro, M., Lesizza, P., . . . Giacca, M. (2017). In Vivo Functional Selection Identifies Cardiotrophin-1 as a Cardiac Engraftment Factor for Mesenchymal Stromal Cells. *Circulation, 136*(16), 1509-1524. doi: 10.1161/CIRCULATIONAHA.117.029003

Cannata, A., Ali, H., Sinagra, G., & Giacca, M. (2020). Gene Therapy for the Heart Lessons Learned and Future Perspectives. *Circ Res, 126*(10), 1394-1414. doi: 10.1161/CIRCRESAHA.120.315855

Cao, X., Gao, Z., Robert, C. E., Greene, S., Xu, G., Xu, W., . . . Wolf, B. A. (2003). Pancreatic-derived factor (FAM3B), a novel islet cytokine, induces apoptosis of insulin-secreting beta-cells. *Diabetes, 52*(9), 2296-2303. doi: 10.2337/diabetes.52.9.2296

Cao, X., Yang, J., Burkhardt, B. R., Gao, Z., Wong, R. K., Greene, S. R., . . . Wolf, B. A. (2005). Effects of overexpression of pancreatic derived factor (FAM3B) in isolated mouse islets and insulin-secreting betaTC3 cells. *Am J Physiol Endocrinol Metab, 289*(4), E543-550. doi: 10.1152/ajpendo.00113.2005

Chaudhury, A., Hussey, G. S., Ray, P. S., Jin, G., Fox, P. L., & Howe, P. H. (2010). TGF-beta-mediated phosphorylation of hnRNP E1 induces EMT via transcript-selective translational induction of Dab2 and ILEI. *Nat Cell Biol, 12*(3), 286-293. doi: 10.1038/ncb2029

Chen, G., Li, H., Li, X., Li, B., Zhong, L., Huang, S., . . . Bin, J. (2018). Loss of long non-coding RNA CRRL promotes cardiomyocyte regeneration and improves cardiac repair by functioning as a competing endogenous RNA. *J Mol Cell Cardiol, 122*, 152-164. doi: 10.1016/j.yjmcc.2018.08.013

Chen, H., Sun, X., Ge, W., Qian, Y., Bai, R., & Zheng, S. (2017). A seven-gene signature predicts overall survival of patients with colorectal cancer. *Oncotarget, 8*(56), 95054-95065. doi: 10.18632/oncotarget.10982

Chen, Z., Ding, L., Yang, W., Wang, J., Chen, L., Chang, Y., . . . Yang, J. (2017). Hepatic Activation of the FAM3C-HSF1-CaM Pathway Attenuates Hyperglycemia of Obese Diabetic Mice. *Diabetes, 66*(5), 1185-1197. doi: 10.2337/db16-0993

Chen, Z., Wang, J., Yang, W., Chen, J., Meng, Y., Geng, B., . . . Yang, J. (2017). FAM3A mediates PPARgamma's protection in liver ischemia-reperfusion injury by activating Akt survival pathway and repressing inflammation and

oxidative stress. *Oncotarget, 8*(30), 49882-49896. doi: 10.18632/oncotarget.17805

Chien, K. R., Frisen, J., Fritsche-Danielson, R., Melton, D. A., Murry, C. E., & Weissman, I. L. (2019). Regenerating the field of cardiovascular cell therapy. *Nat Biotechnol, 37*(3), 232-237. doi: 10.1038/s41587-019-0042-1

Chiong, M., Wang, Z. V., Pedrozo, Z., Cao, D. J., Troncoso, R., Ibacache, M., . . . Lavandero, S. (2011). Cardiomyocyte death: mechanisms and translational implications. *Cell Death Dis, 2*, e244. doi: 10.1038/cddis.2011.130

Cho, Y. S., Go, M. J., Kim, Y. J., Heo, J. Y., Oh, J. H., Ban, H. J., . . . Kim, H. L. (2009). A large-scale genome-wide association study of Asian populations uncovers genetic factors influencing eight quantitative traits. *Nat Genet, 41*(5), 527-534. doi: 10.1038/ng.357

Chong, J. J., Yang, X., Don, C. W., Minami, E., Liu, Y. W., Weyers, J. J., . . . Murry, C. E. (2014). Human embryonic-stem-cell-derived cardiomyocytes regenerate non-human primate hearts. *Nature, 510*(7504), 273-277. doi: 10.1038/nature13233

Chu, D., Sullivan, C. C., Weitzman, M. D., Du, L., Wolf, P. L., Jamieson, S. W., & Thistlethwaite, P. A. (2003). Direct comparison of efficiency and stability of gene transfer into the mammalian heart using adeno-associated virus versus adenovirus vectors. *J Thorac Cardiovasc Surg, 126*(3), 671-679. doi: 10.1016/s0022-5223(03)00082-5

Condorelli, G., Morisco, C., Stassi, G., Notte, A., Farina, F., Sgaramella, G., . . . Lembo, G. (1999). Increased cardiomyocyte apoptosis and changes in proapoptotic and antiapoptotic genes bax and bcl-2 during left ventricular adaptations to chronic pressure overload in the rat. *Circulation, 99*(23), 3071-3078. doi: 10.1161/01.cir.99.23.3071

Crespo-Leiro, M. G., Anker, S. D., Maggioni, A. P., Coats, A. J., Filippatos, G., Ruschitzka, F., . . . Heart Failure Association of the European Society of, C. (2016). European Society of Cardiology Heart Failure Long-Term Registry (ESC-HF-LT): 1-year follow-up outcomes and differences across regions. *Eur J Heart Fail, 18*(6), 613-625. doi: 10.1002/ejhf.566

Csiszar, A., Kutay, B., Wirth, S., Schmidt, U., Macho-Maschler, S., Schreiber, M., . . . Beug, H. (2014). Interleukin-like epithelial-to-mesenchymal transition inducer activity is controlled by proteolytic processing and plasminogen-urokinase plasminogen activator receptor system-regulated secretion during breast cancer progression. *Breast Cancer Res, 16*(5), 433. doi: 10.1186/s13058-014-0433-7

Cuervo, A. M., & Dice, J. F. (1996). A receptor for the selective uptake and degradation of proteins by lysosomes. *Science, 273*(5274), 501-503. doi: 10.1126/science.273.5274.501

Cuervo, A. M., & Wong, E. (2014). Chaperone-mediated autophagy: roles in disease and aging. *Cell Res, 24*(1), 92-104. doi: 10.1038/cr.2013.153

Darnell, J. E., Jr., Kerr, I. M., & Stark, G. R. (1994). Jak-STAT pathways and transcriptional activation in response to IFNs and other extracellular signaling proteins. *Science, 264*(5164), 1415-1421. doi: 10.1126/science.8197455

De Duve, C., & Wattiaux, R. (1966). Functions of lysosomes. *Annu Rev Physiol, 28*, 435-492. doi: 10.1146/annurev.ph.28.030166.002251

de Wit, N. J., N, I. J., Oosterink, E., Keshtkar, S., Hooiveld, G. J., Mensink, R. P., . . . van der Meer, R. (2012). Oit1/Fam3D, a gut-secreted protein displaying nutritional status-dependent regulation. *J Nutr Biochem, 23*(11), 1425-1433. doi: 10.1016/j.jnutbio.2011.09.003

Dice, J. F. (1990). Peptide sequences that target cytosolic proteins for lysosomal proteolysis. *Trends Biochem Sci, 15*(8), 305-309. doi: 10.1016/0968-0004(90)90019-8

Doroshow, J. H., & Davies, K. J. (1986). Redox cycling of anthracyclines by cardiac mitochondria. II. Formation of superoxide anion, hydrogen peroxide, and hydroxyl radical. *J Biol Chem, 261*(7), 3068-3074.

Eschenhagen, T., Bolli, R., Braun, T., Field, L. J., Fleischmann, B. K., Frisen, J., . . . Hill, J. A. (2017). Cardiomyocyte Regeneration: A Consensus Statement. *Circulation, 136*(7), 680-686. doi: 10.1161/CIRCULATIONAHA.117.029343

Eulalio, A., Mano, M., Dal Ferro, M., Zentilin, L., Sinagra, G., Zacchigna, S., & Giacca, M. (2012). Functional screening identifies miRNAs inducing cardiac regeneration. *Nature, 492*(7429), 376-381. doi: 10.1038/nature11739

Frangogiannis, N. (2020). Transforming growth factor-beta in tissue fibrosis. *J Exp Med, 217*(3), e20190103. doi: 10.1084/jem.20190103

Frangogiannis, N. G., Michael, L. H., & Entman, M. L. (2000). Myofibroblasts in reperfused myocardial infarcts express the embryonic form of smooth muscle myosin heavy chain (SMemb). *Cardiovasc Res, 48*(1), 89-100. doi: 10.1016/s0008-6363(00)00158-9

French, B. A., Mazur, W., Geske, R. S., & Bolli, R. (1994). Direct in vivo gene transfer into porcine myocardium using replication-deficient adenoviral vectors. *Circulation, 90*(5), 2414-2424. doi: 10.1161/01.cir.90.5.2414

Fuglesteg, B. N., Suleman, N., Tiron, C., Kanhema, T., Lacerda, L., Andreasen, T. V., . . . Lecour, S. (2008). Signal transducer and activator of transcription 3 is involved in the cardioprotective signalling pathway activated by insulin therapy at reperfusion. *Basic Res Cardiol, 103*(5), 444-453. doi: 10.1007/s00395-008-0728-x

Gabisonia, K., Prosdocimo, G., Aquaro, G. D., Carlucci, L., Zentilin, L., Secco, I., . . . Giacca, M. (2019). MicroRNA therapy stimulates uncontrolled cardiac repair after myocardial infarction in pigs. *Nature, 569*(7756), 418-422. doi: 10.1038/s41586-019-1191-6

Galluzzi, L., Vitale, I., Aaronson, S. A., Abrams, J. M., Adam, D., Agostinis, P., . . . Kroemer, G. (2018). Molecular mechanisms of cell death: recommendations of the Nomenclature Committee on Cell Death 2018. *Cell Death Differ, 25*(3), 486-541. doi: 10.1038/s41418-017-0012-4

Gao, F., Kataoka, M., Liu, N., Liang, T., Huang, Z. P., Gu, F., . . . Wang, D. Z. (2019). Therapeutic role of miR-19a/19b in cardiac regeneration and protection from myocardial infarction. *Nat Commun, 10*(1), 1802. doi: 10.1038/s41467-019-09530-1

Gao, G. P., Alvira, M. R., Wang, L., Calcedo, R., Johnston, J., & Wilson, J. M. (2002). Novel adeno-associated viruses from rhesus monkeys as vectors for human gene therapy. *Proc Natl Acad Sci U S A, 99*(18), 11854-11859. doi: 10.1073/pnas.182412299

Gao, Z. H., Lu, C., Wang, Z. N., Song, Y. X., Zhu, J. L., Gao, P., . . . Xu, H. M. (2014). ILEI: a novel marker for epithelial-mesenchymal transition and poor prognosis in colorectal cancer. *Histopathology, 65*(4), 527-538. doi: 10.1111/his.12435

Garbers, C., Hermanns, H. M., Schaper, F., Muller-Newen, G., Grotzinger, J., Rose-John, S., & Scheller, J. (2012). Plasticity and cross-talk of interleukin 6-type cytokines. *Cytokine Growth Factor Rev, 23*(3), 85-97. doi: 10.1016/j.cytogfr.2012.04.001

Ghosh, R. K., Banerjee, K., Tummala, R., Ball, S., Ravakhah, K., & Gupta, A. (2017). Serelaxin in acute heart failure: Most recent update on clinical and preclinical evidence. *Cardiovasc Ther, 35*(1), 55-63. doi: 10.1111/1755-5922.12231

Giacca, M. (2020). Cardiac Regeneration After Myocardial Infarction: an Approachable Goal. *Curr Cardiol Rep, 22*(10), 122. doi: 10.1007/s11886-020-01361-7

Giese, B., Roderburg, C., Sommerauer, M., Wortmann, S. B., Metz, S., Heinrich, P. C., & Muller-Newen, G. (2005). Dimerization of the cytokine receptors gp130 and LIFR analysed in single cells. *J Cell Sci, 118*(Pt 21), 5129-5140. doi: 10.1242/jcs.02628

Golstein, P., & Kroemer, G. (2007). Cell death by necrosis: towards a molecular definition. *Trends Biochem Sci, 32*(1), 37-43. doi: 10.1016/j.tibs.2006.11.001

Gonzalez-Rosa, J. M., & Mercader, N. (2012). Cryoinjury as a myocardial infarction model for the study of cardiac regeneration in the zebrafish. *Nat Protoc, 7*(4), 782-788. doi: 10.1038/nprot.2012.025

Gottlieb, S. S., Kukin, M. L., Penn, J., Fisher, M. L., Cines, M., Medina, N., . . . Packer, M. (1993). Sustained hemodynamic response to flosequinan in patients with heart failure receiving angiotensin-converting enzyme inhibitors. *J Am Coll Cardiol, 22*(4), 963-967. doi: 10.1016/0735-1097(93)90404-o

Gupta, S. K., Garg, A., Bar, C., Chatterjee, S., Foinquinos, A., Milting, H., . . . Thum, T. (2018). Quaking Inhibits Doxorubicin-Mediated Cardiotoxicity Through Regulation of Cardiac Circular RNA Expression. *Circ Res, 122*(2), 246-254. doi: 10.1161/CIRCRESAHA.117.311335

Hansen, A., Eder, A., Bonstrup, M., Flato, M., Mewe, M., Schaaf, S., . . . Eschenhagen, T. (2010). Development of a drug screening platform based on engineered heart tissue. *Circ Res, 107*(1), 35-44. doi: 10.1161/CIRCRESAHA.109.211458

Haranath Chinthaginjala, K. K., Sai Priyanka Manchikanti, Pushpalatha Gutty Reddy, Sumala Karamthoy and Navyalatha Reddy Vennapusa. (2021). BIOTHERAPEUTICS AS DRUGS, ITS DELIVERY ROUTES AND IMPORTANCE OF NOVEL CARRIERS IN BIOTHERAPEUTICS. *International Journal of Pharmaceutical Sciences and Research*. doi: 10.13040/IJPSR.0975-8232.12(1).44-56

Harhous, Z., Booz, G. W., Ovize, M., Bidaux, G., & Kurdi, M. (2019). An Update on the Multifaceted Roles of STAT3 in the Heart. *Front Cardiovasc Med, 6*, 150. doi: 10.3389/fcvm.2019.00150

Hasegawa, H., Liu, L., Tooyama, I., Murayama, S., & Nishimura, M. (2014). The FAM3 superfamily member ILEI ameliorates Alzheimer's disease-like pathology by destabilizing the penultimate amyloid-beta precursor. *Nat Commun, 5*, 3917. doi: 10.1038/ncomms4917

Hausenloy, D. J., Baxter, G., Bell, R., Botker, H. E., Davidson, S. M., Downey, J., . . . Yellon, D. M. (2010). Translating novel strategies for cardioprotection: the Hatter Workshop Recommendations. *Basic Res Cardiol, 105*(6), 677-686. doi: 10.1007/s00395-010-0121-4

Hausenloy, D. J., Kharbanda, R. K., Moller, U. K., Ramlall, M., Aaroe, J., Butler, R., . . . Investigators, C.-E.-P. (2019). Effect of remote ischaemic conditioning on clinical outcomes in patients with acute myocardial infarction (CONDI-2/ERIC-PPCI): a single-blind randomised controlled trial. *Lancet, 394*(10207), 1415-1424. doi: 10.1016/S0140-6736(19)32039-2

Hausenloy, D. J., & Yellon, D. M. (2008). Remote ischaemic preconditioning: underlying mechanisms and clinical application. *Cardiovasc Res, 79*(3), 377-386. doi: 10.1093/cvr/cvn114

Heidenreich, P. A., Bozkurt, B., Aguilar, D., Allen, L. A., Byun, J. J., Colvin, M. M., . . . Yancy, C. W. (2022). 2022 AHA/ACC/HFSA Guideline for the Management of Heart Failure: A Report of the American College of Cardiology/American Heart Association Joint Committee on Clinical Practice Guidelines. *Circulation, 145*(18), e895-e1032. doi: 10.1161/CIR.0000000000001063

Heusch, G., & Gersh, B. J. (2017). The pathophysiology of acute myocardial infarction and strategies of protection beyond reperfusion: a continual challenge. *Eur Heart J, 38*(11), 774-784. doi: 10.1093/eurheartj/ehw224

Hilfiker-Kleiner, D., Hilfiker, A., Fuchs, M., Kaminski, K., Schaefer, A., Schieffer, B., . . . Drexler, H. (2004). Signal transducer and activator of transcription 3 is required for myocardial capillary growth, control of interstitial matrix deposition, and heart protection from ischemic injury. *Circ Res, 95*(2), 187-195. doi: 10.1161/01.RES.0000134921.50377.61

Hu, T., Yeh, J. E., Pinello, L., Jacob, J., Chakravarthy, S., Yuan, G. C., . . . Frank, D. A. (2015). Impact of the N-Terminal Domain of STAT3 in STAT3-Dependent Transcriptional Activity. *Mol Cell Biol, 35*(19), 3284-3300. doi: 10.1128/MCB.00060-15

Hutt, K. J. (2015). The role of BH3-only proteins in apoptosis within the ovary. *Reproduction, 149*(2), R81-89. doi: 10.1530/REP-14-0422

Ibanez, B., James, S., Agewall, S., Antunes, M. J., Bucciarelli-Ducci, C., Bueno, H., . . . Widimsky, P. (2018). [2017 ESC Guidelines for the management of acute myocardial infarction in patients presenting with ST-segment elevation.]. *Kardiol Pol, 76*(2), 229-313. doi: 10.5603/KP.2018.0041

Ichikawa, Y., Ghanefar, M., Bayeva, M., Wu, R., Khechaduri, A., Naga Prasad, S. V., . . . Ardehali, H. (2014). Cardiotoxicity of doxorubicin is mediated through mitochondrial iron accumulation. *J Clin Invest, 124*(2), 617-630. doi: 10.1172/JCI72931

Ikeuchi, M., Tsutsui, H., Shiomi, T., Matsusaka, H., Matsushima, S., Wen, J., . . . Takeshita, A. (2004). Inhibition of TGF-beta signaling exacerbates early cardiac dysfunction but prevents late remodeling after infarction. *Cardiovasc Res, 64*(3), 526-535. doi: 10.1016/j.cardiores.2004.07.017

Jansson, A. M., Csiszar, A., Maier, J., Nystrom, A. C., Ax, E., Johansson, P., & Schiavone, L. H. (2017). The interleukin-like epithelial-mesenchymal transition inducer ILEI exhibits a non-interleukin-like fold and is active as a domain-swapped dimer. *J Biol Chem, 292*(37), 15501-15511. doi: 10.1074/jbc.M117.782904

Johansson, P., Bernstrom, J., Gorman, T., Oster, L., Backstrom, S., Schweikart, F., . . . Schiavone, L. H. (2013). FAM3B PANDER and FAM3C ILEI represent a distinct class of signaling molecules with a non-cytokine-like fold. *Structure, 21*(2), 306-313. doi: 10.1016/j.str.2012.12.009

Johnston, P. A., & Grandis, J. R. (2011). STAT3 signaling: anticancer strategies and challenges. *Mol Interv, 11*(1), 18-26. doi: 10.1124/mi.11.1.4

Jones, S. A., & Jenkins, B. J. (2018). Recent insights into targeting the IL-6 cytokine family in inflammatory diseases and cancer. *Nat Rev Immunol, 18*(12), 773-789. doi: 10.1038/s41577-018-0066-7

Kanamori, H., Takemura, G., Goto, K., Maruyama, R., Ono, K., Nagao, K., . . . Minatoguchi, S. (2011). Autophagy limits acute myocardial infarction induced by permanent coronary artery occlusion. *Am J Physiol Heart Circ Physiol, 300*(6), H2261-2271. doi: 10.1152/ajpheart.01056.2010

Katahira, T., Nakagiri, S., Terada, K., & Furukawa, T. (2010). Secreted factor FAM3C (ILEI) is involved in retinal laminar formation. *Biochem Biophys Res Commun, 392*(3), 301-306. doi: 10.1016/j.bbrc.2009.12.180

Kerr, J. F., Wyllie, A. H., & Currie, A. R. (1972). Apoptosis: a basic biological phenomenon with wide-ranging implications in tissue kinetics. *Br J Cancer, 26*(4), 239-257. doi: 10.1038/bjc.1972.33

Kirchner, P., Bourdenx, M., Madrigal-Matute, J., Tiano, S., Diaz, A., Bartholdy, B. A., . . . Cuervo, A. M. (2019). Proteome-wide analysis of chaperone-mediated autophagy targeting motifs. *PLoS Biol, 17*(5), e3000301. doi: 10.1371/journal.pbio.3000301

Kral, M., Klimek, C., Kutay, B., Timelthaler, G., Lendl, T., Neuditschko, B., . . . Csiszar, A. (2017). Covalent dimerization of interleukin-like epithelial-to-mesenchymal transition (EMT) inducer (ILEI) facilitates EMT, invasion, and late aspects of metastasis. *FEBS J, 284*(20), 3484-3505. doi: 10.1111/febs.14207

Kraya, A. A., Piao, S., Xu, X., Zhang, G., Herlyn, M., Gimotty, P., . . . Speicher, D. W. (2015). Identification of secreted proteins that reflect autophagy dynamics within tumor cells. *Autophagy, 11*(1), 60-74. doi: 10.4161/15548627.2014.984273

Kubler, W., & Haass, M. (1996). Cardioprotection: definition, classification, and fundamental principles. *Heart, 75*(4), 330-333. doi: 10.1136/hrt.75.4.330

Lahsnig, C., Mikula, M., Petz, M., Zulehner, G., Schneller, D., van Zijl, F., . . . Mikulits, W. (2009). ILEI requires oncogenic Ras for the epithelial to mesenchymal transition of hepatocytes and liver carcinoma progression. *Oncogene, 28*(5), 638-650. doi: 10.1038/onc.2008.418

Lee, J. T., Ideker, R. E., & Reimer, K. A. (1981). Myocardial infarct size and location in relation to the coronary vascular bed at risk in man. *Circulation, 64*(3), 526-534. doi: 10.1161/01.cir.64.3.526

Levine, B., & Kroemer, G. (2008). Autophagy in the pathogenesis of disease. *Cell, 132*(1), 27-42. doi: 10.1016/j.cell.2007.12.018

Levy, D. E., & Inghirami, G. (2006). STAT3: a multifaceted oncogene. *Proc Natl Acad Sci U S A, 103*(27), 10151-10152. doi: 10.1073/pnas.0604042103

Li, D. L., Wang, Z. V., Ding, G., Tan, W., Luo, X., Criollo, A., . . . Hill, J. A. (2016). Doxorubicin Blocks Cardiomyocyte Autophagic Flux by Inhibiting Lysosome Acidification. *Circulation, 133*(17), 1668-1687. doi: 10.1161/CIRCULATIONAHA.115.017443

Li, J., Chi, Y., Wang, C., Wu, J., Yang, H., Zhang, D., . . . Guan, Y. (2011). Pancreatic-derived factor promotes lipogenesis in the mouse liver: role of the Forkhead box 1 signaling pathway. *Hepatology, 53*(6), 1906-1916. doi: 10.1002/hep.24295

Liang, W., Peng, X., Li, Q., Wang, P., Lv, P., Song, Q., . . . Wang, Y. (2020). FAM3D is essential for colon homeostasis and host defense against inflammation associated carcinogenesis. *Nat Commun, 11*(1), 5912. doi: 10.1038/s41467-020-19691-z

Lijnen, P., Petrov, V., Rumilla, K., & Fagard, R. (2003). Transforming growth factor-beta 1 promotes contraction of collagen gel by cardiac fibroblasts through their differentiation into myofibroblasts. *Methods Find Exp Clin Pharmacol, 25*(2), 79-86. doi: 10.1358/mf.2003.25.2.723680

Lipsic, E., Schoemaker, R. G., van der Meer, P., Voors, A. A., van Veldhuisen, D. J., & van Gilst, W. H. (2006). Protective effects of erythropoietin in cardiac ischemia: from bench to bedside. *J Am Coll Cardiol, 48*(11), 2161-2167. doi: 10.1016/j.jacc.2006.08.031

Liu, J., Wang, H., & Li, J. (2016). Inflammation and Inflammatory Cells in Myocardial Infarction and Reperfusion Injury: A Double-Edged Sword. *Clin Med Insights Cardiol, 10*, 79-84. doi: 10.4137/CMC.S33164

Liu, L., Watanabe, N., Akatsu, H., & Nishimura, M. (2016). Neuronal expression of ILEI/FAM3C and its reduction in Alzheimer's disease. *Neuroscience, 330*, 236-246. doi: 10.1016/j.neuroscience.2016.05.050

Liu, Y. W., Chen, B., Yang, X., Fugate, J. A., Kalucki, F. A., Futakuchi-Tsuchida, A., . . . Murry, C. E. (2018). Human embryonic stem cell-derived cardiomyocytes restore function in infarcted hearts of non-human primates. *Nat Biotechnol, 36*(7), 597-605. doi: 10.1038/nbt.4162

Lo, H. W., Hsu, S. C., Ali-Seyed, M., Gunduz, M., Xia, W., Wei, Y., . . . Hung, M. C. (2005). Nuclear interaction of EGFR and STAT3 in the activation of the iNOS/NO pathway. *Cancer Cell, 7*(6), 575-589. doi: 10.1016/j.ccr.2005.05.007

Luck, K., Kim, D. K., Lambourne, L., Spirohn, K., Begg, B. E., Bian, W., . . . Calderwood, M. A. (2020). A reference map of the human binary protein interactome. *Nature, 580*(7803), 402-408. doi: 10.1038/s41586-020-2188-x

Ludman, A. J., Yellon, D. M., & Hausenloy, D. J. (2010). Cardiac preconditioning for ischaemia: lost in translation. *Dis Model Mech, 3*(1-2), 35-38. doi: 10.1242/dmm.003855

Lymperopoulos, A., Suster, M. S., & Borges, J. I. (2022). Short-Chain Fatty Acid Receptors and Cardiovascular Function. *Int J Mol Sci, 23*(6). doi: 10.3390/ijms23063303

Ma, J. H., Qin, L., & Li, X. (2020). Role of STAT3 signaling pathway in breast cancer. *Cell Commun Signal, 18*(1), 33. doi: 10.1186/s12964-020-0527-z

Maatta, J. A., Bendre, A., Laanti, M., Buki, K. G., Rantakari, P., Tervola, P., . . . Vaananen, K. (2016). Fam3c modulates osteogenic cell differentiation and affects bone volume and cortical bone mineral density. *Bonekey Rep, 5*, 787. doi: 10.1038/bonekey.2016.14

Martin, B., Romero, G., & Salama, G. (2019). Cardioprotective actions of relaxin. *Mol Cell Endocrinol, 487*, 45-53. doi: 10.1016/j.mce.2018.12.016

Martinez-Gil, N., Roca-Ayats, N., Monistrol-Mula, A., Garcia-Giralt, N., Diez-Perez, A., Nogues, X., . . . Balcells, S. (2018). Common and rare variants of WNT16, DKK1 and SOST and their relationship with bone mineral density. *Sci Rep, 8*(1), 10951. doi: 10.1038/s41598-018-29242-8

Mijaljica, D., Prescott, M., & Devenish, R. J. (2011). Microautophagy in mammalian cells: revisiting a 40-year-old conundrum. *Autophagy, 7*(7), 673-682. doi: 10.4161/auto.7.7.14733

Mitsuyama, K., Matsumoto, S., Masuda, J., Yamasakii, H., Kuwaki, K., Takedatsu, H., & Sata, M. (2007). Therapeutic strategies for targeting the IL-6/STAT3 cytokine signaling pathway in inflammatory bowel disease. *Anticancer Res, 27*(6A), 3749-3756.

Montero, P., Flandes-Iparraguirre, M., Musquiz, S., Perez Araluce, M., Plano, D., Sanmartin, C., . . . Mazo, M. M. (2020). Cells, Materials, and Fabrication Processes for Cardiac Tissue Engineering. *Front Bioeng Biotechnol, 8*, 955. doi: 10.3389/fbioe.2020.00955

Moon, C., Krawczyk, M., Ahn, D., Ahmet, I., Paik, D., Lakatta, E. G., & Talan, M. I. (2003). Erythropoietin reduces myocardial infarction and left ventricular functional decline after coronary artery ligation in rats. *Proc Natl Acad Sci U S A, 100*(20), 11612-11617. doi: 10.1073/pnas.1930406100

Mori, K., Ikari, Y., Jono, S., Shioi, A., Ishimura, E., Emoto, M., . . . Nishizawa, Y. (2010). Association of serum TRAIL level with coronary artery disease. *Thromb Res, 125*(4), 322-325. doi: 10.1016/j.thromres.2009.11.024

Mou, H., Li, Z., Yao, P., Zhuo, S., Luan, W., Deng, B., . . . Le, Y. (2013). Knockdown of FAM3B triggers cell apoptosis through p53-dependent

pathway. *Int J Biochem Cell Biol, 45*(3), 684-691. doi: 10.1016/j.biocel.2012.12.003

Murry, C. E., Jennings, R. B., & Reimer, K. A. (1986). Preconditioning with ischemia: a delay of lethal cell injury in ischemic myocardium. *Circulation, 74*(5), 1124-1136. doi: 10.1161/01.cir.74.5.1124

Murry, C. E., Reinecke, H., & Pabon, L. M. (2006). Regeneration gaps: observations on stem cells and cardiac repair. *J Am Coll Cardiol, 47*(9), 1777-1785. doi: 10.1016/j.jacc.2006.02.002

Nakai, A., Yamaguchi, O., Takeda, T., Higuchi, Y., Hikoso, S., Taniike, M., . . . Otsu, K. (2007). The role of autophagy in cardiomyocytes in the basal state and in response to hemodynamic stress. *Nat Med, 13*(5), 619-624. doi: 10.1038/nm1574

Nakayama, N., Han, C. E., Scully, S., Nishinakamura, R., He, C., Zeni, L., . . . Wen, D. (2001). A novel chordin-like protein inhibitor for bone morphogenetic proteins expressed preferentially in mesenchymal cell lineages. *Dev Biol, 232*(2), 372-387. doi: 10.1006/dbio.2001.0200

Noguchi, K., Dalton, A. C., Howley, B. V., McCall, B. J., Yoshida, A., Diehl, J. A., & Howe, P. H. (2017). Interleukin-like EMT inducer regulates partial phenotype switching in MITF-low melanoma cell lines. *PLoS One, 12*(5), e0177830. doi: 10.1371/journal.pone.0177830

O'Gorman, S., Fox, D. T., & Wahl, G. M. (1991). Recombinase-mediated gene activation and site-specific integration in mammalian cells. *Science, 251*(4999), 1351-1355. doi: 10.1126/science.1900642

O'Sullivan, K. E., Breen, E. P., Gallagher, H. C., Buggy, D. J., & Hurley, J. P. (2016). Understanding STAT3 signaling in cardiac ischemia. *Basic Res Cardiol, 111*(3), 27. doi: 10.1007/s00395-016-0543-8

Osmancik, P., Teringova, E., Tousek, P., Paulu, P., & Widimsky, P. (2013). Prognostic value of TNF-related apoptosis inducing ligand (TRAIL) in acute coronary syndrome patients. *PLoS One, 8*(2), e53860. doi: 10.1371/journal.pone.0053860

Packer, M. (2018). Heart Failure: The Most Important, Preventable, and Treatable Cardiovascular Complication of Type 2 Diabetes. *Diabetes Care, 41*(1), 11-13. doi: 10.2337/dci17-0052

Pallen, M. J., & Wren, B. W. (1997). The HtrA family of serine proteases. *Mol Microbiol, 26*(2), 209-221. doi: 10.1046/j.1365-2958.1997.5601928.x

Peng, X., Xu, E., Liang, W., Pei, X., Chen, D., Zheng, D., . . . Wang, Y. (2016). Identification of FAM3D as a new endogenous chemotaxis agonist for the formyl peptide receptors. *J Cell Sci, 129*(9), 1831-1842. doi: 10.1242/jcs.183053

Penna, C., Cappello, S., Mancardi, D., Raimondo, S., Rastaldo, R., Gattullo, D., . . . Pagliaro, P. (2006). Post-conditioning reduces infarct size in the isolated rat heart: role of coronary flow and pressure and the nitric oxide/cGMP pathway. *Basic Res Cardiol, 101*(2), 168-179. doi: 10.1007/s00395-005-0543-6

Penna, C., Mancardi, D., Raimondo, S., Geuna, S., & Pagliaro, P. (2008). The paradigm of postconditioning to protect the heart. *J Cell Mol Med, 12*(2), 435-458. doi: 10.1111/j.1582-4934.2007.00210.x

Pilipenko, V. V., Reece, A., Choo, D. I., & Greinwald, J. H., Jr. (2004). Genomic organization and expression analysis of the murine Fam3c gene. *Gene, 335*, 159-168. doi: 10.1016/j.gene.2004.03.026

Porrello, E. R., Mahmoud, A. I., Simpson, E., Hill, J. A., Richardson, J. A., Olson, E. N., & Sadek, H. A. (2011). Transient regenerative potential of the neonatal mouse heart. *Science, 331*(6020), 1078-1080. doi: 10.1126/science.1200708

Poss, K. D., Wilson, L. G., & Keating, M. T. (2002). Heart regeneration in zebrafish. *Science, 298*(5601), 2188-2190. doi: 10.1126/science.1077857

Przyklenk, K., Undyala, V. V., Wider, J., Sala-Mercado, J. A., Gottlieb, R. A., & Mentzer, R. M., Jr. (2011). Acute induction of autophagy as a novel strategy for cardioprotection: getting to the heart of the matter. *Autophagy, 7*(4), 432-433. doi: 10.4161/auto.7.4.14395

Raso, A., Dirkx, E., Sampaio-Pinto, V., El Azzouzi, H., Cubero, R. J., Sorensen, D. W., . . . De Windt, L. J. (2021). A microRNA program regulates the balance between cardiomyocyte hyperplasia and hypertrophy and stimulates cardiac regeneration. *Nat Commun, 12*(1), 4808. doi: 10.1038/s41467-021-25211-4

Razazan, A., Karunakar, P., Mishra, S. P., Sharma, S., Miller, B., Jain, S., & Yadav, H. (2021). Activation of Microbiota Sensing - Free Fatty Acid Receptor 2 Signaling Ameliorates Amyloid-beta Induced Neurotoxicity by Modulating Proteolysis-Senescence Axis. *Front Aging Neurosci, 13*, 735933. doi: 10.3389/fnagi.2021.735933

Robert-Cooperman, C. E., Carnegie, J. R., Wilson, C. G., Yang, J., Cook, J. R., Wu, J., . . . Burkhardt, B. R. (2010). Targeted disruption of pancreatic-derived factor (PANDER, FAM3B) impairs pancreatic beta-cell function. *Diabetes, 59*(9), 2209-2218. doi: 10.2337/db09-1552

Roger, V. L., Go, A. S., Lloyd-Jones, D. M., Benjamin, E. J., Berry, J. D., Borden, W. B., . . . Stroke Statistics, S. (2012). Heart disease and stroke statistics--2012 update: a report from the American Heart Association. *Circulation, 125*(1), e2-e220. doi: 10.1161/CIR.0b013e31823ac046

Ruozi, G., Bortolotti, F., Falcione, A., Dal Ferro, M., Ukovich, L., Macedo, A., . . . Giacca, M. (2015). AAV-mediated in vivo functional selection of tissue-protective factors against ischaemia. *Nat Commun, 6*, 7388. doi: 10.1038/ncomms8388

Ruozi, G., Bortolotti, F., Mura, A., Tomczyk, M., Falcione, A., Martinelli, V., . . . Giacca, M. (2022). Cardioprotective factors against myocardial infarction selected in vivo from an AAV secretome library. *Sci Transl Med, 14*(660), eabo0699. doi: 10.1126/scitranslmed.abo0699

Sanders, L. N., Schoenhard, J. A., Saleh, M. A., Mukherjee, A., Ryzhov, S., McMaster, W. G., Jr., . . . Hatzopoulos, A. K. (2016). BMP Antagonist Gremlin 2 Limits Inflammation After Myocardial Infarction. *Circ Res, 119*(3), 434-449. doi: 10.1161/CIRCRESAHA.116.308700

Schultz Jel, J., Witt, S. A., Glascock, B. J., Nieman, M. L., Reiser, P. J., Nix, S. L., . . . Doetschman, T. (2002). TGF-beta1 mediates the hypertrophic cardiomyocyte growth induced by angiotensin II. *J Clin Invest, 109*(6), 787-796. doi: 10.1172/JCI14190

Schultz, N., Byman, E., Fex, M., & Wennstrom, M. (2017). Amylin alters human brain pericyte viability and NG2 expression. *J Cereb Blood Flow Metab, 37*(4), 1470-1482. doi: 10.1177/0271678X16657093

Schwartz Longacre, L., Kloner, R. A., Arai, A. E., Baines, C. P., Bolli, R., Braunwald, E., . . . Blood Institute, N. I. o. H. (2011). New horizons in cardioprotection: recommendations from the 2010 National Heart, Lung, and Blood Institute Workshop. *Circulation, 124*(10), 1172-1179. doi: 10.1161/CIRCULATIONAHA.111.032698

Sciarretta, S., Maejima, Y., Zablocki, D., & Sadoshima, J. (2018). The Role of Autophagy in the Heart. *Annu Rev Physiol, 80*, 1-26. doi: 10.1146/annurev-physiol-021317-121427

Shehata, M. M., Kamal, M. M., El-Hefnawy, M. H., & El-Mesallamy, H. O. (2017). Association of serum pancreatic derived factor (PANDER) with beta-cell dysfunction in type 2 diabetes mellitus. *J Diabetes Complications, 31*(4), 748-752. doi: 10.1016/j.jdiacomp.2017.01.001

Slordal, L., & Spigset, O. (2006). Heart failure induced by non-cardiac drugs. *Drug Saf, 29*(7), 567-586. doi: 10.2165/00002018-200629070-00003

Spinella-Jaegle, S., Roman-Roman, S., Faucheu, C., Dunn, F. W., Kawai, S., Gallea, S., . . . Rawadi, G. (2001). Opposite effects of bone morphogenetic protein-2 and transforming growth factor-beta1 on osteoblast differentiation. *Bone, 29*(4), 323-330. doi: 10.1016/s8756-3282(01)00580-4

Steppich, B., Groha, P., Ibrahim, T., Schunkert, H., Laugwitz, K. L., Hadamitzky, M., . . . Regeneration of Vital Myocardium in, S. T. S. E. M. I. b. E. S. I. (2017). Effect of Erythropoietin in patients with acute myocardial infarction:

five-year results of the REVIVAL-3 trial. *BMC Cardiovasc Disord, 17*(1), 38. doi: 10.1186/s12872-016-0464-3

Strungs, E. G., Ongstad, E. L., O'Quinn, M. P., Palatinus, J. A., Jourdan, L. J., & Gourdie, R. G. (2013). Cryoinjury models of the adult and neonatal mouse heart for studies of scarring and regeneration. *Methods Mol Biol, 1037*, 343-353. doi: 10.1007/978-1-62703-505-7_20

Suliman, H. B., Carraway, M. S., Ali, A. S., Reynolds, C. M., Welty-Wolf, K. E., & Piantadosi, C. A. (2007). The CO/HO system reverses inhibition of mitochondrial biogenesis and prevents murine doxorubicin cardiomyopathy. *J Clin Invest, 117*(12), 3730-3741. doi: 10.1172/JCI32967

Sumida, A., Horiba, M., Ishiguro, H., Takenaka, H., Ueda, N., Ooboshi, H., . . . Kodama, I. (2010). Midkine gene transfer after myocardial infarction in rats prevents remodelling and ameliorates cardiac dysfunction. *Cardiovasc Res, 86*(1), 113-121. doi: 10.1093/cvr/cvp386

Tartaglia, L. A., Ayres, T. M., Wong, G. H., & Goeddel, D. V. (1993). A novel domain within the 55 kd TNF receptor signals cell death. *Cell, 74*(5), 845-853. doi: 10.1016/0092-8674(93)90464-2

Teerlink, J. R., Cotter, G., Davison, B. A., Felker, G. M., Filippatos, G., Greenberg, B. H., . . . Investigators, R. E. i. A. H. F. (2013). Serelaxin, recombinant human relaxin-2, for treatment of acute heart failure (RELAX-AHF): a randomised, placebo-controlled trial. *Lancet, 381*(9860), 29-39. doi: 10.1016/S0140-6736(12)61855-8

Teichman, S. L., Unemori, E., Dschietzig, T., Conrad, K., Voors, A. A., Teerlink, J. R., . . . Cotter, G. (2009). Relaxin, a pleiotropic vasodilator for the treatment of heart failure. *Heart Fail Rev, 14*(4), 321-329. doi: 10.1007/s10741-008-9129-3

Tian, Y., Liu, Y., Wang, T., Zhou, N., Kong, J., Chen, L., . . . Morrisey, E. E. (2015). A microRNA-Hippo pathway that promotes cardiomyocyte proliferation and cardiac regeneration in mice. *Sci Transl Med, 7*(279), 279ra238. doi: 10.1126/scitranslmed.3010841

Tiburcy, M., Hudson, J. E., Balfanz, P., Schlick, S., Meyer, T., Chang Liao, M. L., . . . Zimmermann, W. H. (2017). Defined Engineered Human Myocardium With Advanced Maturation for Applications in Heart Failure Modeling and Repair. *Circulation, 135*(19), 1832-1847. doi: 10.1161/CIRCULATIONAHA.116.024145

Turkson, J., & Jove, R. (2000). STAT proteins: novel molecular targets for cancer drug discovery. *Oncogene, 19*(56), 6613-6626. doi: 10.1038/sj.onc.1204086

Valle Raleigh, J., Mauro, A. G., Devarakonda, T., Marchetti, C., He, J., Kim, E., . . . Salloum, F. N. (2017). Reperfusion therapy with recombinant human relaxin-2 (Serelaxin) attenuates myocardial infarct size and NLRP3

inflammasome following ischemia/reperfusion injury via eNOS-dependent mechanism. *Cardiovasc Res, 113*(6), 609-619. doi: 10.1093/cvr/cvw246

Waerner, T., Alacakaptan, M., Tamir, I., Oberauer, R., Gal, A., Brabletz, T., . . . Beug, H. (2006). ILEI: a cytokine essential for EMT, tumor formation, and late events in metastasis in epithelial cells. *Cancer Cell, 10*(3), 227-239. doi: 10.1016/j.ccr.2006.07.020

Wang, A., Gu, Z., Heid, B., Akers, R. M., & Jiang, H. (2009). Identification and characterization of the bovine G protein-coupled receptor GPR41 and GPR43 genes. *J Dairy Sci, 92*(6), 2696-2705. doi: 10.3168/jds.2009-2037

Wang, C., Chi, Y., Li, J., Miao, Y., Li, S., Su, W., . . . Guan, Y. (2014). FAM3A activates PI3K p110alpha/Akt signaling to ameliorate hepatic gluconeogenesis and lipogenesis. *Hepatology, 59*(5), 1779-1790. doi: 10.1002/hep.26945

Wang, L., Klionsky, D. J., & Shen, H. M. (2022). The emerging mechanisms and functions of microautophagy. *Nat Rev Mol Cell Biol*. doi: 10.1038/s41580-022-00529-z

Weinberger, F., Breckwoldt, K., Pecha, S., Kelly, A., Geertz, B., Starbatty, J., . . . Eschenhagen, T. (2016). Cardiac repair in guinea pigs with human engineered heart tissue from induced pluripotent stem cells. *Sci Transl Med, 8*(363), 363ra148. doi: 10.1126/scitranslmed.aaf8781

Wen, Z., & Darnell, J. E., Jr. (1997). Mapping of Stat3 serine phosphorylation to a single residue (727) and evidence that serine phosphorylation has no influence on DNA binding of Stat1 and Stat3. *Nucleic Acids Res, 25*(11), 2062-2067. doi: 10.1093/nar/25.11.2062

Wen, Z., Zhong, Z., & Darnell, J. E., Jr. (1995). Maximal activation of transcription by Stat1 and Stat3 requires both tyrosine and serine phosphorylation. *Cell, 82*(2), 241-250. doi: 10.1016/0092-8674(95)90311-9

Whelan, R. S., Kaplinskiy, V., & Kitsis, R. N. (2010). Cell death in the pathogenesis of heart disease: mechanisms and significance. *Annu Rev Physiol, 72*, 19-44. doi: 10.1146/annurev.physiol.010908.163111

Wilson, C. G., Robert-Cooperman, C. E., & Burkhardt, B. R. (2011). PANcreatic-DERived factor: novel hormone PANDERing to glucose regulation. *FEBS Lett, 585*(14), 2137-2143. doi: 10.1016/j.febslet.2011.05.059

Witman, N., Murtuza, B., Davis, B., Arner, A., & Morrison, J. I. (2011). Recapitulation of developmental cardiogenesis governs the morphological and functional regeneration of adult newt hearts following injury. *Dev Biol, 354*(1), 67-76. doi: 10.1016/j.ydbio.2011.03.021

Woosley, A. N., Dalton, A. C., Hussey, G. S., Howley, B. V., Mohanty, B. K., Grelet, S., . . . Howe, P. H. (2019). TGFbeta promotes breast cancer stem

cell self-renewal through an ILEI/LIFR signaling axis. *Oncogene, 38*(20), 3794-3811. doi: 10.1038/s41388-019-0703-z

Wu, D., Zhang, K., & Hu, P. (2019). The Role of Autophagy in Acute Myocardial Infarction. *Front Pharmacol, 10*, 551. doi: 10.3389/fphar.2019.00551

Wu, X., He, L., Chen, F., He, X., Cai, Y., Zhang, G., . . . Luo, J. (2014). Impaired autophagy contributes to adverse cardiac remodeling in acute myocardial infarction. *PLoS One, 9*(11), e112891. doi: 10.1371/journal.pone.0112891

Wyllie, A. H. (1980). Glucocorticoid-induced thymocyte apoptosis is associated with endogenous endonuclease activation. *Nature, 284*(5756), 555-556. doi: 10.1038/284555a0

Yang, J., Gao, Z., Robert, C. E., Burkhardt, B. R., Gaweska, H., Wagner, A., . . . Wolf, B. A. (2005). Structure-function studies of PANDER, an islet specific cytokine inducing cell death of insulin-secreting beta cells. *Biochemistry, 44*(34), 11342-11352. doi: 10.1021/bi0503908

Yao, L., Zhang, Y., Chen, K., Hu, X., & Xu, L. X. (2011). Discovery of IL-18 as a novel secreted protein contributing to doxorubicin resistance by comparative secretome analysis of MCF-7 and MCF-7/Dox. *PLoS One, 6*(9), e24684. doi: 10.1371/journal.pone.0024684

Yellon, D. M., & Downey, J. M. (2003). Preconditioning the myocardium: from cellular physiology to clinical cardiology. *Physiol Rev, 83*(4), 1113-1151. doi: 10.1152/physrev.00009.2003

Yorimitsu, T., & Klionsky, D. J. (2005). Autophagy: molecular machinery for self-eating. *Cell Death Differ, 12 Suppl 2*, 1542-1552. doi: 10.1038/sj.cdd.4401765

You, L., Wang, Z., Li, H., Shou, J., Jing, Z., Xie, J., . . . Han, W. (2015). The role of STAT3 in autophagy. *Autophagy, 11*(5), 729-739. doi: 10.1080/15548627.2015.1017192

Youssef, G., & Links, M. (2005). The prevention and management of cardiovascular complications of chemotherapy in patients with cancer. *Am J Cardiovasc Drugs, 5*(4), 233-243. doi: 10.2165/00129784-200505040-00003

Zhang, F., Zhu, X., Wang, P., He, Q., Huang, H., Zheng, T., . . . Ding, Y. (2021). The cytokine FAM3B/PANDER is an FGFR ligand that promotes posterior development in Xenopus. *Proc Natl Acad Sci U S A, 118*(20). doi: 10.1073/pnas.2100342118

Zhang, L. S., Hu, H. G., Liu, Y. J., Li, J., Yu, P., Zhang, F., . . . Deng, H. W. (2012). A follow-up association study of two genetic variants for bone mineral density variation in Caucasians. *Osteoporos Int, 23*(7), 1867-1875. doi: 10.1007/s00198-011-1863-z

Zhang, S., Liu, X., Bawa-Khalfe, T., Lu, L. S., Lyu, Y. L., Liu, L. F., & Yeh, E. T. (2012). Identification of the molecular basis of doxorubicin-induced cardiotoxicity. *Nat Med, 18*(11), 1639-1642. doi: 10.1038/nm.2919

Zhang, X., Yang, W., Wang, J., Meng, Y., Guan, Y., & Yang, J. (2018). FAM3 gene family: A promising therapeutical target for NAFLD and type 2 diabetes. *Metabolism, 81*, 71-82. doi: 10.1016/j.metabol.2017.12.001

Zhao, L., & Zhang, B. (2017). Doxorubicin induces cardiotoxicity through upregulation of death receptors mediated apoptosis in cardiomyocytes. *Sci Rep, 7*, 44735. doi: 10.1038/srep44735

Zhao, X., Luo, G., Fan, Y., Ma, X., Zhou, J., & Jiang, H. (2018). ILEI is an important intermediate participating in the formation of TGF-beta1-induced renal tubular EMT. *Cell Biochem Funct, 36*(2), 46-55. doi: 10.1002/cbf.3316

Zhao, Z. Q., Corvera, J. S., Halkos, M. E., Kerendi, F., Wang, N. P., Guyton, R. A., & Vinten-Johansen, J. (2003). Inhibition of myocardial injury by ischemic postconditioning during reperfusion: comparison with ischemic preconditioning. *Am J Physiol Heart Circ Physiol, 285*(2), H579-588. doi: 10.1152/ajpheart.01064.2002

Zhong, X., Neumann, P., Corbo, M., & Loh, E. (2011). *Recent Advances in Biotherapeutics Drug Discovery and Development*.

Zhu, Y., Pu, Z., Wang, G., Li, Y., Wang, Y., Li, N., & Peng, F. (2021). FAM3C: an emerging biomarker and potential therapeutic target for cancer. *Biomark Med, 15*(5), 373-384. doi: 10.2217/bmm-2020-0179

Zhu, Y., Xu, G., Patel, A., McLaughlin, M. M., Silverman, C., Knecht, K., . . . Young, P. R. (2002). Cloning, expression, and initial characterization of a novel cytokine-like gene family. *Genomics, 80*(2), 144-150. doi: 10.1006/geno.2002.6816

Zhu, Y. H., Zhang, B., Li, M., Huang, P., Sun, J., Fu, J., & Guan, X. Y. (2015). Prognostic significance of FAM3C in esophageal squamous cell carcinoma. *Diagn Pathol, 10*, 192. doi: 10.1186/s13000-015-0424-8

Zimmermann, W. H., Melnychenko, I., Wasmeier, G., Didie, M., Naito, H., Nixdorff, U., . . . Eschenhagen, T. (2006). Engineered heart tissue grafts improve systolic and diastolic function in infarcted rat hearts. *Nat Med, 12*(4), 452-458. doi: 10.1038/nm1394

Zouein, F. A., Altara, R., Chen, Q., Lesnefsky, E. J., Kurdi, M., & Booz, G. W. (2015). Pivotal Importance of STAT3 in Protecting the Heart from Acute and Chronic Stress: New Advancement and Unresolved Issues. *Front Cardiovasc Med, 2*, 36. doi: 10.3389/fcvm.2015.00036